Investigating the absorptive and secretory transport of selected anti-malarial drugs

JJ Heyns

orcid.org/ 0000-0003-0053-948X

Dissertation submitted in fulfilment of the requirements for the degree *Master of Science* in *Pharmaceutics* at the North-West University

Supervisor:	Dr C Gouws
Co-supervisor:	Prof JH Hamman
Assistant supervisor:	Dr C Willers

Examination November 2017

Student number: 23376856

This dissertation is dedicated to Jesus Christ, who is my Lord and Saviour. All of this, was by His grace and mercy alone. May the Lamb that was slain, receive the reward of His suffering. Secondly, I want to dedicate this to my parents, Cecil and Elize Heyns, who have always loved me unconditionally and supported me until the end.

ACKNOWLEDGEMENT

I would like to express my deepest and greatest appreciation to my Lord and Saviour, **Jesus Christ**. His love, grace, and mercy is always sufficient and may all my life and work glorify Him until eternity.

- My parents, **Cecil and Elize Heyns**. No words can describe what both of you mean to me. I want to honour both of you for what you have sowed into my life and always cared about me. I am truly blessed with wonderful parents and thank you for teaching me the value of humbleness.

- My brother, **Muller Heyns**. Thank you for all the moral support and always being intrigued with what I am doing and how things are going. Thank you for always helping me out when I was short on gaming money and that your heart was always open to help, and that is why you are an amazing brother.

- To my sister and brother-in-law, **Ilze and Meyer Dalton**. I want to thank you both for everything you have done until this day. Meyer, you are a blessing in my life and thank you for who you are, especially the time you let me shoot my first Springbok. Ilze, thank you for always caring about me and my well-being.

- My supervisor, **Dr. Chrisna Gouws**. Thank you for your support and guidance throughout the two years and I want to thank you for your endless patience and kindness towards me, especially when it comes to the writing part. I am very grateful to have such an excellent supervisor who oversaw everything and I want to honour you for the hard work and everything you have done.

- My assistant supervisor, **Dr. Clarissa Willers**. I am very grateful for all the support and work you have done during these two years. I want to honour you for the kindness and patience you bestowed upon me and above all, the person you are. I have learned so much from you and my appreciation stretches far more than words can say.

- My co-supervisor, **Prof. Josias Hamman**. Thank you for your guidance and patiences during the evaluation of all the permeability studies. I have learned so much from you as a researcher and I want to honour you for the time and input you have given over these two years.

- To **Prof. Jan du Preez** and **Mr. Francois Viljoen**. Thank you for always assisting me when I was in trouble with the HPLC and I want to honour you for your patients, time and input in this two years

- My best friend, **Stefan Cloete**. “Greater love has no one than this: to lay down one’s life for one’s friends” – John 15:13. I want to thank and honour you as my friend and brother. These past two years was something else and you were always there supporting me every step of the way. One thing that I want to honour you for, is your endless support and encouragement in times when it was difficult. I am looking forward to what the next three years are holding for us during our Ph.D.’s.

- To my friend, **Douw Steyn**. Thank you for the times we drank coffee at the P.O.K and for every squash session we had. Thank you for the moral support you gave me in these two years and I want to honour you as a true friend. I will certainly miss all of this in the future.

- To my mentor in life, **Jaco Bekker**. Thank you for the brother and also the father-figure that you have been these 5 years, and words cannot express what a blessing you are. Thank you for always guiding me to the Truth and I honour you for that.

- To all my other close friends, **Jan Oberholzer**, **Jaco Diederiks**, **Wikus Roestorf**. Your moral support over these two years is something I really hold dear to my heart. I am truly blessed with great friends that I can count on even in difficult times.

- To my fellow fraternity member in De Wilgers Men’s Residence, **Alex “Gemmer” Laux**. Your friendship means a lot to me and the fact that we went through O’n’B together until the day we submitted our dissertations was really an honour and I hope we can work together in the future.

- To my colleague, **Anja Haasbroek**. Thank you for the support during each experiment, and the muffins you blessed me with. Thank you for always being willing to help when it came to measuring the TEER values. I really appreciate you as a friend and I really hope to work with you in the future.

- To **Carlemi Calitz**. Thank you for your guidance during my training at the cell culture lab and I appreciate every input and wisdom you bestowed upon me regarding this area.

The financial assistance of the National Research Foundation (NRF) towards this research is hereby acknowledged. Opinions expressed and conclusions arrived at, are those of the author and are not necessarily to be attributed to the NRF.

ABSTRACT

Malaria is one of the predominant infectious diseases affecting more than 200 million people a year worldwide. Artemisinin combination therapy (ACT) is currently the frontline treatment against the *Plasmodium falciparum* parasite, but reports of resistance developed against the ACT has started to surface in Cambodia and Thailand. New derivatives of artemisinin, such as such as artemisone and artemiside, are therefore being established in an effort to overcome this resistance, whereas artemether is already being used clinically. Knowledge regarding the membrane permeability properties of the newly developed anti-malarial drugs is limited, and treatment failure caused by sub-optimal drug concentrations at the site of action can give rise to drug resistance. The aim of this study was to use the Caco-2 cell-based *in vitro* model to evaluate intestinal membrane permeability and P-glycoprotein (P-gp) related efflux of these orally administered drugs, which can provide an estimation of the bioavailability of the compounds.

The Caco-2 model was validated to confirm monolayer integrity using Lucifer yellow, and subsequently the expression of P-gp was confirmed with the P-gp substrate, vinblastine. Furthermore, high-performance liquid chromatography (HPLC) analytical methods to quantify the various compounds studied were validated. Bi-directional transport of the selected anti-malarial drugs across Caco-2 cell monolayer was measured in the presence and absence of verapamil, a known P-gp inhibitor, and samples obtained during the transport studies were analysed. The relative percentage transport of each compound in both directions were used to calculate the apparent permeability coefficient (P_{app}) values, as well as the efflux ratios (ER) for each anti-malarial.

The relative percentage transport of artemisone and artemether appeared to be moderate in comparison to the reference compounds, caffeine and atenolol, while very low permeation levels of artemiside could be detected. The bi-directional transport results revealed that artemether was probably a very poor P-gp substrate, while artemisone and artemiside were both susceptible to P-gp mediated efflux to some extent. In an effort to potentially increase the bioavailability of these P-gp substrates, the potentially beneficial herb-drug interaction with piperine extracted from black pepper was investigated. Piperine has been shown to inhibit P-gp, which could then potentially reduce the efflux of artemisone and artemiside. It reduced the efflux of artemisone slightly more than verapamil, but solicited an increase in artemiside efflux, thus revealing the possible involvement of other efflux transporters. The transport studies of the artemisinin derivatives clearly suggests these compounds to have moderate to low bioavailability, and low affinity for the P-gp efflux protein.

Keywords: Artemisinin, Caco-2, drug permeability, efflux, herb-drug interactions, malaria, P-glycoprotein

TABLE OF CONTENTS

LIST OF TABLES

LIST OF FIGURES

LIST OF ABBREVIATIONS

%RSD	Relative standard deviation
ABC	ATP-binding cassette
ACT	Artemisinin combination therapy
ANOVA	One-way analysis of variance
AP-BL	Apical to basolateral
ATL	Analytical Technology Laboratory
ATP	Adenosine triphosphate
AUC	Area under the curve
BL-AP	Basolateral to apical
Caco-2	Human Caucasian colon adenocarcinoma cell lines
CDC	Centers of Disease Control and Prevention
CO_2	Carbon dioxide
CYP	Cytochrome P450
DHA	Dihydroartemisinin
DMEM	Dulbecco's Modified Eagle's medium
DMT	Drug/metabolite transporter
ECACC	European Collection of Cell Cultures
EDTA	Trypsin-Versene
ER	Efflux ratio
FBS	Foetal bovine serum

GIT	Gastrointestinal tract
HDI	Herb-drug interactions
HEPES	2-[4-(2-hydroxyethyl)piperazin-1-yl]ethanesulfonic acid
HPLC	High-performance liquid chromatography
HREC	Health Research Ethics Committee
H_3PO_4	Orthophosphoric acid
ICH	International Council on Harmonisation
LOD	Limit of detection
LOQ	Limit of quantification
LY	Lucifer yellow
MRCSA	Medical Research Council of South Africa
MRP	Multi-drug resistance-associated protein
NADH	Nicotinamide adenine dinucleotide phosphate
NADPH	Reduced nicotinamide adenine dinucleotide phosphate
NA_2HPO_4	Di-potasium hydrophosphate
NBDs	Nucleotide binding domains
NEAA	Non-essential amino acids
O_2	Oxygen
P_{app}	Apparent permeability coefficient
PBS	Phosphate buffered saline
P. falciparum	*Plasmodium falciparum*
P-gp	P-glycoprotein
pfcrt	*P. falciparum* chloroquine-resistant transporter

pfmdr1	*P. falciparum* multidrug-resistance-1
P. knowlesi	*Plasmodium knowlesi*
P. malariae	*Plasmodium malariae*
P. ovale	*Plasmodium ovale*
P. vivax	*Plasmodium vivax*
ROS	Reactive oxygen species
RNS	Reactive nitrogen species
SD	Standard deviation
TEER	Transepithelial electrical resistance
UV	Ultraviolet
WHO	World Health Organization

CHAPTER 1: INTRODUCTION

1.1 Background.

Malaria is one of the most prevalent parasitic diseases in the world, and specifically in sub-Saharan Africa. Transmission of this parasite occurs primarily via bites of infected female Anopheles mosquitoes that carry one of the *Plasmodium* species (Karamati *et al.*, 2014:599). A total of 212 million cases of malaria have been reported in 2015, and have resulted in 429 000 deaths (World Health Organization (WHO), 2016:40, 42). New strains of the malaria parasite, *Plasmodium falciparum*, showing resistance to anti-malarial drugs have caused resurgence in malarial morbidity and mortality rates (Valderramos & Fidock, 2006:594). Chloroquine has been the first line of defence against malaria infection for decades, but since resistance towards chloroquine was reported in South-East Asia and South America it has spread to the majority of malaria-endemic countries (Sidhu *et al.*, 2002:210).

Currently, artemisinin combination therapy (ACT) is the recommended course of treatment for *Plasmodium falciparum* malaria. The current front-line combination of ACT is dihidroartemisinin-piperaquine, which is being used worldwide but especially in Cambodia, Vietnam, Thailand, Myanmar, China and Indonesia, although resistance incidents against this treatment have been reported and is spreading (Amato *et al.*, 2017:164). This has prompted research on new drug development against malaria. In South-Africa the first-line treatment for uncomplicated malaria due to *P. falciparum* is artemether-lumefantrine (Coartem®) (Blumberg, 2015:175).

The majority of prescribed drugs are administered orally (Gavhane & Yadav, 2012:331). The villi of the proximal small intestines are the optimal site for drug absorption because of the large epithelial surface area (Gavhane & Yadav, 2012:331; Schellack, 2011:13). Permeability of a drug across the intestinal epithelium is essential in the drug discovery process and therefore the aqueous and intestinal permeability characteristics are fundamental to oral absorption (Estudante *et al.*, 2015:118). The efficacy and safety of a drug molecule is not only dependent on its pharmacodynamics, but the biopharmaceutical and pharmacokinetic properties determine the rate and extent to which the drug reaches its therapeutic target (Panchagnula & Thomas, 2000:132). Permeability of drug compounds across the intestinal epithelia can occur through different transport mechanisms such as passive diffusion, active uptake, efflux, endocytosis and paracellular transport (Kerns & Di, 2008:86).

Active transport, in short, uses an energy-coupling mechanism to create an ion/solute gradient across the epithelial membranes. This mechanism is divided into primary and secondary active transport, which depends on whether energy is generated from ATP hydrolysis, or from ion gradients that were created by active transporters such as ion pumps (Estudante *et al.*, 2013:1341). Secretory transport (i.e. efflux) is a crucial mechanism that actively transports molecules from the epithelial cells back into the intestinal lumen as a protective measure against xenobiotics (Chan *et al.*, 2004:25; Kerns & Di, 2008:89). Intestinal efflux transporters that are investigated primarily, includes the ABC (ATP binding cassette) family of efflux transporters and more specifically, P-glycoprotein (P-gp). P-gp is well recognized for modulating the pharmacokinetic profiles of drug compounds, and this protein's net efflux effect is the prevention of drug permeation across epithelial membranes, reducing the drug concentration within the cells (Kerns & Di, 2008:89; Oga *et al.*, 2012:612). Furthermore, efflux transporter proteins are also responsible for resistance in microorganisms (Willers *et al.*, 2017).

1.1.1 Research Problem

The current management of malaria faces various problems, but the main and foremost is the resistance of the malaria-causing parasites against current drug treatments. New anti-malarial drugs are being developed to overcome resistance, but information regarding their membrane permeability properties is limited while this can significantly affect potential bioavailability in patients. Therefore, the *in vitro* membrane permeability of these drugs across intestinal epithelial cell monolayers can provide an indication of their uptake and efflux and potential bioavailability after oral administration, and can aid in their biopharmaceutical classification. Furthermore, although not the purpose of this study, should any of these compounds be identified to be substrates for the efflux transporter, P-gp, it may indicate potential susceptibility to resistance of the parasite, by means of drug efflux.

1.1.2 Aim and objectives

The aim of this study is to investigate the *in vitro* bi-directional (i.e. absorptive and secretory) transport of selected anti-malaria drugs that are currently in development across cultured Caco-2 cell monolayers.

The specific objectives include:

- To validate existing high performance liquid chromatography (HPLC) analytical methods for the analysis of all the selected anti-malarial drugs (i.e. artemether, artemisone and artemiside) and reference compounds (i.e. vinblastine, caffeine and atenolol).

- To culture Caco-2 cells as a differentiated monolayer on polycarbonate membranes in Transwell® plates, and to validate the model with a known P-gp substrate (i.e. vinblastine).

- To determine absorption reference values through the transport of caffeine and atenolol across Caco-2 cell monolayer.

- To conduct bi-directional transport studies across Caco-2 cell monolayers cultured on Transwell® membranes for each of the selected anti-malarial drugs, and to determine if the addition of a P-gp inhibitor (i.e. verapamil) modulates the transport.

- To interpret the *in vitro* transport results of the selected anti-malaria drugs across Caco-2 cell monolayers in order to identify to what extent absorption and efflux occurred as indicators of human oral bioavailability.

- To identify potential herb-drug pharmacokinetic interactions with the known P-gp inhibiting herbal extract, piperine.

1.1.3 Dissertation organisation

Chapter 1 is an introduction to the study, providing important information with regards to the research problem, aim and specific objectives. Chapter 2 provides a literature review, describing the impact of malaria on humanity, the life cycle of the malaria parasite, anti-malarial drugs currently used to treat the disease and the potential efflux transporters contributing to drug resistance in malaria parasites. The selected anti-malarial drugs (still in the development phase), possible pharmacokinetic herb-drug interactions and the different screening models to investigate various absorptive and secretory transport mechanisms, are also discussed. Chapter 3 contains the validation methods and results for the analytical methods used to study the selected anti-malarial drugs that are used in the *in vitro* studies, whereas the *in vitro* transport methods and results are presented and discussed in Chapter 4. The final conclusions, future recommendations and potential limitations of the study are given in Chapter 5.

CHAPTER 2: LITERATURE REVIEW ON THE ARTIMISININ DERIVATIVES

2.1 Malaria

2.1.1 The impact malaria has on humanity

Malaria is a devastating infectious disease caused by protozoan parasites belonging to the *Plasmodium* genus. These parasites are transmitted from one human to another via female Anopheles mosquitoes (Carter & Mendis, 2002:565). Five species of *Plasmodium* can cause malaria, namely *P. falciparum, P. vivax, P. malariae, P. ovale* and *P. knowlesi*. Of these, only *P. knowlesi* causes malaria in primates, which is found in certain forested areas of South-East Asia. The other four species are responsible for transferring malaria infections to humans. Recently, human cases of *P. knowlesi* have been reported, but were not transmitted from person to person, rather from monkey to human by an infected *Anopheles* mosquito (World Health Organization (WHO), 2015:2). Out of all the malaria species, *P. falciparum* is predominant in the world, especially in Africa. *P. falciparum* infection is the most complicated form of the disease and more than 90% of reported deaths were affected by it. *P. vivax* has a tendency to cause a relapsing form of malaria, and is mainly located in Asia and South America (Petersen *et al.*, 2011:1551; White, 2011:1). This life-threatening disease was responsible for 212 million new cases and 429 000 deaths at the end of 2015 (WHO, 2016:40, 42). These concerning statistics can be attributed to the emergence of drug resistance of the malaria parasite, the increasing migration of refugees from conflict stricken areas to endemic regions and uncontrolled demographic growth leading to the deterioration of vector control measures (Bourdy *et al.*, 2008:33).

Two types of malaria infection exist: uncomplicated malaria results in recurring coldness, rigors and fever, lasting for up to 6 h over 2 to 3 days. If not treated properly, uncomplicated malaria can progress into severe malaria (Bell & Winstanley, 2005:29). Its symptoms are severe headaches, cerebral ischemia and -malaria, hepatomegaly, splenomegaly, hypoglycaemia, haemoglobinuria with kidney failure and subsequent coma, and finally death (De Ridder *et al.*, 2008:304; Medana & Turner, 2006:555). These underlying complications can develop rapidly, and the progress to death may be within several hours or days as most patients have more than one complication developing at the same time (Trampuz *et al.*, 2003:316). The malaria parasite has a complex life cycle, making successful treatment regimens a challenging task.

2.1.2 The life cycle of the malaria parasite

The life cycle of *Plasmodium* parasites consists of several stages, with minor differences occurring among the different species. As illustrated in Figure 2.1, the lifespan of the malaria parasite spreads across two hosts, namely the female *Anopheles* mosquito and a human. The infection starts when an infected *Anopheles* mosquito transfers sporozoite-bearing saliva into a human host. The sporozoites act as the infectious stage of malaria (Cox, 2010:1; Moreno & Joyner, 2015:98). These sporozoites are carried throughout the host until they are able to invade the parenchymal cells of the liver.

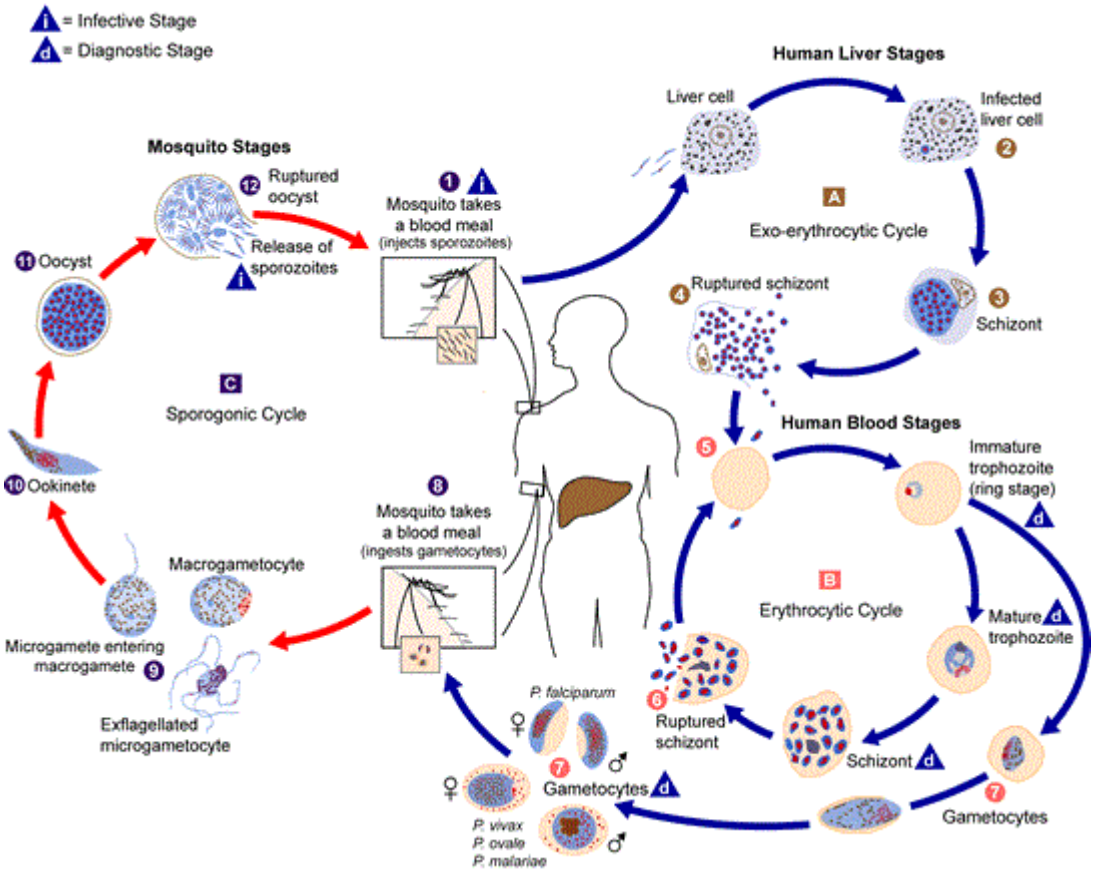

Figure 2.1: Schematic life cycle of *Plasmodium* species between the *Anopheles* mosquito and human host (CDC, 2016)

Inside the hepatocytes, the sporozoites undergo an asexual amplification phase known as exoerythrocytic schizogony - the production of numerous uni-nucleate merozoites in schizonts. The infected hepatocytes (schizonts) rupture to release the merozoites into the bloodstream, which invade the erythrocytes to enter into a second phase of asexual proliferation (erythrocytic

schizogony). Interestingly, *P. vivax and P. ovale* sporozoites form dormant hypnozoites within the liver, which can remain latent for weeks or months after infection. When activated, these hypnozoites result in recurring malaria episodes (Greenwood & Targett, 2011:1601; Moreno & Joyner, 2015: 98). The proliferated merozoites are released from an infected erythrocyte, and after a short period in the blood plasma, the released merozoites re-infect new erythrocytes (Cox, 2010:2). This process is repeated indefinitely causing the characteristic cyclic fevers and shaking chills and ultimately leading to severe anaemia or cerebral malaria (Valderramos & Fidock, 2006:594). Some of the merozoites develop into male and female gametocytes, with *P. falciparum* having a distinctive crescent shape. The gametocytes are harboured inside erythrocytes, which are again transferred to a mosquito upon feeding. The consumed gametocytes, inside the mosquito, mature into male and female gametes. As fertilization occurs, a motile zygote (ookinete) is formed inside the lumen of the anopheline gut, signifying the initiation of the process of sporogony (Moreno & Joyner, 2015:99). The ookinete penetrates the gut wall and develops into an oocyst, which continues to proliferate into sporozoites. The sporozoites migrate to the salivary glands of the mosquito and the life cycle repeats when such an infected mosquito feeds upon a new human host (Cox, 2010:2). This complex life cycle substantiates the vast number of anti-malarial drugs available, focusing on eliminating or suppressing different parasitic life stages, for successful malaria treatment.

2.1.3 Established anti-malarial drugs

Chemotherapeutic treatment regimens form an important contributing factor in combating malaria infections. A wide range of established anti-malarial drugs are available, several of which are derived from natural plant products (Müller & Hyde, 2010). Quinoline drugs, including quinine (derived from Cinchona tree bark), chloroquine, amodiaquine, primaquine, mefloquine and piperaquine, interfere with the parasite's heme detoxification process resulting in lethal complexes against the parasite.

During the intraerythrocytic stage of a *P. falciparum* infection, the parasite requires large amounts of haemoglobin from the host erythrocytes to fulfil its nutritional needs. This is to help counter the threat of oxidative stress that arises from an increased ion permeability of infected erythrocytes (Sanchez *et al.*, 2010:1110). The digestive vacuole is an acidic, lysosome-like organelle in which haemoglobin is degraded and detoxified. The toxic heme is released after haemoglobin is proteolyzed and mineralized inside the vacuole to inert hemozoin, which is then catalysed by a heme detoxification protein. The drug chloroquine for example, in its deprotonated form, is accumulated inside the digestive vacuole and binds to a dimeric form of oxidized heme, called

hematin. Therefore, it interferes with the heme-mineralization process by producing a toxic complex with heme that kills the parasite by perforating the intracellular membranes (Valderramos & Fidock, 2006:594; Sanchez *et al.*, 2010:1110).

Antifolate drugs used against malaria infections are pyrimethamine, proguanil, sulfonamide, sulfadoxine, sulfone and dapsone (Müller & Hyde, 2010). These drugs target the activity of several important enzymes, competing against their natural substrates and acting as possible inhibitors. Artemisinin and its derivatives are peroxidic anti-malarial drugs that are highly effective against the intra-erythrocytic stages of *P. falciparum* (White, 1997:1416). Artemisinins induce the fastest reduction in parasitemia compared to other anti-malarial drug compounds (White, 1997:1415). It is naturally derived from the Chinese plant *Artemisia annua*, and several derivatives have been developed (will be discussed in a later section). However, due to the rapid clearance of circulating parasites, artemisinins have a short half-life of less than an hour, therefore if a radical parasitological cure is not achieved, treatment failure will occur with potential recrudescence (Borrmann *et al.*,2003:903).

It is important to note that several of the abovementioned drugs, which were forerunners in the quest against malaria infections, are currently ineffective in the majority of *P. falciparum* infested areas (De Ridder *et al.*, 2008:303). According to the World Malaria Report 2015 (WHO, 2015: 202-203), the former widely-used chloroquine is presently only prescribed for severe *P. falciparum* cases in the Dominican Republic. Similarly, mefloquine is only used in Peru, but in combination with the artemisinin, artesunate (WHO, 2015: 203). For this reason, artemisinin combination therapies that consist of a potent, short-acting artemisinin drug with a less-potent, long-acting partner drug is a prerequisite for *Plasmodium falciparum* malaria in endemic areas (Amaratunga *et al.*, 2016:357). Examples of such fixed dose combination treatments against uncomplicated malaria due to *P. falciparum* infection include atovaquone-proguanil (Malarone™) and artemether-lumefantrine (Coartem™), whereas other artemisinin combination therapies include artesunate and amodiaquine, artesunate and mefloquine and artesunate in combination with sulfadoxine-pyrimethamine (De Ridder *et al.*, 2008:311; WHO, 2015:32). A decrease in drug efficacy can be ascribed to the increasing emergence of drug resistance in the *Plasmodium* parasite.

2.1.4 Drug resistance in the malaria parasite

The efficacy of multiple anti-malarial drugs is limited by widespread drug resistance, and recent evidence indicates that malaria parasites are also becoming resistant to newer anti-malarial drugs (Cui *et al.*, 2015:58). As a consequence, human morbidity and mortality rates have drastically

increased in areas where drug resistance has been reported (Mita *et al.*, 2009:201,202). From the *P. falciparum* genome, a specific gene was identified as the *P. falciparum* chloroquine-resistant transporter (*pfcrt*), in which a mutation led to an amino acid change at position 76 (K76T), which is believed to be responsible for the resistant phenotype (Hyde, 2005:495; Takala-Harrison & Laufer, 2015:63). This mutation resulted in the replacement of a lysine amino acid by a threonine amino acid in the protein, which is located on the membrane of the digestive vacuole, facing the cytosolic side of the organelle (Petersen *et al.*, 2011:1557; Sanchez *et al.*, 2010:1110). Biochemical studies have been conducted on the vacuoles of parasites with a mutant and wild-type *pfcrt* allele and found that the accumulation of chloroquine in the digestive vacuole was less in the mutant *pfcrt* allele than in the wild type allele (Petersen *et al.*, 2011:1557). The dissimilarity between the two alleles was a result of the amino acid substitution of the positively charged lysine, with an uncharged threonine within the first transmembrane domain of the mutant *pfcrt* allele. Once the electrostatic charge is removed, the protonated chloroquine is prevented from entering the digestive vacuole; therefore, chloroquine is exported via active transport (Petersen *et al.*, 2011:1557). The *pfcrt* protein can also be categorized as a carrier transporter and bioinformatic analyses have revealed that this protein falls within the drug/metabolite transporter (DMT) superfamily. This protein demonstrates a trans-stimulated chloroquine movement, by the chloroquine-resistant strains in live *P. falciparum*-infected erythrocytes. This movement is intrinsic to the characteristic of a carrier, in which the substrate at the trans face of the membrane stimulates the flow of substrate from the cis to the trans direction (Sanchez *et al.*, 2007:332; Sanchez *et al.*, 2010:1111-1112). In both the resistant and sensitive chloroquine strains, the extracellular chloroquine stimulated the efflux of pre-loaded radiolabelled chloroquine (in the presence and absence of metabolic energy), but with different kinetic profiles. In reverse experiments, a low concentration of the pre-loaded unlabelled chloroquine could stimulate uptake of the radiolabelled chloroquine, albeit only in the resistant strains with the mutated *pfcrt* (Sanchez *et al.*, 2010:1112).

Transport studies on intact parasitized erythrocytes have shown evidence that efflux of chloroquine occurs in chloroquine-resistant parasites. These findings were either interpreted in terms of an energy-dependent chloroquine transport or a “charged drug leak” model, from which protonated chloroquine will diffuse passively down its concentration gradient out of the parasitic digestive vacuole (Lehane & Kirk, 2008:4374-4375). The acidity of the vacuole is predominantly maintained by inwardly directed H^+ pumps, which counter the outward movement of H^+ from the digestive vacuole. The presence of chloroquine in chloroquine-resistant parasites has a direct influence on the outward movement of H^+ from the digestive vacuole, but not in chloroquine-

sensitive parasites. This phenomenon was observed by inhibiting the chloroquine associated H^+ leak with verapamil in three *P. falciparum* strains that only differed in their *pfcrt* allele. This showed enhanced H^+ efflux out of the digestive vacuole in chloroquine-resistant parasites, as a consequence of the *pfcrt* mutation (Lehane & Kirk, 2008:4375).

There are numerous plasmodial proteins on the parasites' membrane that can transport different drug molecules. Polymorphisms in the transporter protein genes act as intermediaries of drug resistance by inducing changes in the protein expression. The efflux capabilities of the parasites may be enhanced, leading to the reduced sensitivity of the parasites to drugs (Cui *et al.*, 2015:58). The well-known P-glycoprotein (P-gp) transporter responsible for several drug efflux occurrences in humans has been associated with cancer multidrug-resistance. A P-gp homolog was identified in the *P. falciparum* parasite that is located on the 5th chromosome and encodes a predicted 12-transmembrane-domain protein, called the *P. falciparum* multidrug-resistance-1 (*pfmdr1*) gene (Sidhu *et al.*, 2006:529). This protein also resides within the membrane of the digestive vacuole, which is a common site of action for anti-malarial drugs, but its specific function is still unknown (Cui *et al.*, 2015:59). Therefore, the possibility does exist that the *pfmdr1* transporter is a major contributor to plasmodial drug resistance, by actively effluxing anti-malarial drugs out of the parasitic cell. Consequently, if an anti-malarial drug is susceptible to efflux by transporters such as P-gp, the malaria parasite has a high probability of developing resistance to the particular drug, in time.

Although the focus of this study is intestinal absorption and efflux of anti-malarial drugs after oral administration, identification of potential selectivity of these drugs for P-gp efflux may indicate similar effects in the parasite. Therefore these P-gp substrates drugs may be subjected to drug resistance.

2.1.5 Anti-malarial drug development

With the increased use and availability of artemisinin-based combination therapies (ACTs) worldwide, overall morbidity and mortality rates caused by malaria outbreaks have decreased (Ashley *et al.*, 2014:412). However, the effectiveness of ACTs is becoming a concern, as the malaria parasite is showing an increased tolerance to ACTs. This was first reported from both sides of the Thai and Cambodian border in 2008 (WHO, 2016:6). Recent ACT resistant cases have also been confirmed in several South-East Asian regions such as Laos, Thailand, Cambodia, Vietnam and Myanmar (Ashley *et al.*, 2014:415). Given the fact that artemisinin-based drugs are still effective in several malaria endemic areas, new derivatives from the parent molecule is being synthesised and tested for anti-malarial potential.

New concepts that form part of the Medical Research Council of South Africa (MRCSA) Flagship program under the leadership of Prof R.K. Haynes: Development to the clinical phase of oxidant and redox drug combinations for treatment of malaria, tuberculosis and related diseases, which include drugs that enhance oxidative stress with synergistic action against co-factors of flavoenzymes corresponding with redox homeostasis and other functions. The redox homeostasis in the *Plasmodium* parasite cell synthesizes reduced glutathione and thioredoxin, to protect against oxidative stress. Oxidative stress is an imbalanced production of pro-oxidants to anti-oxidants, such as reactive oxygen species (ROS) and reactive nitrogen species (RNS), and the intracellular system should be capable of detoxifying these species (Percario *et al.*, 2012:16358; Rahman *et al.*, 2012:997). Existing molecules (e.g. methylene blue) contain chemical groups with a redox potential that is converted to its reduced conjugate by nicotinamide adenine dinucleotide phosphate (NADPH)-dependent flavoenzyme-catalyzed reactions in the cytosol of infected blood cells. The reduced conjugate is oxidized into ROS by molecular oxygen and migrates to the digestive vacuole for re-oxidization into the original redox molecule, therefore repeating the cycle (Belorgey *et al.*, 2013:15). The natural defence mechanism of the host is activated with the involvement of phagocytes upon infection with *Plasmodium* parasites. During this stage, oxidative stress occurs and forms part of the defence mechanism in a human host, which acts upon malaria infection and can lead to the death of the parasite (Percario *et al.*, 2012:16348).

Artemisinins act as oxidant molecules that oxidize reduced flavin co-factors and interfere with electron transfer inside the redox homeostasis (Guo *et al.*, 2012:171-172). The reduced conjugates of methylene blue are oxidized by artemisinins, thus accelerating the futile cycling of NADPH with methylene blue. Increased turnover of methylene blue and ROS is also apparent in the single electron transfer processes involving artemisinins and methylene blue under aerobic conditions (Haynes *et al.*, 2010:9). Thus, a considerable number of novel artemisinin derivatives exist for the possible control of malaria infections, as displayed in Figure 2.2, of which only three will be investigated in this study. Artemisinin represents the parent drug; dihydroartemisinin (DHA) is an active metabolite; arteether and artemether are lipid-based derivatives; artesunate is a polar derivative; SM905 (1-(12β-dihydroartemisininoxy)-2-hydroxy-3-tert-butyla1minopropane maleate) is a new water soluble derivative; SM934 (β-aminoarteether maleate); artemiside is a 10-alkylamino sulphide derivative and artemisone is a new 10-alkylamino sulfone derivative (Ho *et al.*, 2014:127).

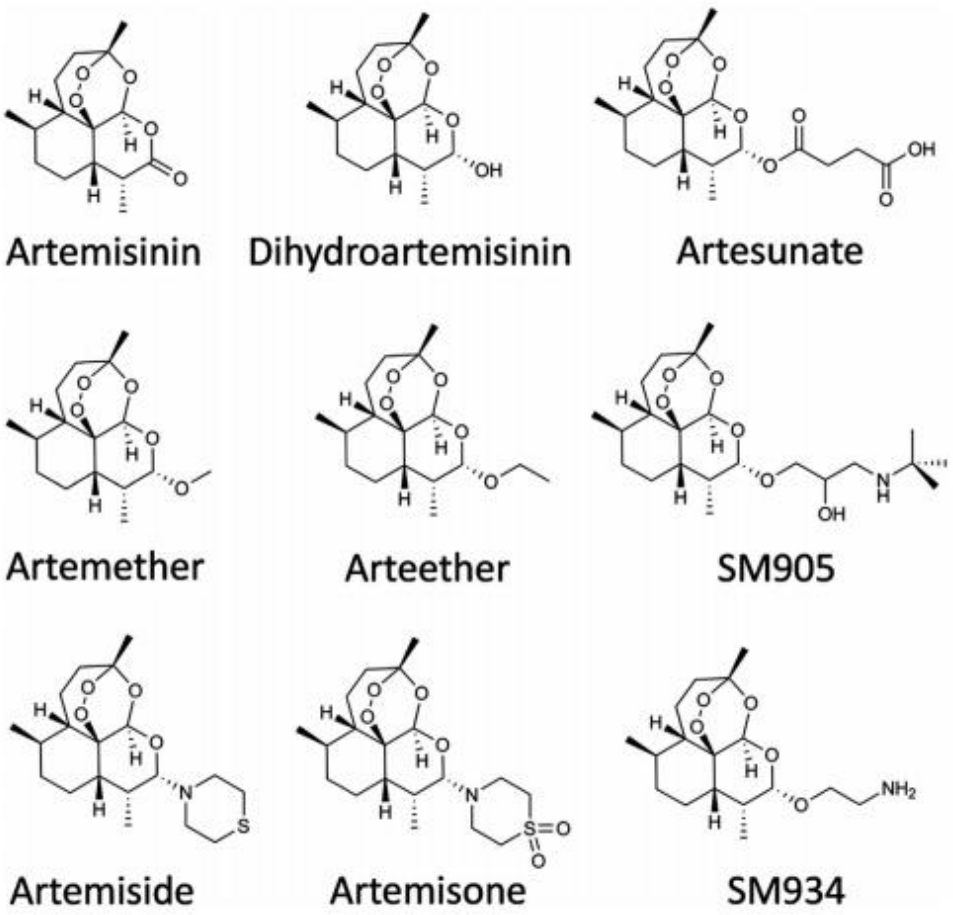

Figure 2.2: Chemical structures of artemisinin and its derivatives. (Ho *et al.*, 2014:127)

2.1.5.1 Artemether

Artemether belongs to the artemisinin anti-malarial drug family (chemical structure shown Figure 2.2). After administration, it is rapidly metabolized by cytochrome P450 enzymes to dihydroartemisinin (DHA) (Ali *et al.*, 2010:1). Artemether interacts with ferriprotoporphyrin IX or ferrous iron in the digestive vacuole of the parasite, which produces cytotoxic radical species in the treatment of malaria. Artemether is given clinically in combination with lumefantrine against chloroquine-sensitive and resistant *P. falciparum* malaria (Makanga, 2014:292; Olliaro, 2001:215).

2.1.5.2 Artemiside

Artemiside is part of the semi-synthetic 10 alkylamino-artemisinins that is synthesised from DHA (chemical structure shown in Figure 2.2). This compound is superior to artemisone in both *in vitro* and *in vivo* studies against Toxoplasma gondii. It is also potent in the treatment of cerebral malaria due to its anti-plasmodial capacity and synergistic relationship with the immune system (Guo *et al.*, 2012:163).

2.1.5.3 Artemisone

Artemisone is one of the new semi-synthetic 10 alkylamino-artemisinins that can be synthesized from dihydroartemisinin (DHA) (chemical structure shown in Figure 2.2). This compound is highly effective against *P. falciparum* in primates, but is less effective than artemiside in experimental cerebral malaria (Guo *et al.*, 2012:163). Treatment of malaria with artemisone led to complete cure, or recrudescence and results also showed that experimental cerebral malaria may be completely cured in late stages of pathogenesis (Waknine-Grineberg *et al.*, 2010:12).

It is necessary to investigate the membrane permeability of the abovementioned anti-malarial (artemisinin) drugs because relatively little is known in terms of these properties, and to identify the potential of drug resistance via efflux.

2.2 Herb-drug pharmacokinetic interactions

Medicinal plants have been the fundamental aspect of primary health care before the invention of modern medicine (Fasinu *et al.*, 2012:1). The frequent usage of herbal medicine continues to increase in both developing and developed countries worldwide (Fasinu *et al.*, 2012:1; Posadzki *et al.*, 2013:603). Traditional medicine is being consumed by more than 80% of the population in some developing countries, mostly in Africa and Asia where herbal medicine is used for primary health care (Brijlal *et al.*, 2011:35). The use of herbal medicine was intended for health improvement and also for treating common diseases such as colds, inflammatory disorders and chronic diseases. This has led people to think that these herbal medicines are safe and non-toxic with limited interaction with other compounds (Liu *et al.*, 2011:835). However, it is important to be aware that herbal medicine may also contain pharmacologically active ingredients, which can have an interaction with modern synthetic drugs (Posadzki *et al.*, 2013:603). The combination of synthetic drugs and herbal medicines can induce changes in the pharmacodynamic and/or pharmacokinetic profiles of the drugs, which alters its physiological responses (Cordier & Steenkamp, 2011:54). The resulting pharmacokinetic interaction between herbal medicines and

allopathic medicines, may involve induction and/or inhibition of intestinal efflux proteins as well as intestinal and hepatic metabolizing enzymes (Pal & Mitra, 2006:2132).

Herb-drug interactions (HDI) are mainly associated with cytochrome P450 (CYP450) enzymes and/or P-glycoprotein (P-gp) (Liu *et al.*, 2015:2). Alteration in absorption, distribution, metabolism or elimination of the drug compound can pose two major extremities that include pharmacotoxicity and treatment failure (Cordier & Steenkamp, 2011:54; Fasinu *et al.*, 2012:2). Pharmacodynamic interactions that can occur will either enhance or negate each other's effect, so it can either produce an increase or decrease of the physiological response (Gurley, 2012:1479). Most drug molecules undergo biotransformation by the CYP450 enzymes and more specifically by the CYP3A4 isoform. These enzymes are highly expressed in the liver and in the small intestines. The ABC efflux transporters (including P-gp) is also located on the apical surface of the intestinal epithelium and the synergistic action by both the efflux pumps (P-gp) and CYP450 will reduce the oral bioavailability of drug compounds such as, protease inhibitors, macrolides and azoles (Gurley, 2012:1483; Pal & Mitra, 2006:2132). The quantity of drug compounds that reach the systemic circulation will be altered when modulation of transporter proteins or metabolizing enzymes occur (Pal & Mitra, 2006:2132).

2.2.1 Piperine

The natural occurring alkaloid, piperine, has been extracted from *Piper nigrum* Linn (black pepper) and *Piper longum* Linn (Long pepper), both from the Piperaceae family (Ajazuddin *et al.*, 2014:2). Black pepper powder was used in ancient times as a means of flavouring food, but also as a medicine (Gurley *et al.*, 2012:1499). Piperine has been indicated to have various medicinal activities such as anti-inflammatory, antipyretic, analgesic and immunomodulatory effects (Ajazuddin *et al.*, 2014:2; Li *et al.*, 2016:287). Piperine is described as a bio-enhancer that improves the absorption of drugs/nutrients, and inhibits metabolic enzymes in the biotransformation of drug molecules (Ajazuddin *et al.*, 2014:2). The piperine alkaloid (1-Piperoyl piperidine) enhances the bioavailability of drug molecules by inhibiting the metabolic pathway of glucuronidation, metabolic enzymes including the cytochrome P450 in both the liver and small intestines, and changes the lipid dynamics of cell membranes (Ajazuddin *et al.*, 2014:3; Li *et al.*, 2016:287; Shoba *et al.*, 1998:353). Piperine has been shown to be a potent inhibitor of the P-gp efflux transporter in gastrointestinal epithelial cells (i.e. Caco-2 cell line) (Ajazuddin *et al.*, 2014:2). According to Bhardwaj *et al.* (2002:647) a transport study for the two known P-gp substrates, digoxin and cyclosporine A, revealed a dose-dependent decrease in secretory transport, whereas the absorptive transport increased.

2.3 Absorptive and secretory drug transport

The oral route is the most convenient way of drug administration, with the small intestine being the primary absorption site of orally administered drugs because of its large epithelial surface area (Schellack, 2011:13). The villi on the enterocytes of the intestinal epithelium are a contributing factor to the rate and extent of drug absorption, and consequently also the bioavailability of drugs administered orally (Nožinić *et al.*, 2010:323). Transport across biological membranes is therefore an important parameter in the field of biopharmaceutics, which governs the pharmacokinetics of a drug (Panchagnula & Thomas, 2000:137). Drug absorption involves the movement of drug molecules across the intestinal epithelium into the capillary blood vessels surrounding the gastrointestinal tract (GIT) (El-Kattan & Varma, 2012:3; Schellack, 2011:13). The ability of a drug molecule to cross the intestinal epithelium is crucial because a compound must be capable of permeating through the epithelium to reach its specific therapeutic target.

Oral absorption of drug molecules is primarily dependent on their aqueous solubility and intestinal permeability (El-Kattan & Varma, 2012:1; Estudante *et al.*, 2015:118; Kerns & Di, 2008:86). Several physiochemical properties determine the ability of molecules to cross the intestinal membrane, namely molecular size, electrochemical charge, lipophilicity and hydrogen bonding potential. Polar molecules usually have lower permeability potential, by means of passive diffusion, in comparison to lipophilic molecules because of the non-polar lipid bilayer functioning as the biological membrane. The permeability of neutral, anionic molecules is also higher than that of ionic forms (Hunter & Hirst, 1997:132; Kerns & Di, 2008:87).

During absorption and distribution, drug molecules come in contact with several different biological membrane barriers inside the human body, including the gastrointestinal epithelial cells, blood capillary walls, hepatocyte membranes, blood-brain barrier, glomerulus and most importantly, the target cell membrane. The permeation of drugs across the intestinal epithelial cell layer can occur through various mechanisms such as passive diffusion, active transport, facilitated transport and phagocytosis (Hunter & Hirst, 1997:131; Kerns & Di, 2008:86). Figure 2.3 illustrates the various mechanisms of drug transport across the intestinal epithelium.

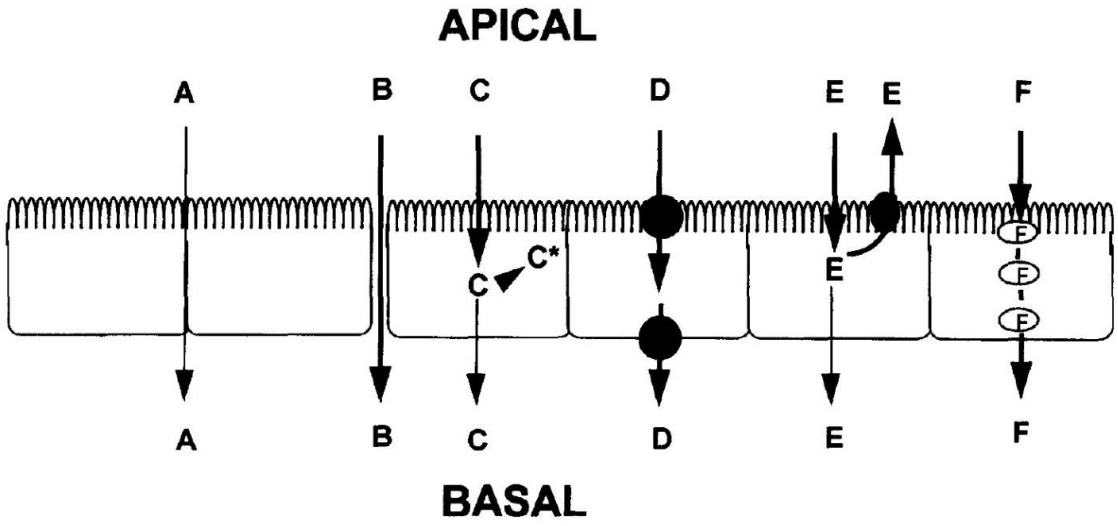

Figure 2.3: **The different transport mechanisms of intestinal absorption: (A) passive paracellular diffusion; (B) passive paracellular diffusion enhanced by a modulator of tight junctions; (C) passive transcellular diffusion; (C*) intracellular metabolism; (D) carrier-mediated active transport, (E) passive trancellular diffusion coupled with an efflux mechanism, (F) endocytosis. (Hunter & Hirst, 1997:131)**

2.3.1 Passive diffusion

Passive diffusion is in general considered to be the main mechanism of drug transport across the intestinal epithelial membrane. This mechanism involves the energy-independent movement of molecules from a high concentration to a low concentration (Kerns & Di, 2008:87). Passive diffusion can occur via the transcellular or paracellular transport pathways. For transcellular diffusion, molecules permeate through the cells, whereas diffusion between adjacent cells through tight junctions and intercellular spaces is termed paracellular diffusion. Paracellular diffusion is limited to small hydrophilic drug molecules, due to the very small fenestrae in the tight junctions (Daugherty & Mrsny, 1999:147). Tight junctions form a continuous intercellular barrier between epithelial cells, which separates tissue spaces and regulate the selective movement of solutes and molecules across the epithelium. These tight junctions determine whether the transepithelial electrical resistance (TEER) is high or low and therefore differs by several orders of magnitude between so-called “tight” and “leaky” epithelia. The relevance of TEER is that epithelia with “tight” tight junctions can maintain the high electrochemical gradient in secondary active transport, whereas epithelia with “leaky” tight junctions can transfer large amounts of iso-

osmotic fluids and ions because tight junctions have an ionic charge selectivity (Anderson & Van Itallie, 2009:3).

2.3.2 Active transport

Active transport is an energy-dependent (forced) movement of molecules against a concentration gradient, across a membrane, by using active transporter proteins. Active transport can be divided into primary and secondary active transport. Primary active transport utilises chemical energy in the form of adenosine triphosphate (ATP) to phosphorylate the transporter. Phosphorylation changes the conformation of the protein and also the affinity of the transporter's solute-binding site (Widmaier *et al.*, 2011:102). Secondary active transport involves the use of an electrochemical gradient as a source of energy. The movement of an ion down its electrochemical gradient is coupled to the transporter, to increase the affinity for another molecule such as a nutrient or an amino acid (Widmaier *et al.*, 2011:104). This transport mechanism requires the binding of a drug molecule to a transmembrane protein, which carries it across the membrane. The drug molecule should therefore have an affinity for a transporter before it can be transported via the secondary active transport mechanism (Kerns & Di, 2008:89).

2.3.3 Efflux of drugs

In contrast to uptake transport (absorptive direction), efflux (secretory direction) is an important mechanism during which molecules are actively transported out of the epithelial cells back into the intestinal lumen (Chan *et al.*, 2004:26; Kerns & Di, 2008:89). This efflux mechanism is necessary for the survival of an organism, as it reduces the concentration of potentially harmful compounds within epithelial cells and, therefore, the quantity that moves across the epithelial lining. Consequently, the bioavailability of the compound is regulated within the human body. Reduced bioavailability, as a result of efflux, is known for its negative effect on drug pharmacodynamics because sub-therapeutic levels may be reached. Furthermore, it is detrimental to the effective treatment of cancer cells, as it reduces the intracellular concentration of anti-cancer drugs, contributing to multi-drug resistance (Chan *et al.*, 2004:25; Kerns & Di, 2008:89). The P-gp transporter, also known as multi-drug resistance protein 1 (MDR1), is one of the foremost efflux transporters in mammalian cells (Oga *et al.*, 2012:612).

2.3.3.1 P-glycoprotein transporter

The P-gp transporter was first expressed as a surface phosphoglycoprotein in drug-resistant Chinese hamster ovary cells and characterized by Juliano and Ling (Lin & Yamazakie, 2003:60). They confirmed that P-gp is an ATP hydrolysis driven, energy-dependent efflux transporter. This protein forms part of the ATP-binding cassette (ABC) superfamily of transporter proteins and was one of the first active efflux transporters to be identified (Chan *et al.*, 2004:25; Lin & Yamazakie, 2003:60). This protein is located in the apical membrane of intestinal epithelial cells, renal epithelial cells, bile canaliculi and the blood-brain barrier (Oga *et al.*, 2012:612). The ABC transporter protein is composed of at least four core domains; two membrane-bound domains that form the permeation pathway for substrate transport and two nucleotide binding domains (NBDs) that hydrolyse ATP for energy (Sharom, 2008:105). The P-glycoprotein structure consists of two homologous and symmetrical halves (cassettes), as illustrated in Figure 2.4. These cassettes contain six transmembrane domains, with a putative alpha-helix structure, separated by extracellular hydrophilic loops (of which one is glycosylated) (Lin & Yamazakie, 2003:61; Rosenberg *et al.*, 1997:10685, 10693). Each of these cassettes is separated by an intracellular flexible linker polypeptide loop with an ATP-binding motif. The two cassettes interact cooperatively in order to form a single functional unit that plays a critical role in ATPase and transport activity. The flexible linker region ensures the proper interaction between the cassettes (Lin & Yamazakie, 2003:61).

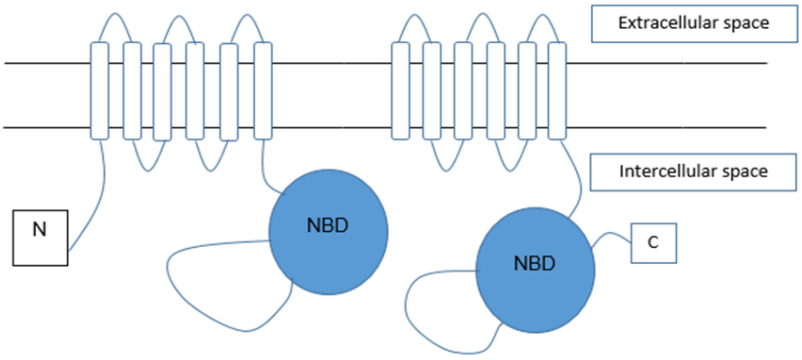

Figure 2.4: **Transmembrane arrangement of P-gp. This protein has 12 transmembrane regions and two nucleotide binding domains (NBDs). The "N" symbolizes the nitrogen-terminus and "C" symbolizes the carboxylic terminus of the amino acid chain. (Adapted from Chan *et al.*, 2004:28)**

The small intestinal enterocytes represent the first region where cytochrome P450 (CYP450)-mediated metabolism of orally administrated drugs occurs (Chan *et al.*, 2004:27). This metabolism modifies drugs into metabolites that can potentially be substrates for P-gp efflux, thus having a synergistic relationship by increasing efflux transport (Chan *et al.*, 2004:26). Table 2.1 lists some of the clinically relevant drugs and other compounds that are known to be substrates of the P-gp transporter.

Table 2.1: Examples of clinically relevant drugs known to be substrates of the P-gp transporter. (Adapted from Sharom, 2008:107)

Anti-cancer drugs	Vinca Alkaloids (vinblastine and vincristine)
	Anthracyclines (doxorubicin and daunorubicin)
	Taxanes (paclitaxel and docetaxel)
	Epipodophyllotoxins (etoposide and teniposide)
	Camptothecins (topotecan)
	Anthracenes (bisantrene and mitoxantrone)
HIV protease inhibitors	Ritonavir; saquinavir; nelfinavir
Analgesics	Morphine
Antihistamines	Terfenadine; fexofenadine
H2-receptor antagonists	Cimetidine
Immunosuppressive agents	Cyclosporine A; tacrolimus (FK506)
Anti-arrhythmics	Quinidine; amiodarone; propafenone
Anti-epileptic	Felbamate; topiramate
Fluorescent compounds	Calcein-AM; Hoechst 33342; Rhodamine 123
HMG-CoA reductase inhibitors	Lovastatin; simvastatin
Anti-emetics	Ondansetron
Tyrosine kinase inhibitors	Imatinib mesylate; gefitinib
Cardiac glycosides	Digoxin
Anti-helminthics	Ivermectin
Calcium-channel blockers	Verapamil (Known P-gp inhibitor)
	Nifedipine; aziodopine; diltiazem
Calmodulin antagonist	Trifluoperazine; chlorpromazine; trans-flupentixol
Anti-hypertensives	Reserpine; propranolol
Antibiotics	Erythromycin; gramicidin A
Steroids	Corticosterone; dexamethasone; aldosterone; cortisol
Pesticides	Methylparathion; endosulfan; cypermethrin; fenvalerate
Natural products	Curcuminoids; colchicine
Anti-alcoholism drug	Disulfiram

The P-gp protein is vulnerable to inhibition, activation and induction, which may alter the pharmacokinetics of co-administered drug substrates by increasing or decreasing drug transport from the intestinal lumen into the epithelial cells (Izzo, 2005:3). Inhibition of the P-gp protein can either be competitive or non-competitive. Competitive inhibition (e.g. verapamil) of the P-gp

transporter refers to competition between two drug substrates for the same drug-binding sites. In contrast, non-competitive inhibition ensues when the ATP hydrolysis process is inhibited by a drug substrate, thereby changing the conformation of the binding site (Marchetti *et al.*, 2007:930). Grapefruit juice is one of the best known inhibitors of P-gp related efflux. The bioavailability of cyclosporine A has been shown to dramatically increase with the co-administration of grapefruit juice (Colombo *et al.*, 2014:2).

Various transport models have been proposed, as illustrated in Figure 2.5, to clarify the mechanism upon which the P-gp protein transports drugs out of the epithelial cell. The first mechanistic model shows P-gp as an ion channel protein pump: the hydrophobic membrane-spanning regions and hydrophilic elements of the protein act as an aqueous transmembrane pore, through which drugs are extruded from the cytosol to the extracellular space (Lin & Yamazakie, 2003:61). The vacuum cleaner model suggests that an interaction between the protein and the substrate takes place before the molecule is extruded back into the extracellular space before they reach the cytoplasm (Lin & Yamazakie, 2003:62; Sharom, 2014:3). In the flippase model, an interaction occurs between the lipophilic drugs that partitioned in the lipid bilayer membrane. The P-gp protein intercepts the lipophilic drug molecule as they cross the lipid membrane and flips the molecule from the inner leaflet to the outer leaflet of the bilayer, therefore extruding the drug molecule back into the extracellular medium (Lin & Yamazakie, 2003:62).

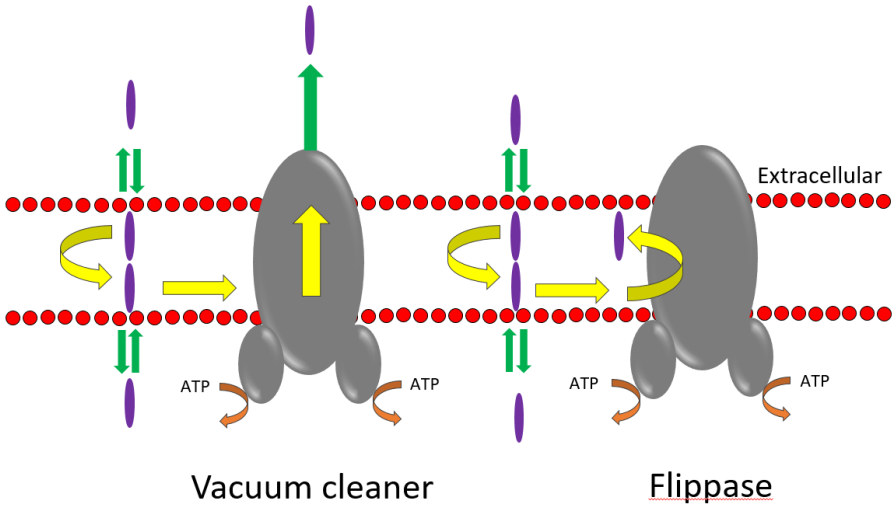

Figure 2.5: Illustration of the proposed P-gp mechanisms of action (adapted from Sharom, 2014:3)

2.4 Screening models to investigate absorptive and secretory drug transport

Drug metabolism and pharmacokinetic studies are crucial in drug discovery and development. Pharmacokinetic screening models can aid in the prediction of drug behaviour in patients. From this, decisions can be made whether a new candidate drug should continue with development trials or be completely removed from the development program (Zhang *et al.*, 2012:550). The models available for intestinal permeation studies can be divided into the following categories (Alqahtani *et al.*, 2013:1-14):

- *In vivo* models (e.g. whole living animals such as rats).
- *Ex vivo* models (Zhang *et al.*, 2012) (e.g., making liver into microsomes).
- *In situ* perfusion models (e.g. segments of intestine as part of living animals).
- *In vitro* models (e.g. cell lines derived from human colon carcinoma (Caco-2) and Mardin-Darby canine kidney (MDCK) cells).

Ethical considerations are important in pharmacokinetic research, especially when animals are involved. The "3R" concept (i.e. replace, refinement and reduce) should be implemented as a guideline to improve animal wellbeing in research. The term "replace" refers to the substitution of animals with a different model, such as *in vitro* techniques. "Refinement" refers to the alteration in procedures to improve animal welfare and reduce the pain and distress experienced by experimental animals. "Reduce" refers to using a minimum number of animals for experimental procedures and applying different strategies for data acquisition (Fenwick *et al.*, 2009:523-524).

2.4.1 *In vivo* models

Animal models are commonly used in pre-clinical studies to predict the extent of intestinal drug absorption and metabolism in humans. The absolute extent of in vivo absorption can be indicated by the comparison of AUC (area under the curve of plasma concentration vs. time curve) after a drug is administered via the intravenous, intraperitoneal and oral route. During *in vivo* pharmacokinetic studies after oral administration, blood samples are withdrawn at pre-determined time intervals and analysed to determine specific plasma concentrations at each of the particular time points. Animals that are primarily used for drug absorption and metabolism studies include rats, dogs, monkeys and pigs (Balimane *et al.*, 2000:309). The primary advantage of in vivo models is their intact organ systems (e.g. blood supply, nervous system), providing excellent predictions for the pharmacokinetics of drug compounds (Alqahtani *et al.*, 2013:5). Anatomical

and physiological differences between animals and humans do, however, harbour constraints for effective predictions. Differences such as transporter protein expression, differential distribution of enzymes, pH, transit time and gastrointestinal motility need to be considered when extrapolating data from animals to humans (Alqahtani *et al.*, 2013:5; Balimane *et al.*, 2000:309). Other than anatomical and physiological differences, another disadvantage of this model includes the requirement of large quantities of resources, time and labour. Therefore, this screening model is too complex for individual drug permeability studies and is not practical for high-throughput screening (Alqahtani *et al.*, 2013:6).

2.4.2 *Ex vivo* models

The process of *ex vivo* studies is based on the injection of animals with drugs, followed by the removal and processing (e.g., making liver into microsomes) of organ tissue afterwards, to investigate the changes in enzyme activity or drug permeability during treatment periods (Zhang *et al.*, 2012:554).

2.4.3 *In situ* perfusion models

The perfusion model mimics drug absorption, distribution, metabolism and excretion closely with that obtained *in vivo* (Zhang *et al.*, 2012:554). With this method, the small intestinal segments used for experimental purposes are still tethered to the test animal, although the animal is under sedation (Balimane *et al.*, 2000:308). This method has several advantages over *in vivo* models, as it can bypass the stomach so that acidic compounds do not precipitate and dissolution rates do not interfere with intestinal drug concentrations, and therefore also not with plasma levels. Information on the function of regional variances in coupled and separate contributions of intestinal drug permeability, drug metabolism, variability and dose-dependent pharmacokinetics, can be obtained from the *in situ* intestinal perfusion model. Furthermore, secretory transport after intravenous administration can also be studied with this model. The efflux of xenobiotics, into the intestinal lumen, by P-gp and multi-drug resistance-associated protein (MRP) can also be investigated (Le Ferrec *et al.*, 2001:653). Drug permeability is determined by calculating the difference in the concentration between the inlet and outlet flow (Alqahtani *et al.*, 2013:5). The *in situ* model's major advantages is that it functions under the same conditions as in vivo models with intact intestinal mucosa, blood supply, a nervous system and expression of membrane enzymes and transporters (Holmstock *et al.*, 2012:1474). Limitations of this model include the negative effect anaesthesia may have on drug absorption, which is not practical for high-throughput screening as the permeability of drugs is based on the disappearance of molecules

from the luminal side. Therefore, it can lead to overestimation of intestinal drug absorption (Alqahtani *et al.*, 2013:5).

2.4.4 *In vitro* models

Due to ethical considerations, animal testing are not appropriate for high-throughput screening. The Ussing chamber has different features that distinguish it from the *in vitro* Caco-2 cell culture model. The small intestinal epithelium provides an adequate paracellular permeability for drugs, it also contains transport proteins and metabolic enzymes, and a mucous layer is present (Luo *et al.*, 2013:209). This method measures apparent permeability across epithelial tissue, providing an indication of intestinal drug absorption, the drug's interaction with influx or efflux transporter proteins and drug metabolism (Algahtani *et al.*, 2013:3). This model consists of an excised intestinal segment from rat, rabbit, dog, monkey and, recently, human segments as well (Miyake *et al.*, 2017:374; Sjöberg *et al.*, 2013:167). The diffusion compartments are mainly filled with Krebs-Ringer bicarbonate buffer and supplied with nutrients such as glucose, pyruvate and glutamate with additional oxygenated air (95% O_2: 5% CO_2) to maintain tissue viability (Alqahtani *et al.*, 2013:3). In this model, the drug solution can be subjected to either the apical or the basolateral side of the enterocytes, making it an attractive *in vitro* model system to study drug absorption or efflux (Le Ferrec *et al.*, 2001:654). The benefit of using this technique is that studies can be done on different regions of the gastrointestinal tract to investigate the difference in absorption and metabolism of drugs as they move along the gastrointestinal tract (Balimane *et al.*, 2000:305; Sjöberg *et al.*, 2013:167).

Another well-known *in vitro* model is the everted intestinal sac, which is mainly used to study the extent of transfer and metabolism of drug molecules (Luo *et al.*, 2013:210). An everted sac is obtained from freshly isolated animal intestine and is divided into segments of approximately 5-6 cm. The sacs are washed with an ice-cold physiological solution (oxygenated Krebs solution) and then everted on a glass rod filled with oxygenated medium. Each everted sac is submerged in a beaker that contains the drug solution (Alam *et al.*, 2012:327; Dixit *et al.*, 2012:14). This model can be used to investigate drug absorption, drug metabolism or pro-drug conversion in the GIT, multi-drug resistance, and efflux transport, and to evaluate the role of P-gp in drug absorption (Alam *et al.*, 2012:327). In a study by Alam *et al.* (2012), this model was applied by everting a rat's intestinal sac to study the P-gp-mediated efflux of [^{3}H] vinblastine, [^{14}C] doxorubicin and verapamil, as reference compounds. They proposed that this particular everted intestinal sac model could be a useful screening tool to investigate the mechanisms and kinetics of drug transport (i.e. P-gp) (Alam *et al.*, 2012:327; Barthe *et al.*, 1998:322). Limiting parameters such

as a lack of active blood and nerve supply can decrease tissue viability in everted intestine sacs. The presence of muscularis mucosa is another potential disadvantage of this model, as the mucosa is not removed and can induce an underestimation of the permeability of a compound with a tendency to bind with muscle cells. Morphological damage can occur when everting the intestinal tissue and structural integrity diminish over time (Alam *et al.*, 2012:327; Dixit *et al.*, 2011:13; Luo *et al.*, 2013:211).

The utilisation of *in vitro* cell cultures is a suitable alternative to study drug pharmacokinetics. Mammalian cell cultures have been developed to imitate the human intestinal epithelium, in order to study drug absorption by the intestine (Van Breemen & Li, 2005:179). The Caco-2 cell line, derived from human colorectal adenocarcinoma, is used as a permeability-screening assay for the prediction of drug permeability and fraction of oral dose absorbed in human intestines (Shah *et al.*, 2006:186). Caco-2 cell cultures express the majority of the morphological and functional similarities of the human small intestinal epithelia, regardless of its colonic origin (Le Ferrec *et al.*, 2001:655). During culturing, the Caco-2 cells undergo spontaneous enterocytic differentiation presenting them with microvilli, tight junctions between adjacent cells and increased brush border hydrolytic enzymes (Küblbeck *et al.*, 2016:941). Figure 2.6A illustrates the different transporter proteins and metabolizing enzymes expressed by Caco-2 cell monolayers.

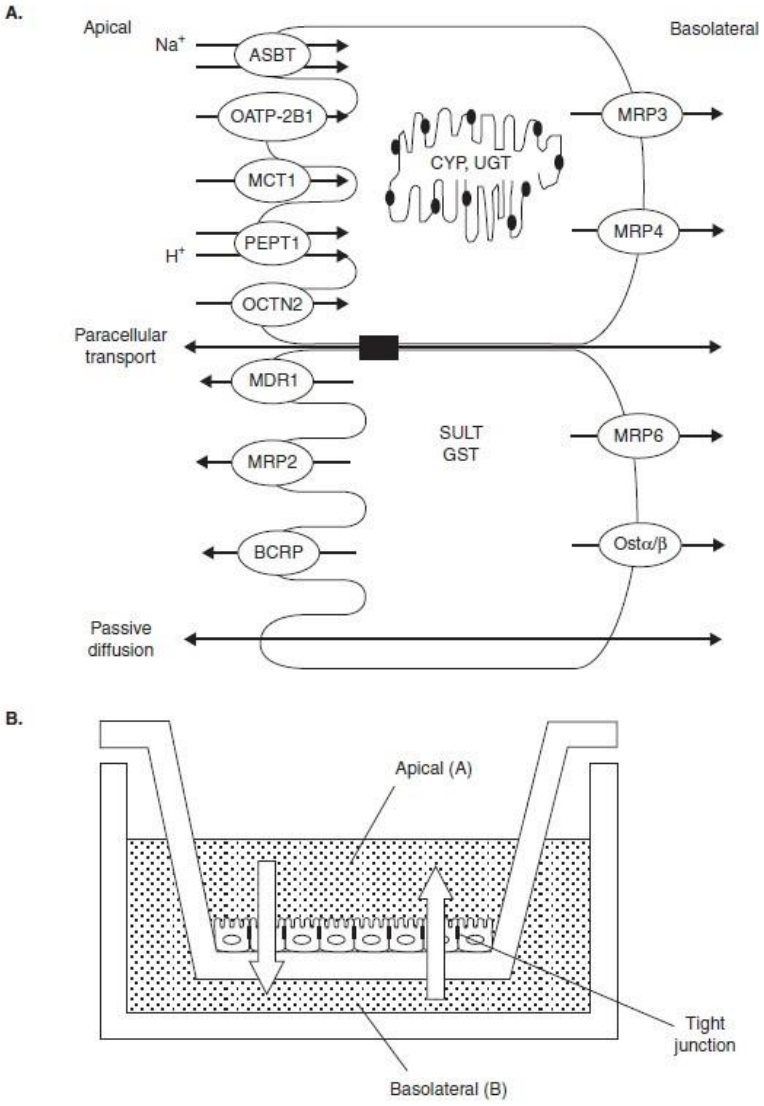

Figure 2.6: **A: The drug transporter proteins and metabolizing enzymes present in Caco-2 cell monolayers. B: Schematic illustration of the bi-directional transwell plate transport system of a Caco-2 cell monolayer (Sun *et al.*, 2008:396)**

Caco-2 cells express important uptake and efflux transporters for predicting drug permeability, such as the P-gp efflux transporter (Küblbeck *et al.*, 2016:941; Shah *et al.*, 2006:186). The preferred method for identifying P-gp substrates or inhibitors is the study of bi-directional transport of drugs across a polarised Caco-2 cell monolayer (Figure 2.6B). The difference in drug transport between the apical (intestinal lumen) and basolateral (blood) compartments can provide an indication of drug absorption or efflux. If the permeation is higher from the apical to basolateral

chambers, the drug is highly permeable. However, when the basolateral to apical transport is higher, the drug is likely to be a P-gp substrate susceptible to efflux (Wessler *et al.*, 2013:2501). Caco-2 cell monolayers are useful to study the mechanism of drug-drug interactions and to identify drug transporter affinities. Through this model, the susceptibility of a drug to potential drug resistance can be determined (Sun *et al.*, 2008:405-406). For this reason, the permeability of the three anti-malarial drugs described in Sections 2.1.5.1 to 2.1.5.3 will be investigated using Caco-2 cell monolayers in this study.

2.5 Summary

Malaria remains a health-intimidating disease worldwide, especially with continuous reports of drug resistance occurring. Drug resistant infections have recently been reported for the artemisinin derivatives, causing mono-therapeutic treatments to be restricted to uncomplicated malaria infections only. Therefore, several novel artemisinin derivatives have been synthesised and pharmacokinetic investigations are required to test their absorptive transport across intestinal epithelia.

Drugs can either be passively transported through the tight junctions between adjacent epithelial cells or actively transported via carrier proteins present in the cell membranes. If a transporter protein actively effluxes a drug out of the epithelial cell, the required drug plasma concentration for pharmacological activity may not be reached. The P-gp transporter is an example of such an efflux active transporter protein. Malaria parasites over-expressing efflux transporters may develop drug resistance. Hence, it is necessary to investigate the susceptibility of the novel artemisinin derivatives towards efflux as a possible measure of drug resistance development in the future. The *in vitro* Caco-2 cell culture model is one of the most appropriate models for investigation of drug transport in the absorptive and secretory direction.

CHAPTER 3: VALIDATION OF THE HIGH PERFORMANCE LIQUID CHROMATOGRAPHY (HPLC) ANALYTICAL METHODS USED FOR DRUG QUANTIFICATION

3.1 Introduction

In this study, the bi-directional permeability of the artemisinin derivatives, artemiside, artemisone and artemether were tested across Caco-2 cell monolayer alone and in the presence of the P-gp inhibitor, verapamil. Caffeine was included as a highly permeable reference compound, whereas atenolol was applied as a reference compound with low permeability. Lucifer yellow was used as an integrity marker to confirm the cell monolayer integrity, while the known P-gp substrate, vinblastine, was used to confirm the appropriateness of the cell-based model to study efflux transport. All the samples from the permeability studies were analysed by means of high performance liquid chromatography (HPLC) to determine the concentration of the permeant. The HPLC methods for each of the selected compounds were validated to ensure the data obtained are reliable and valid.

3.2 High-Performance Liquid Chromatography method validation of selected compounds for the *in vitro* transport studies

High-performance liquid chromatography (HPLC) is a distinctive form of column chromatography that pumps a solution in a constituted liquid phase (mobile phase) at high pressure through a column (stationary phase), which consists of solid adsorbent material (Thammana, 2016:22; Dong, 2006:2). The HPLC technique is commonly used as a means to separate, identify and also quantify the active components in a sample (Malviya *et al.*, 2010:22; Thammana, 2016:22). Pharmaceutical industries predominantly use HPLC for evaluating a large diversity of samples with the following purposes: to determine the purity of chemical entities, to detect impurities during drug development, for quality control and lastly, it is a useful method during dissolution studies (Ahuja, 2007:1, 2; Thammana, 2016:25).

In normal-phase chromatography, the stationary phase is polar whereas, the mobile phase is relatively non-polar. During normal-phase chromatography, the non-polar molecules will be

eluted first through the stationary phase, and the polar molecules will be eluted last. In other words, the polar molecules will move slower through the stationary phase (column) than the non-polar analytes. Reverse-phase chromatography, on the other hand, is the exact opposite of normal-phase chromatography, where the stationary phase is non-polar and the mobile phase is polar. This specific phase allows the polar molecules to be eluted first, followed by the non-polar molecules at the end (Wilson & Walker, 2000:650,651). Therefore, the non-polar molecules will move at a slower rate through the column than the polar analytes due to the strong interaction with the hydrophobic (C_{18}) molecules that reside within the column (Dong, 2006:7). Solvents that are typically used for reverse-phase chromatography include acetonitrile, methanol or tetrahydrofuran, seeing as they are miscible with water. The best option for a mobile phase in method development is a mixture of acetonitrile and water (Singh, 2013:28).

3.2.1 Analytical method validation

The term “method validation” is defined as the process used to confirm that a developed analytical method is adequate for its predetermined use (Singh, 2013:26). It is a regulatory requirement during an analytical process. Method validation is an ongoing process, and the fulfilment of a verified analytical method is to establish if future measurements and use of the method will provide a value that is as close as possible to the unknown true value of an analyte in a sample (Kumar *et al.*, 2012:4). The method can be validated for the use on a single instrument, by different instruments in the same laboratory or even in different laboratories (Singh, 2013:28, 29). The necessary validation parameters that should be addressed include accuracy, precision, specificity, detection limit, quantification limit, linearity and ruggedness/robustness (Shabir, 2004:29; Singh, 2013:29).

For this study, the purpose of the validation process is to confirm that the analytical method used to determine the amount of the selected compounds in the samples, is both reliable and suitable for the assay of the compounds in the transport samples. A complete validation for all of the artemisinin-based derivatives and vinblastine was required, whereas previously validated HPLC methods for caffeine and atenolol were used. Therefore, only the linearity as well as the limit of detection and limit of quantification were determined for the latter compounds. The fluorometric method for Lucifer yellow quantification was also validated.

The methods described in this section were developed under the supervision of Professor Jan L. du Preez in the Analytical Technology Laboratory (ATL) at the North-West University, Potchefstroom, South Africa.

3.2.2 Chromatographic conditions

The HPLC instrument and the parameters used for the different compounds analysed in this study are summarised in Table 3.1.

Table 3.1: Chromatographic conditions used for compound analysis with HPLC

Analytical instrument	HP1100 and HP1200 series HPLC equipped with a pump, autosampler, UV detector and Chemstation Rev.A.08.03 Agilent® Technologies data acquisition and analysis software (Hewlet-Packard, Palo Alto, California, USA)
Column	Venusil XBP C_{18}(2) column, 150 x 4.6 mm, 5 µm, 100 Å (Agela technologies, Newark, DE)
Mobile phase for each compound	
Caffeine	Acetonitrile/water (15:85) with 0.1% acetic acid; isocratic elution mode; (HP1100 series).
Atenolol	Acetonitrile/water (20:80) with 0.005 M Sodium 1-octanesulfonate adjusted to pH 3.5 with orthophosphoric acid (H_3PO_4); isocratic elution mode; (HP1100 series).
Artemiside	Acetonitrile/water (75:25) with 0.1% orthophosphoric acid (H_3PO_4); isocratic elution mode; (HP1100 series).
Artemisone	Acetonitrile/water (70:30) with 0.1% orthophosphoric acid (H_3PO_4); isocratic elution mode; (HP1100 series).
Artemether	Acetonitrile/water solvent (70:30); isocratic elution mode; (HP1100 series).
Vinblastine	Acetonitrile (75) and water (25) with 0.005 M Na_2HPO_4 adjusted to pH 6; isocratic elution mode; (HP1100 series).
Injection volume	50 µl
Flow rate	1.0 ml/min
Detection and retention time	
Caffeine	UV detector set at 275 nm; retention time was ± 5.8 min.
Atenolol	UV detector set at 225 nm; retention time was ± 6.4 min.
Artemiside	UV detector set at 205 nm; retention time was ± 7 min.
Artemisone	UV detector set at 200 nm; retention time was ± 6.8 min.
Artemether	UV detector set at 216 nm; retention time was ± 11.8 min.
Vinblastine	UV detector set at 220 nm; retention time was ± 4.0 min.

3.3 Validation parameters

3.3.1 Linearity

Linearity of an analytical method refers to its ability to produce a response (i.e. measurement values) that is directly proportional to the analyte concentrations within a given range (Kumar *et al.*, 2012:7). The correlation coefficient of the standard/regression line of the response plotted as a function of the concentration indicates the acceptability of linearity. A correlation coefficient (R2) > 0.998 is considered acceptable (Singh, 2013:29).

A stock solution of each compound was prepared by weighing the compound and diluting it, by a factor of 10, into three different concentrations. Each sample was injected into the column of the HPLC instrument at different volumes (representing a series of different concentrations). The standard/regression curve was constructed and analysed with the Analysis Toolpak in Excel™.

3.3.2 Accuracy

Accuracy is defined as the closeness of the obtained test results, by the analytical method, to the true value (Shabir, 2003:61). Accuracy is represented by an inverse relation to both systematic and random errors, where a higher accuracy means a lower error (Singh, 2013:29). The guideline to measure accuracy, stipulated by the International Council on Harmonisation (ICH), is to collect data from a minimum of nine determinations over a minimum of three concentration levels covering a specified range (Shabir, 2004:32). The assay method criterion for accuracy is 100 ± 2% recovery at each concentration over the range of 80 – 120% of target the concentration (Shabir, 2004:32).

3.3.3 Precision

Precision is the degree of agreement between repeatability of an analytical method of a homogenous sample, conducted under normal operation conditions. In most cases, precision is conveyed as the percentage relative standard deviation (%RSD) for the response of a number of samples. It may be considered at three different levels namely repeatability, reproducibility and intermediate precision (Shabir, 2003:61).

Repeatability is determined as intra-day precision, where a method operates under the same conditions over a short period of time (Shabir, 2004:33). It should be determined from a minimum of six determinations at 100% of the target concentration (Shabir 2003:62). The acceptable criterion for repeatability is that the %RSD should be ≤ 2% (Shabir 2003:62).

Reproducibility is determined when homogenous samples are tested in numerous laboratories and it is often part of the inter-laboratory crossover studies (Shabir, 2004:34). The acceptable criterion for reproducibility is that the mean results between the various laboratories will be within 2% of the value by the primary testing laboratory (Shabir, 2004:34).

Intermediate precision (inter-day precision) is the results obtained when various laboratory conditions differ. Parameters such as experimental days, equipment and analysts can vary. The inter-day precision should have a %RSD of ≤ 5% (Shabir, 2003:34).

3.3.4 Ruggedness and robustness

The ruggedness of an analytical procedure can be defined as a molecule's capacity to remain unaffected by small, but deliberate, variations in the parameters of the method. This provides an indication of the reliability during normal usage (Vander Heyden *et al.*, 2001:724). Robustness, on the other hand, can be described as the ability to repeat an analytical method in different laboratories without a difference in the results (Vander Heyden *et al.*, 2001:724, 725). An acceptable criterion for sample degradation is ≤ 2%.

3.3.5 Limit of detection and quantification

The limit of detection (LOD) and limit of quantification (LOQ) should be determined when a method is performed on samples containing a very low concentration of the analyte. The LOD is defined as the lowest quantity of the analyte that can be detected above the baseline noise and in this case, three times the noise level (Shabir, 2004:34). The LOQ can be defined as the lowest concentration of the analyte which can be reproducibly quantitated above the baseline noise, in order to give a signal to noise value of 10 (Shabir, 2004:36).

The LOD and LOQ can be expressed as follow:

$$LOD = \frac{3.3\sigma}{S}$$

$$LOQ = \frac{10\sigma}{S}$$

where σ is the standard deviation of the response, and S is the slope of the calibration curve (Kumar *et al.*, 2012:7). The values of each analyte is summarised in Table 3.22.

3.3.6 Specificity

Specificity in HPLC validation refers to the ability of the method to unambiguously measure an analyte in the presence of endogenous components (Bressolle *et al.*, 1996:4).

3.4 Sample preparation for each compound during validation

All the compounds listed in Table 3.1 were analysed by means of a HPLC instrument, except for Lucifer yellow. The integrity marker, Lucifer yellow, was quantified by using a SpectraMax® Paradigm® Multi-Mode Detection Platform Microplate reader (Molecular Devices, LLC, Sunnyvale, California, U.S.A). The method for Lucifer yellow quantification was also validated accordingly, with the fluorescence measured at wavelengths of 485 nm (excitation) and 535 nm (emission) (Wahlang *et al.*, 2011).

3.4.1 Linearity

A stock solution of caffeine (206.8 µg/ml) was prepared and after dilution with Dulbecco's Modified Eagle's medium (DMEM), a concentration of 20.68 µg/ml and 2.68 µg/ml were obtained. The various concentrations were placed into 3 different HPLC vials and injected into the HPLC instrument at the following volumes: 2.5 µl, 5 µl, 10 µl, 20 µl, 30 µl, 40 µl, 50 µl. The injection of each volume was duplicated (n = 2). The concentrations of caffeine ranged between 0.1034 and 206.8 µg/ml.

A stock solution of atenolol (202.1 µg/ml) was prepared with DMEM and diluted to 20.21 µg/ml and 2.021 µg/ml. Therefore, the concentrations used for atenolol were between 0.11105 and 202.1 µg/ml (n = 2), after being injected at 2.5 µl, 5 µl, 10 µl, 20 µl, 30 µl, 40 µl, 50 µl. The injection of each volume was duplicated (n = 2).

A stock solution of artemiside (26.8 µg/ml) was prepared and diluted to 2.68 µg/ml and 0.268 µg/ml, with DMEM. By injecting the three concentrations at 1 µl, 2.5 µl, 5 µl, 10 µl, 20 µl, 30 µl, 40 µl, 50 µl volumes, the concentration ranged between 0.0536 and 26.8 µg/ml as results of 2.68 µg/ml and 26.8 µg/ml concentrations were used. The injection of each volume was duplicated (n = 2).

A stock solution of artemisone (54.4 µg/ml) was prepared and after dilution with DMEM, concentrations of 5.44 µg/ml and 0.544 µg/ml were obtained and placed into 3 separate HPLC vials. The different concentrations were injected at the following volumes: 1 µl, 2.5 µl, 5 µl, 10 µl,

20 µl, 30 µl, 40 µl, 50 µl. The concentration range of artemisone was between 0.1088 and 54.4 µg/ml. The injection of each volume was duplicated (n = 2).

A stock solution of artemether (100.0 µg/ml) was prepared and diluted to 10.0 µg/ml and 1.0 µg/ml with DMEM. After injecting the three concentrations at 10 µl, 20 µl, 30 µl, 40 µl, 50 µl, the concentrations used for artemether ranged between 0.40 and 100.0 µg/ml. The injection of each volume was duplicated (n = 2).

A stock solution of vinblastine (56.0 µg/ml) was prepared with DMEM and diluted to 5.60 µg/ml and 0.56 µg/ml. The various concentrations were placed into 3 different HPLC vials and injected into the HPLC instrument at the following volumes: 1 µl, 2 µl, 5 µl, 10 µl, 20 µl, 30 µl, 40 µl, 50 µl. The concentrations of vinblastine ranged between 0.0112 and 56.00 µg/ml. The injection of each volume was duplicated (n = 2).

A stock solution of Lucifer yellow at a concentration of 200 µg/ml was prepared and used to make a 1:2 serial dilution with the following concentrations: 100 µg/ml, 50 µg/ml, 25 µg/ml, 12.5 µg/ml, 6.25 µg/ml, 3.125 µg/ml and 1.563 µg/ml. DMEM without additives was used as the dilution agent. The solution was then measured on the SpectraMax® plate reader.

3.4.2 Accuracy

Three stock solutions of artemiside was prepared: 42.8 µg/ml, 41.2 µg/ml and 43.4 µg/ml. Each stock solution was diluted with DMEM by a factor of 2, and the second sample of each concentration was also diluted for a third time by a factor of 2. A total of 9 determinations were injected twice into the HPLC instrument to get a mean value to determine the percentage recovery.

Three stock solutions of artemisone was prepared with the following concentration: 41.4 µg/ml, 43.3 µg/ml and 41.8 µg/ml. Each stock solution was diluted with DMEM by a factor of 2, and the second sample of each concentration was also diluted for a third time by a factor of 2. A total of 9 determinations were injected twice into the HPLC instrument to get a mean value to determine the percentage recovery.

Three stock solutions of artemether was prepared: 42.8 µg/ml, 41.2 µg/ml and 43.4 µg/ml. Each stock solution was diluted with DMEM by a factor of 2, and the second sample of each concentration was also diluted for a third time by a factor of 2. A total of 9 determinations were injected twice into the HPLC instrument to get a mean value to determine the percentage recovery.

Three stock solution of vinblastine was prepared with the following concentrations: 46.0 µg/ml, 47.0 µg/ml and 48.0 µg/ml. Each stock solution was diluted with DMEM by a factor of 2, and the second sample of each concentration was also diluted for a third time also by a factor of 2. A total of 9 determinations were injected twice into the HPLC instrument to get a mean value to determine the percentage recovery.

Three different concentrations of Lucifer yellow was prepared to cover a specified concentration range and three replicates of each were made to form a total of nine determinations. The Lucifer yellow concentrations used to determine the accuracy consisted of 200 µM, 100 µM and 25 µM that were measured on the SpectraMax® plate reader.

3.4.3 Precision

3.4.3.1 Intra-day precision

A single solution of artemiside, artemisone, artemether and vinblastine were prepared and then injected 8 times into the HPLC instrument to record the peak area and retention time of each injection.

Lucifer yellow solution covering a specified concentration range were prepared at the following concentration of 200 µg/ml, 100 µg/ml and 3.125 µg/ml. The solutions was measured on the SpectraMax® plate reader at three different time points (i.e. 08:00, 12:00 and 16:00) during the same day.

3.4.3.2 Inter-day precision

Three solutions of artemiside, artemisone, artemether and vinblastine were prepared and diluted with DMEM by a factor of 2. A total of 3 determinations were injected twice into the HPLC instrument to determine the percentage relative standard deviation. This measurement was repeated on three consecutive days.

Lucifer yellow solutions were prepared in three consecutive days with the same concentration range of 200 µg/ml, 100 µg/ml and 3.125 µg/ml. The samples were measured on the SpectraMax® plate reader at the same time of each day.

3.4.4 Ruggedness and robustness

A single solution of artemiside, artemisone, artemether and vinblastine were prepared and injected 25 times into the HPLC instrument with a run time of 60 min each. The flow rate was reduced every second injection from 1 ml/min to 0.1 ml/min in order to determine degradation over time.

A single solution of Lucifer yellow was prepared and the solution was measured on the SpectraMax® plate reader over a 5 hour period.

3.4.5 Limit of detection and quantification

A solution of 34 µg/ml caffeine was prepared and diluted to a final concentration of 0.34 µg/ml. Subsequently, a series of injections was made into the HPLC instrument at the following volumes: 1 µl, 2 µl, 5 µl, 10 µl, 25 µl, 30 µl, 40 µl and 50 µl. Each volume was injected 7 times.

A solution of 32.65 µg/ml atenolol was prepared and diluted to a final concentration of 0.3265 µg/ml. A series of injections was made into the HPLC instrument at the following volumes: 1 µl, 2 µl, 5 µl, 10 µl, 25 µl, 30 µl, 40 µl and 50 µl and each volume was injected 7 times.

A solution of 40 µg/ml artemiside was prepared and diluted to the following concentrations: 0.4 µg/ml, 0.2 µg/ml and 0.1 µg/ml, respectively. A series of injections was made into the HPLC instrument at the following volumes: 1 µl, 2 µl, 5 µl, 10 µl, 25 µl, 30 µl, 40 µl and 50 µl. Each volume was injected 7 times.

A solution of artemisone (42.6 µg/ml) was prepared and diluted to a final concentration of 0.426 µg/ml and 0.213 µg/ml. Subsequently, a series of injections was made into the HPLC instrument at the following volumes: 1 µl, 2 µl, 5 µl, 10 µl, 25 µl, 30 µl, 40 µl and 50 µl. Each volume was injected 7 times.

A solution of artemether (86.8 µg/ml) was prepared and diluted to a final concentration of 0.868 µg/ml and 0.434 µg/ml, respectively. Thereafter, a series of injections was made into the HPLC instrument at the following volumes: 1 µl, 2 µl, 5 µl, 10 µl, 25 µl, 30 µl, 40 µl and 50 µl. Each volume was injected 7 times.

Two separate solutions of vinblastine (19 µg/ml and 38 µg/ml, respectively) were prepared and diluted into the following concentrations: 0.95 µg/ml, 1.9 µg/ml and 7.6 µg/ml, respectively.

Subsequently, a series of injections was made into the HPLC instrument at the following volumes: 1 µl, 2 µl, 5 µl, 10 µl, 25 µl, 30 µl, 40 µl and 50 µl. Each volume was injected 7 times.

In addition to Lucifer yellow, a blank solution of DMEM were measured 9 times on the SpectraMax® plate reader and the slope of the linear regression curve was used to determine the limit of detection and quantification.

3.5 Validation results

3.5.1 Caffeine

3.5.1.1 Linearity

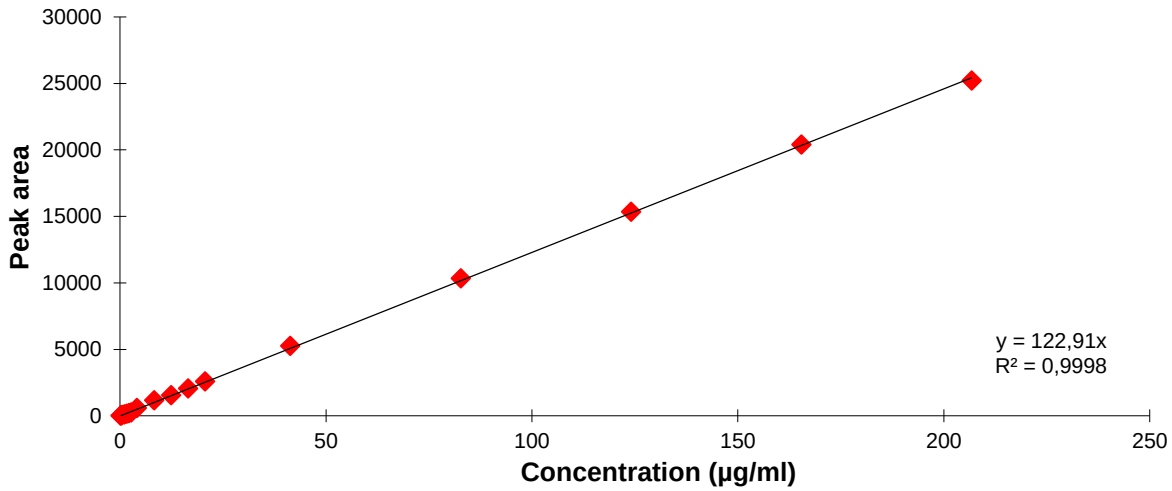

Figure 3.1: The linear regression graph for caffeine, where the mean peak area is plotted as a function of concentration

From the standard curve plotted in Figure 3.1, an R2 value of 0.9998 was obtained. Therefore, it can be concluded that the caffeine HPLC analytical method has met the criteria for linearity.

3.5.1.2 Limit of detection and quantification

The LOD and LOQ values obtained for caffeine are shown in Table 3.2.

Table 3.2: Limit of detection and quantification of caffeine

Analyte	Limit of detection	Limit of quantification
Caffeine	0.0197 µg/ml	0.0597 µg/ml

3.5.1.3 Specificity

The chromatogram for caffeine in the presence of DMEM is shown in Figure 3.2.

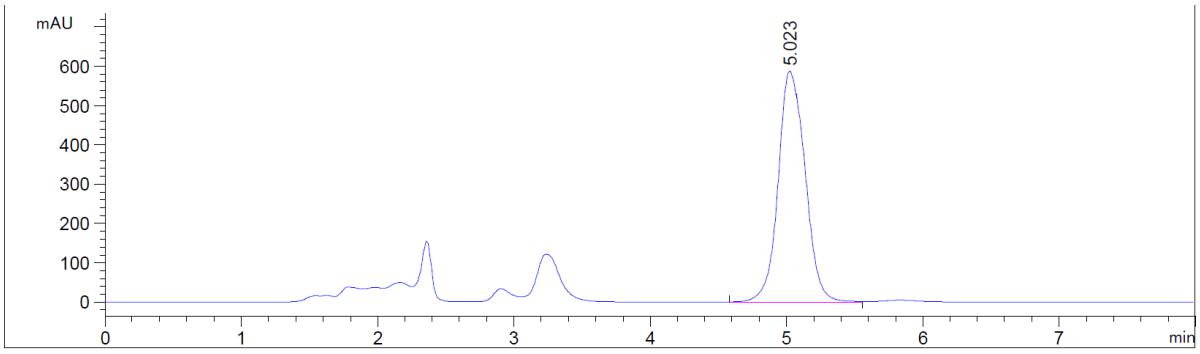

Figure 3.2: Chromatogram for caffeine at wavelength 275 nm

The caffeine peak appeared at 5.023 min on the HPLC chromatogram (Figure 3.2) and was clearly separated from all other compounds. This chromatogram therefore indicated no interference by any other compound, as observed with the HPLC analytical method used to quantify caffeine.

3.5.2 Atenolol

3.5.2.1 Linearity

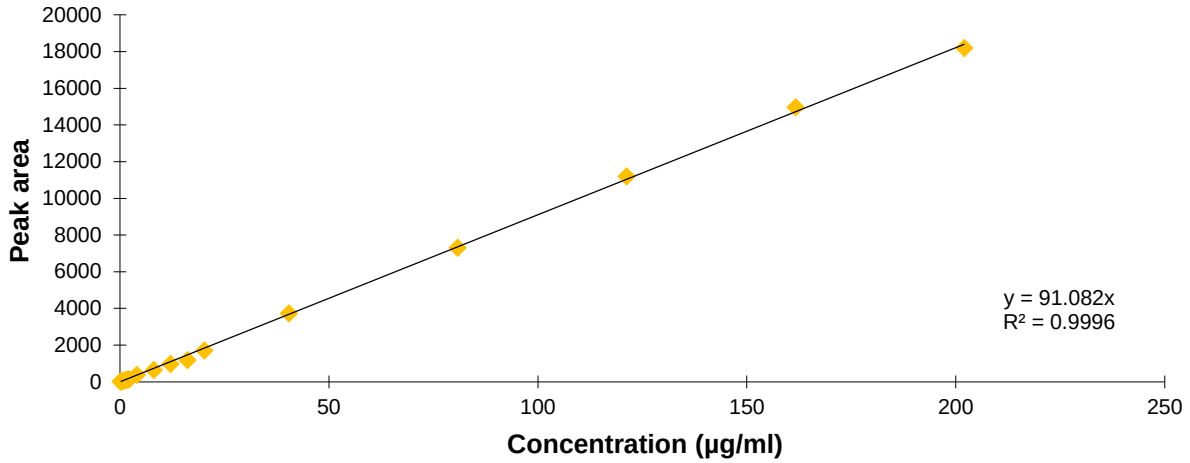

Figure 3.3: The linear regression graph for atenolol, where the mean peak area is plotted as a function of concentration

An R2 value of 0.9996 was obtained for atenolol, as portrayed in Figure 3.3, which indicates compliance of the method for atenolol quantification with the criteria for linearity.

3.5.2.2 Limit of detection and quantification

The LOD and LOQ values obtained for atenolol are shown in Table 3.3.

Table 3.3: Limit of detection and quantification of atenolol

Analyte	Limit of detection	Limit of quantification
Atenolol	0.5435 µg/ml	1.6471 µg/ml

3.5.2.3 Specificity

The chromatogram for atenolol in the presence of DMEM is shown in Figure 3.4.

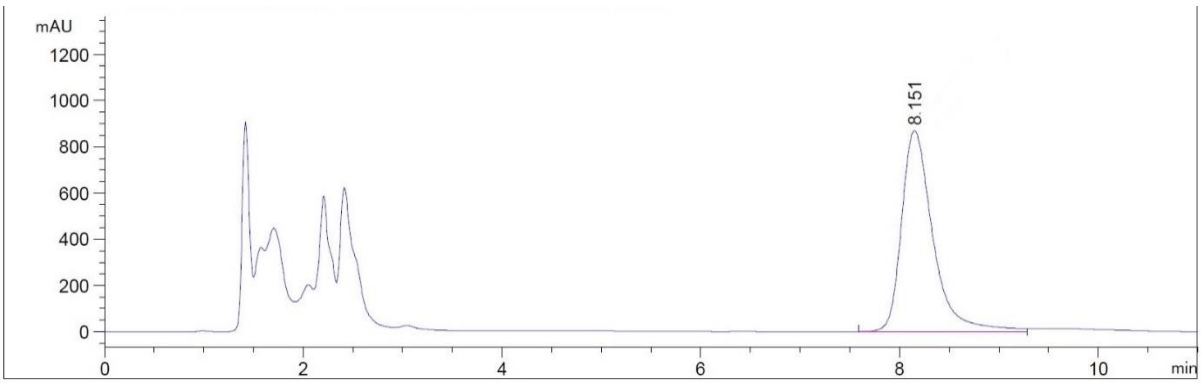

Figure 3.4: Chromatogram for atenolol at wavelength 225 nm

The atenolol peak appeared at 8.151 min on the HPLC chromatogram (Figure 3.4), and was distinctly separated from any other compounds detected. This chromatogram therefore indicates lack of interference by any other compound, as observed with the HPLC analytical method used to quantify atenolol.

3.5.3 Artemiside

3.5.3.1 Linearity

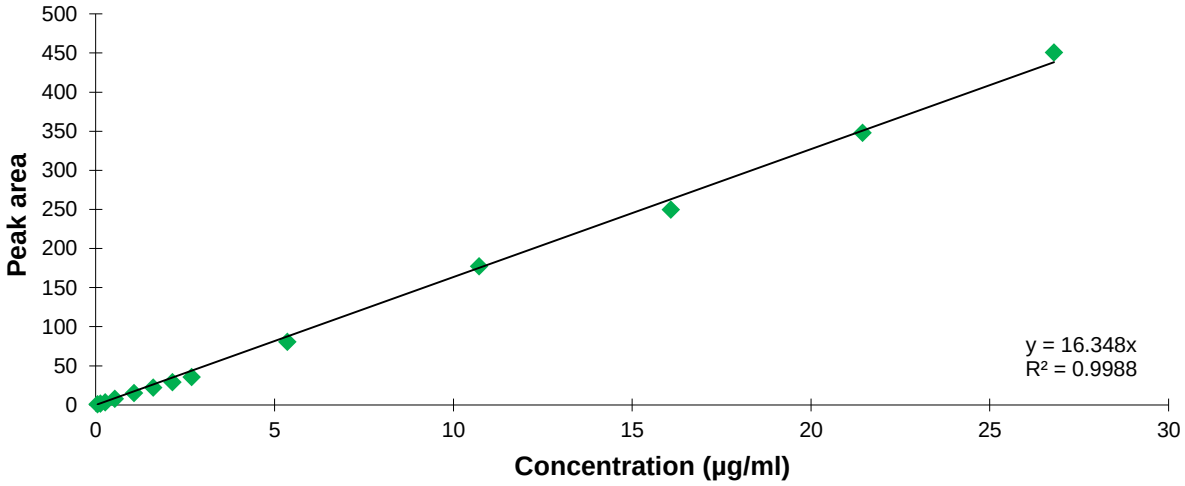

Figure 3.5: The linear regression graph for artemiside, where the mean peak area is plotted as a function of concentration

An R2 value of 0.9988 was obtained for artemiside, as shown in Figure 3.5, which shows that the method for artemiside quantification is in accordance with the linearity criteria.

3.5.3.2 Accuracy

Table 3.4 displays the percentage (%) recovery, standard deviation (SD) and the % relative standard deviation (%RSD) obtained for artemiside from the solutions with different concentrations. The results confirmed that the analytical method yielded an acceptable mean recovery of 102.30%.

Table 3.4: The accuracy results for artemiside solutions

Concentration spiked (µg/ml)	Peak area 1	Peak area 2	Mean peak area	Recovery (µg/ml)	Recovery (%)
10.70	181.39	180.69	181.04	10.12	94.59
10.30	184.62	180.28	182.45	10.20	99.03
10.85	202.78	201.31	202.04	11.30	104.11
21.40	371.09	370.92	371.00	20.74	96.92
20.60	380.83	377.83	379.33	21.21	102.95
21.70	414.88	414.35	414.62	23.18	106.82
42.80	767.32	771.82	769.57	43.02	100.52
41.20	778.31	780.55	779.43	43.57	105.76
43.40	854.14	853.95	854.04	47.75	110.01
				Mean	**102.30**
				SD	**4.688**
				%RSD	**4.583**

3.5.3.3 Precision

3.5.3.3.1 Intra-day Precision

The results illustrated in Table 3.5, clearly show that the %RSD for repeated injections of a single artemiside solution is in accordance with the specified guidelines (Shabir, 2003:62). The %RSD values for both the peak area (0.865%) and the retention time (0.086%) are less than 2%. Therefore, this method has acceptable repeatability.

Table 3.5: Intra-day precision results for artemiside

Injection number	Peak area	Retention time (min)
1	368.70	7.066
2	372.00	7.069
3	371.80	7.079
4	377.00	7.076
5	376.50	7.081
6	373.90	7.085
7	377.10	7.081
8	378.90	7.080
Mean	**374.49**	**7.077**
SD	**3.239**	**0.006**
%RSD	**0.865**	**0.086**

3.5.3.3.2 Inter-day Precision

An acceptable inter-day precision for artemiside was obtained with a %RSD value of 3.358%, as summarised in Table 3.6.

Table 3.6: Inter-day precision results for artemiside on three consecutive days

Days	% Recovery			Mean	SD	%RSD
Day 1	96.92	102.95	106.85	102.23	4.072	3.983
Day 2	106.91	106.00	109.65	107.52	1.552	1.443
Day 3	101.82	100.27	95.35	99.15	2.757	2.781
		Between days		**10297**	**3.457**	**3.358**

3.5.3.4 Ruggedness and robustness

According to the results in Table 3.7, artemiside is stable up to 9 hours.

Table 3.7: The stability of artemiside in solution over a time period of 24 hours

Time (h)	Peak Area	%Remaining
0	377.50	100.00
1	378.60	100.29
2	377.20	99.92
3	375.20	99.39
4	369.70	97.93
5	374.90	99.31
6	374.30	99.15
7	374.70	99.26
8	366.30	97.03
9	373.10	98.83
10	361.90	95.87
11	361.70	95.81
12	359.40	95.21
13	356.40	94.41
14	354.30	93.85
15	353.80	93.72
16	352.60	93.40
17	341.20	90.38
18	340.40	90.17
19	349.80	92.66
20	336.30	89.09
21	337.70	89.46
22	345.30	91.47
23	344.40	91.23
24	343.40	90.97
Mean	**359.20**	**95.15**
SD	**13.989**	**3.706**
%RSD	**3.894**	**3.894**

3.5.3.5 Limit of detection and quantification

The LOD and LOQ values obtained for artemiside are shown in Table 3.8.

Table 3.8: Limit of detection and quantification of artemiside

Analyte	Limit of detection	Limit of quantification
Artemiside	0.0088 µg/ml	0.0265 µg/ml

3.5.3.6 Specificity

The chromatograms for artemiside in the presence of verapamil and piperine is shown in Figure 3.6 and Figure 3.7, respectively. DMEM and methanol were the solvents in which the compounds were dissolved.

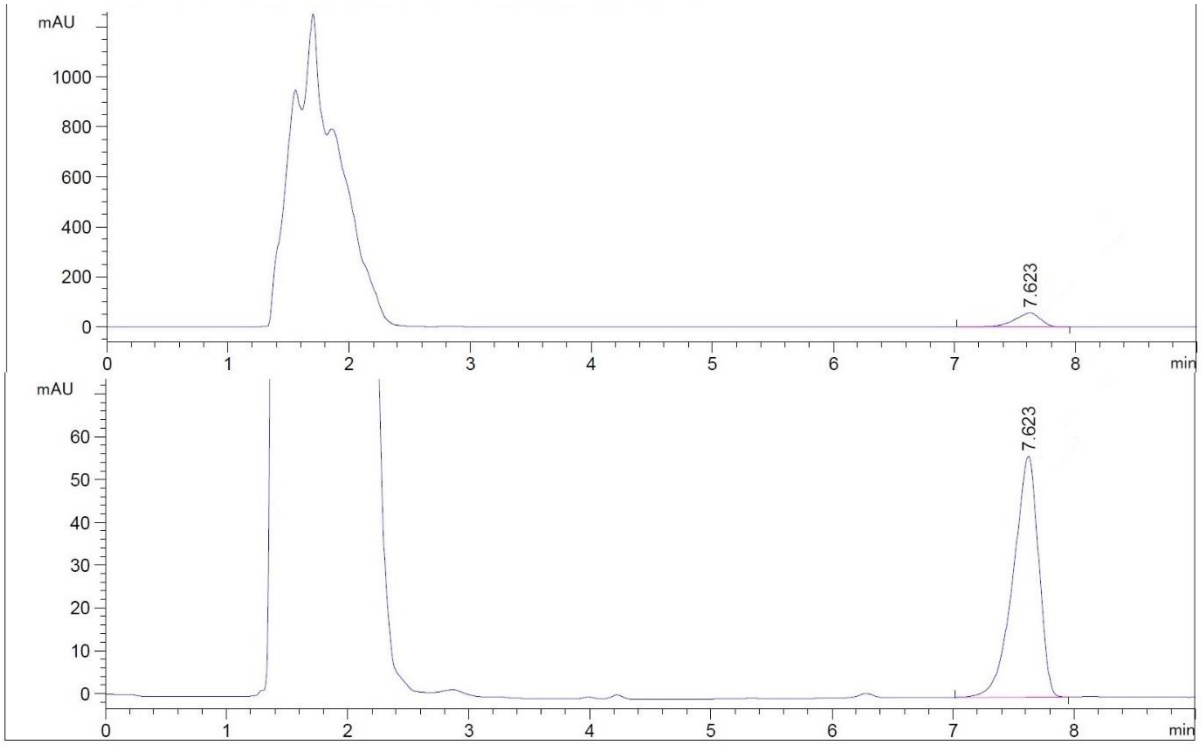

Figure 3.6: Chromatograms for artemiside in the presence of verapamil, at wavelength 205 nm

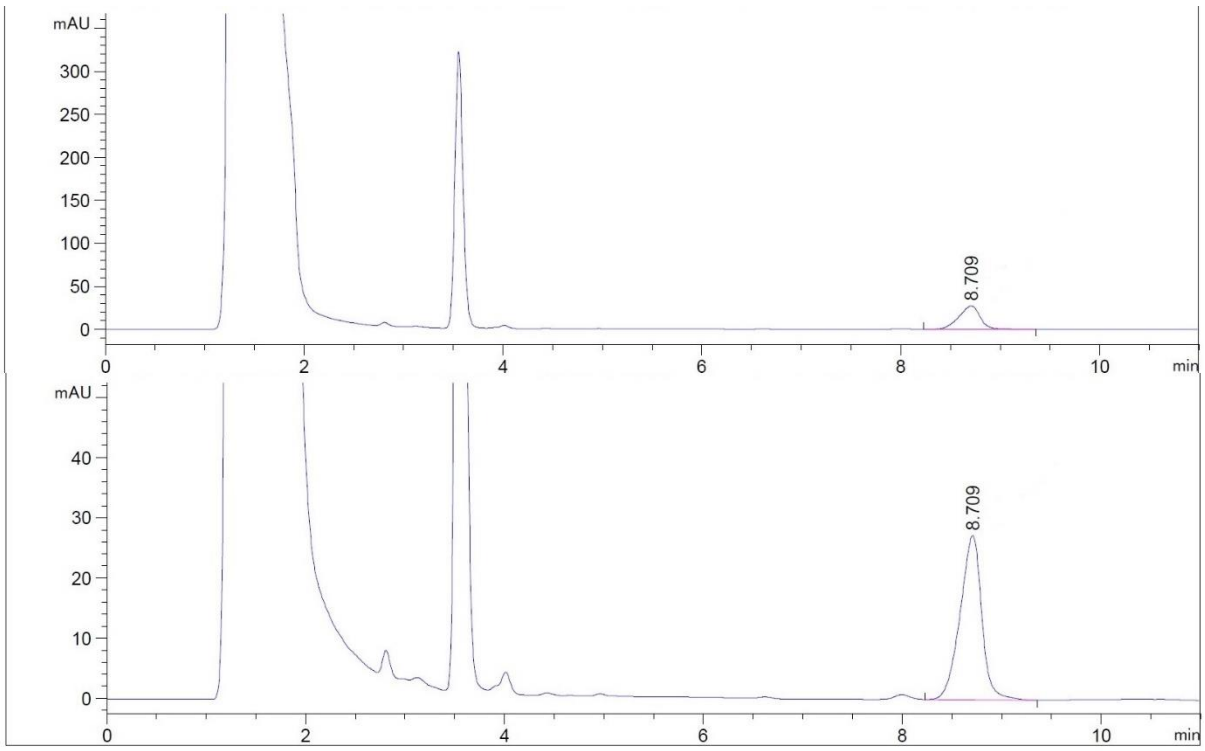

Figure 3.7: Chromatograms for artemiside in the presence of piperine, at wavelength 205 nm

The artemisde peak in the presence of verapamil appeared at 7.623 min on the HPLC chromatogram (Figure 3.6). In the presence of piperine, the peak of artemiside appeared at 8.709 min according to Figure 3.7, and was separated from piperine and the solvents. These chromatograms, therefore indicates no interference by any other compound, as observed with the HPLC analytical method used to quantify artemiside.

3.5.4 Artemisone

3.5.4.1 Linearity

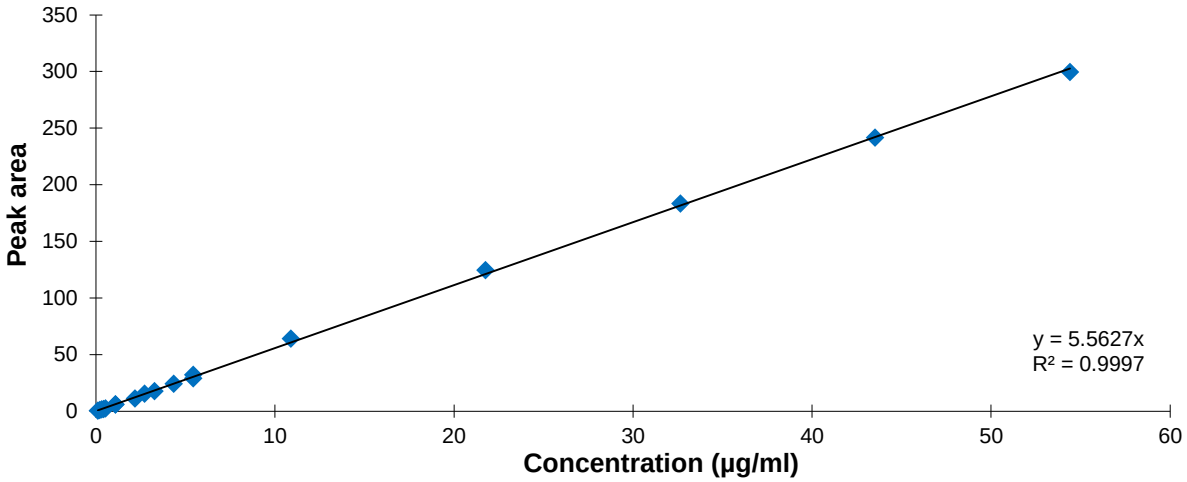

Figure 3.8: The linear regression graph for artemisone, where the mean peak area is plotted as a function of concentration

From the data portrayed in the graph (Figure 3.8), it is evident that an R2 value of 0.9997 was obtained. It can therefore be concluded that the method for artemisone analysis complies with the linearity criteria.

3.5.4.2 Accuracy

From Table 3.9, it is evident that the analytical method yielded an acceptable mean recovery of 98.63%. The standard deviation (SD) and percentage relative standard deviation (%RSD) are also provided in the table.

Table 3.9: The accuracy results for artemisone solutions

Concentration spiked (µg/ml)	Peak area 1	Peak area 2	Mean peak area	Recovery (µg/ml)	Recovery (%)
10.35	65.19	65.99	65.59	10.10	97.61
10.83	68.40	68.22	68.31	10.52	97.19
10.45	67.53	67.39	67.46	10.39	99.43
20.70	136.10	134.76	135.43	20.86	100.77
21.65	136.46	136.27	136.37	21.00	97.01
20.90	135.17	134.99	135.08	20.80	99.54
41.40	265.96	266.22	266.09	40.98	99.00
43.30	273.17	273.06	273.12	42.07	97.15
41.80	271.52	270.88	271.20	41.77	99.93
				Mean	**98.63**
				SD	**1.325**
				%RSD	**1.343**

3.5.4.3 Precision

3.5.4.3.1 Intra-day precision

From the results shown in Table 3.10, it is evident that the intra-day precision of the method used for artemisone quantification falls within the acceptable criteria of ≤ 2% RSD (Shabir, 2003:62). The peak area and retention time provided values of 0.778% and 0.250%, respectively.

Table 3.10: Intra-day precision results for artemisone

Injection number	Peak area	Retention time (min)
1	150.92	6.024
2	151.19	6.033
3	151.06	6.030
4	151.04	6.028
5	154.51	6.048
6	151.80	6.042
7	151.82	6.047
8	150.43	6.074
Mean	**151.60**	**6.041**
SD	**1.180**	**0.015**
%RSD	**0.778**	**0.250**

3.5.4.3.2 Intra-day precision

The results summarised in Table 3.11 confirmed that the inter-day precision of artemisone is acceptable with a %RSD value of 0.957%.

Table 3.11: Inter-day precision results for artemisone on three consecutive days

Days	% Recovery			Mean	SD	%RSD
Day 1	100.77	97.01	99.54	99.11	1.564	1.578
Day 2	98.95	98.74	98.78	98.82	0.090	0.092
Day 3	96.18	96.74	98.04	96.99	0.777	0.801
		Between days		**98.31**	**0.941**	**0.957**

3.5.4.4 Ruggedness and robustness

The results summarised in Table 3.12 reveal that artemisone is sufficiently stable in solution over a period of 24 hours.

Table 3.12: The stability of artemisone in solution over a time period of 24 hours

Time (h)	Peak Area	%Remaining
0	150.35	100.00
1	145.80	96.97
2	146.23	97.26
3	147.02	97.78
4	146.82	97.65
5	146.63	97.53
6	146.99	97.77
7	147.29	97.97
8	147.10	97.84
9	146.79	97.63
10	148.50	98.77
11	149.66	99.54
12	148.51	98.77
13	149.77	99.62
14	149.43	99.39
15	149.81	99.64
16	150.35	100.00
17	150.43	100.06
18	150.35	100.00
19	150.53	100.12
20	151.23	100.58
21	150.89	100.36
22	150.81	100.31
23	150.48	100.08
24	150.38	100.02
Mean	**148.89**	**99.03**
SD	**1.737**	**1.155**
%RSD	**1.167**	**1.167**

3.5.4.5 Limit of detection and quantification

The LOD and LOQ values obtained for artemisone are shown in Table 3.13.

Table 3.13: Limit of detection and quantification of artemisone

Analyte	Limit of detection	Limit of quantification
Artemisone	0.0122 µg/ml	0.0368 µg/ml

3.5.4.6 Specificity

The chromatograms for artemisone in the presence of verapamil and piperine is shown in Figure 3.9 and Figure 3.10, respectively. DMEM and methanol were the solvents in which the compounds were dissolved.

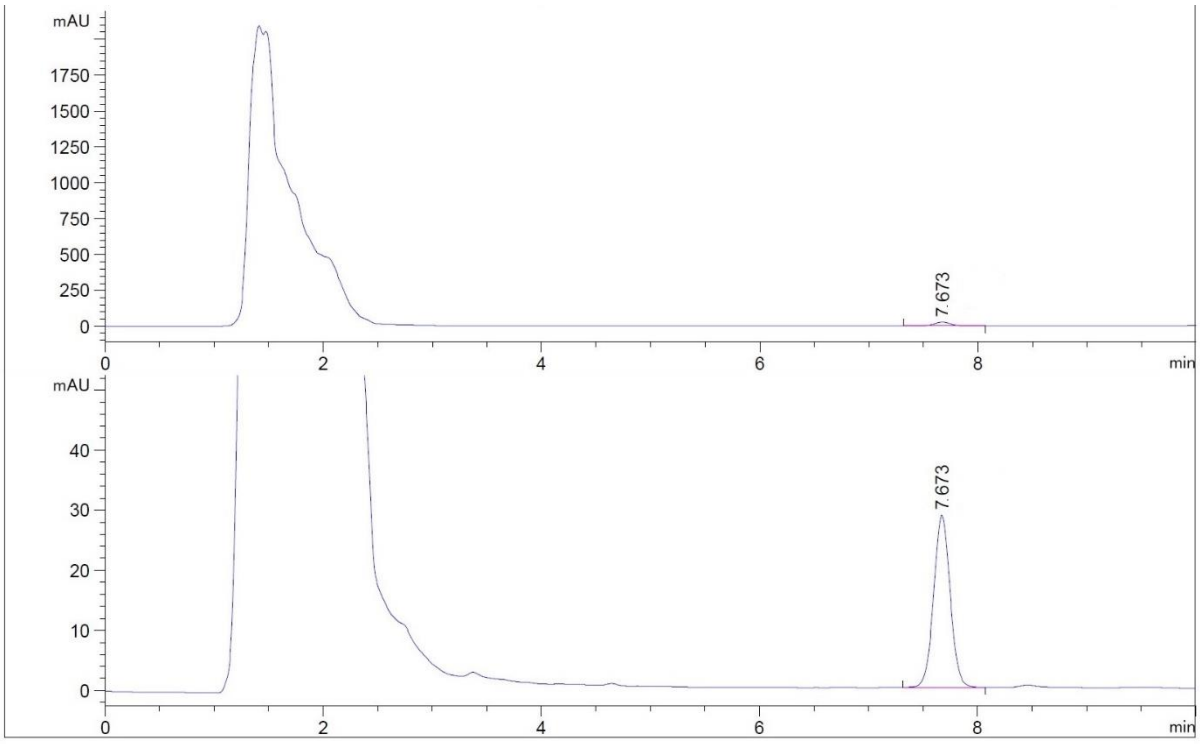

Figure 3.9: Chromatograms for artemisone in the presence of verapamil, at wavelength 200 nm

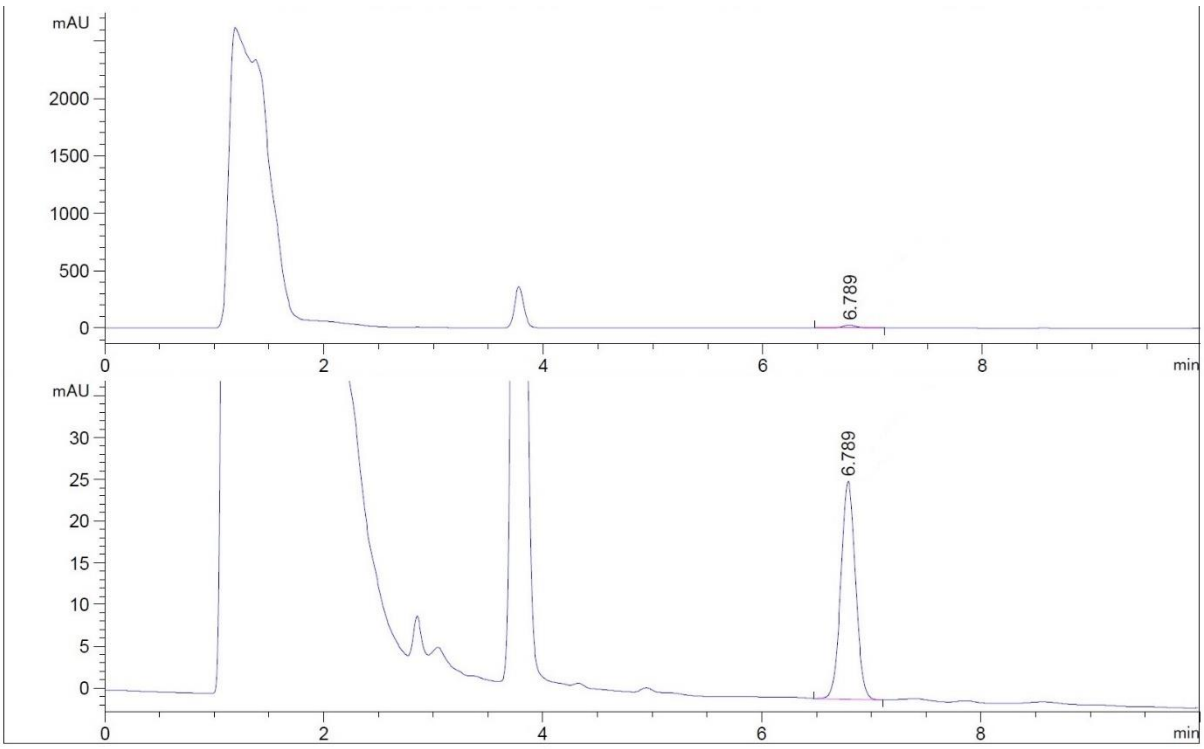

Figure 3.10: Chromatograms for artemisone in the presence of piperine, at wavelength 200 nm

The artemisone peak in the presence of verapamil appeared at 7.673 min on the HPLC chromatogram (Figure 3.9). In the presence of piperine, the peak of artemisone appeared at 6.789 min, indicated in Figure 3.10, and was completely separated from piperine and the solvents. These chromatograms therefore indicate that no interference by any other compound could be observed with the HPLC analytical method used to quantify artemisone.

3.5.5 Artemether

3.5.5.1 Linearity

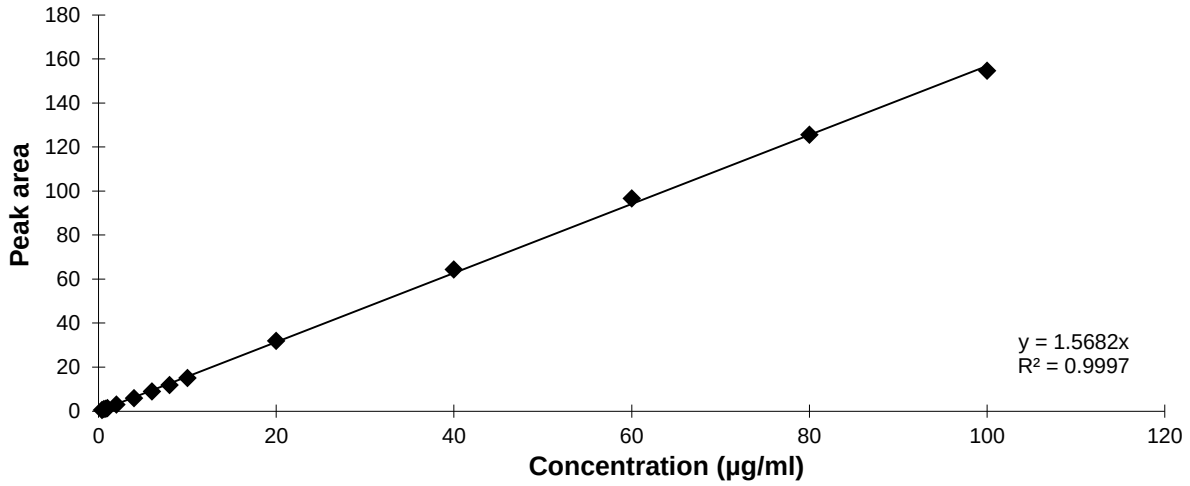

Figure 3.11: The linear regression graph for artemether, where the mean peak area is plotted as a function of concentration

From the standard curve plotted in Figure 3.11, an R2 value of 0.9997 was obtained. Therefore, it can be concluded that artemether HPLC analytical method has met the criteria for linearity.

3.5.5.2 Accuracy

The mean recovery, standard deviation (SD) and the percentage relative standard deviation (%RSD) on the recovery of artemether from the solutions with different concentrations are shown in Table 3.14. The results confirmed that the method yielded an acceptable mean recovery of 102.16%

Table 3.14: The accuracy results for artemether solutions

Concentration spiked (µg/ml)	Peak area 1	Peak area 2	Mean peak area	Recovery (µg/ml)	Recovery (%)
20.45	30.64	30.27	30.46	20.49	100.22
20.80	31.01	31.16	31.08	20.92	100.56
20.80	31.60	31.35	31.48	21.18	101.83
40.90	62.81	61.79	62.30	41.92	102.50
41.60	63.24	63.05	63.15	42.49	102.15
41.60	63.67	62.19	62.93	42.35	101.80
81.80	127.11	127.60	127.35	85.70	104.77
83.20	127.31	124.78	126.05	84.82	101.95
83.20	128.30	128.08	128.19	86.26	103.68
				Mean	**102.16**
				SD	**1.326**
				%RSD	**1.298**

3.5.5.3 Precision

3.5.5.3.1 Intra-day precision

The results portrayed in Table 3.15 clearly show that the %RSD for repeated injections of a single artemether solution is within the acceptable guidelines, with a value of 0.813% for the peak area and 1.037% for the retention time.

Table 3.15 Intra-day precision results for artemether

Injection number	Peak area	Retention time (min)
1	39.45	10.124
2	39.32	10.132
3	39.60	10.130
4	39.54	10.040
5	39.10	10.060
6	38.82	10.053
7	38.76	10.390
8	38.88	10.088
Mean	**39.18**	**10.127**
SD	**0.319**	**0.105**
%RSD	**0.813**	**1.037**

3.5.5.3.2 Inter-day precision

An acceptable inter-day precision was obtained for artemether, with a %RSD value of 0.837%, as shown in Table 3.16.

Table 3.16: Inter-day precision results for artemether on three consecutive days

Days	% Recovery			Mean	SD	%RSD
Day 1	102.50	102.15	101.80	102.15	0.285	0.279
Day 2	98.63	102.08	99.66	100.12	1.443	1.441
Day 3	100.48	101.54	102.58	101.54	0.858	0.845
		Between days		**101.27**	**0.848**	**0.837**

3.5.5.4 Ruggedness and robustness

Artemether is stable in solution over a period of 24 hours, as can be seen from Table 3.17.

Table 3.17: The stability of artemether in solution over a time period of 24 hours

Time (h)	Peak Area	%Remaining
0	47.70	100.00
1	48.08	100.81
2	48.63	101.95
3	49.86	104.53
4	48.24	101.13
5	48.12	100.89
6	47.98	100.58
7	47.98	100.59
8	48.25	101.15
9	48.33	101.32
10	47.20	98.95
11	48.35	101.37
12	47.93	100.49
13	47.32	99.20
14	47.11	98.78
15	47.33	99.23
16	47.27	99.10
17	47.21	98.97
18	47.19	98.93
19	47.58	99.76
20	47.20	98.95
21	47.22	98.99
22	47.34	99.25
23	47.49	99.56
24	47.13	98.82
Mean	**47.76**	**100.13**
SD	**0.630**	**1.321**
%RSD	**1.319**	**1.319**

3.5.5.5 Limit of detection and quantification

The LOD and LOQ values obtained for artemether are shown in Table 3.18.

Table 3.18: Limit of detection and quantification of artemether

Analyte	Limit of detection	Limit of quantification
Artemether	0.0248 µg/ml	0.0752 µg/ml

3.5.5.6 Specificity

The chromatogram (Figure 3.12) for artemether in the presence of verapamil with DMEM and methanol as the solvents.

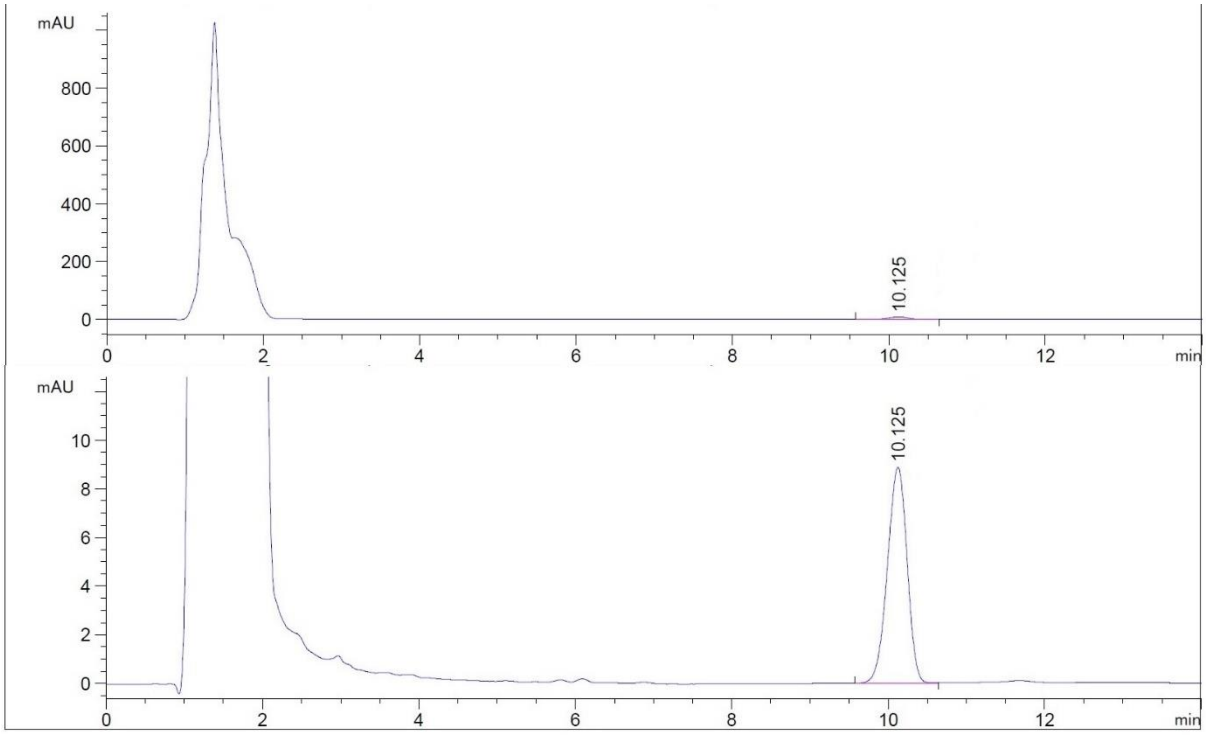

Figure 3.12: Chromatograms for artemether in the presence of verapamil, at wavelength 216 nm

The artemether peak appeared at 10.125 min on the HPLC chromatogram (Figure 3.12) and was completely separated from verapamil and the solvents that were used. This chromatogram therefore indicates that no interference by any other compound could be observed with the HPLC analytical method used to quantify artemether.

3.5.6 Vinblastine

3.5.6.1 Linearity

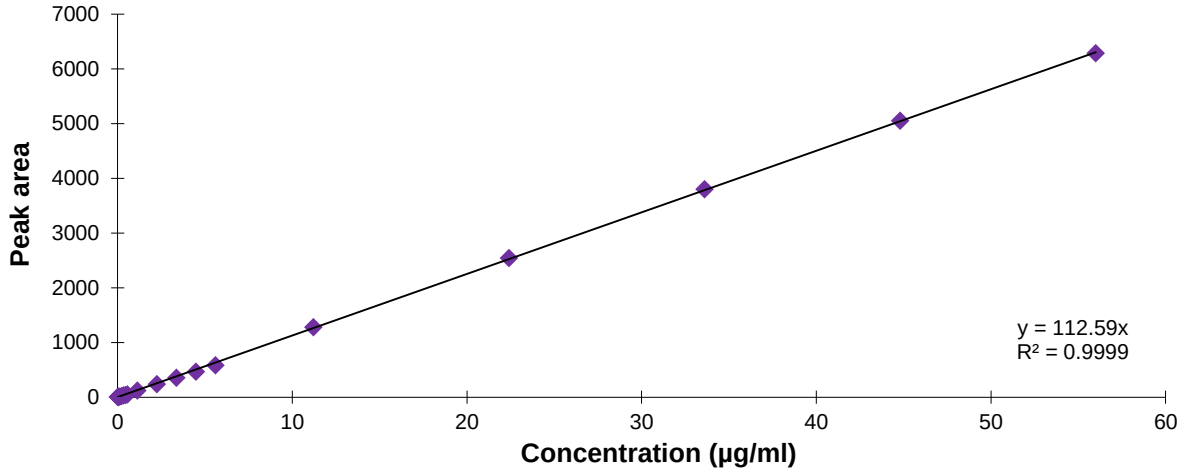

Figure 3.13: The linear regression graph for vinblastine, where the mean peak area is plotted as a function of concentration

An R2 value of 0.9999 was obtained for vinblastine, as shown in Figure 3.13, which implies that the method for vinblastine quantification is in accordance with the criteria for linearity.

3.5.6.2 Accuracy

The accuracy results obtained for vinblastine (seen in Table 3.19), confirmed that the analytical method yielded an acceptable mean recovery of 98.27%.

Table 3.19: The accuracy results for vinblastine solutions

Concentration spiked (µg/ml)	Peak area 1	Peak area 2	Mean peak area	Recovery (µg/ml)	Recovery (%)
11.50	1350.24	1343.49	1346.87	11.22	97.55
11.75	1352.57	1356.82	1354.70	11.28	96.03
12.00	1448.58	1457.27	1452.93	12.10	100.85
23.00	2706.40	2662.64	2684.52	22.36	97.22
23.50	2728.89	2730.61	2729.75	22.74	96.75
24.00	2884.96	2992.14	2938.55	24.48	101.98
46.00	5377.74	5382.97	5380.36	44.81	97.42
47.00	5440.81	5443.34	5437.20	45.29	96.44
48.00	5773.95	5772.76	5773.36	48.09	100.18
				Mean	**98.26**
				SD	**2.039**
				%RSD	**2.075**

3.5.6.3 Precision

3.5.6.3.1 Intra-day precision

From the results shown in Table 3.20, it is evident that the intra-day precision of the method used for vinblastine quantification falls within the acceptable criteria of ≤ 2% (Shabir, 2003:62). The peak area and retention time provided values of 0.335% and 1.433%, respectively.

Table 3.20: Intra-day precision results for vinblastine

Injection number	Peak area	Retention time (min)
1	1168.30	4.117
2	1161.80	4.111
3	1161.44	4.108
4	1167.74	4.284
5	1167.79	4.200
6	1167.01	4.154
7	1174.73	4.103
8	1168.52	4.115
Mean	**1167.17**	**4.149**
SD	**3.916**	**0.059**
%RSD	**0.335**	**1.433**

3.5.6.3.2 Inter-day precision

The results summarised in Table 3.21 confirmed that the inter-day precision of vinblastine is acceptable with a %RSD value of 2.669%.

Table 3.21 Inter-day precision results for vinblastine on three consecutive days

Days	% Recovery			Mean	SD	%RSD
Day 1	97.22	96.75	101.98	98.65	2.364	2.396
Day 2	107.10	106.15	101.60	104.95	2.402	2.288
Day 3	97.02	100.78	102.33	100.04	2.231	2.230
		Between days		**101.21**	**2.702**	**2.669**

3.5.6.4 Ruggedness and robustness

From the results in Table 3.22, it is clear that vinblastine is no longer stable after 11 hours.

Table 3.22: The stability of vinblastine in solution over a time period of 24 hours

Time (h)	Peak Area	%Remaining
0	1025.65	100.00
1	1025.73	100.01
2	1023.17	99.76
3	1026.67	100.10
4	1024.37	99.88
5	1023.99	99.84
6	1019.89	99.44
7	1018.95	99.35
8	1008.09	98.29
9	1028.41	100.27
10	1018.59	99.31
11	1008.43	98.32
12	1002.98	97.79
13	993.79	96.89
14	990.29	96.55
15	983.26	95.87
16	978.92	95.44
17	970.46	94.62
18	966.85	94.27
19	963.57	93.95
20	958.00	93.40
21	952.51	92.87
22	946.60	92.29
23	942.16	91.86
24	935.67	91.23
Mean	**993.48**	**96.86**
SD	**30.489**	**3.297**
%RSD	**3.069**	**3.069**

3.5.6.5 Limit of detection and quantification

The LOD and LOQ values obtained for vinblastine are shown in Table 3.23.

Table 3.23: Limit of detection and quantification of vinblastine

Analyte	Limit of detection	Limit of quantification
Vinblastine	0.0197 µg/ml	0.0597 µg/ml

3.5.6.6 Specificity

The chromatogram (Figure 3.14) for vinblastine in the presence of verapamil, with DMEM and methanol as the solvents.

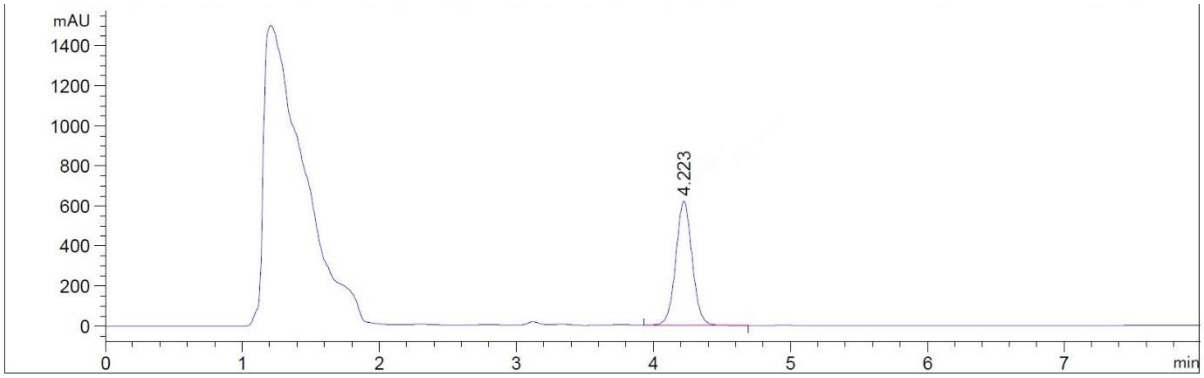

Figure 3.14: Chromatogram for vinblastine in the presence of verapamil, at wavelength 220 nm

The vinblastine peak appeared at 4.223 min on the HPLC chromatogram (Figure 3.14) and was completely separated from verapamil. This chromatogram therefore indicates that no interference by any other compound could be observed with the HPLC analytical method used to quantify vinblastine.

3.5.7 Lucifer yellow

3.5.7.1 Linearity

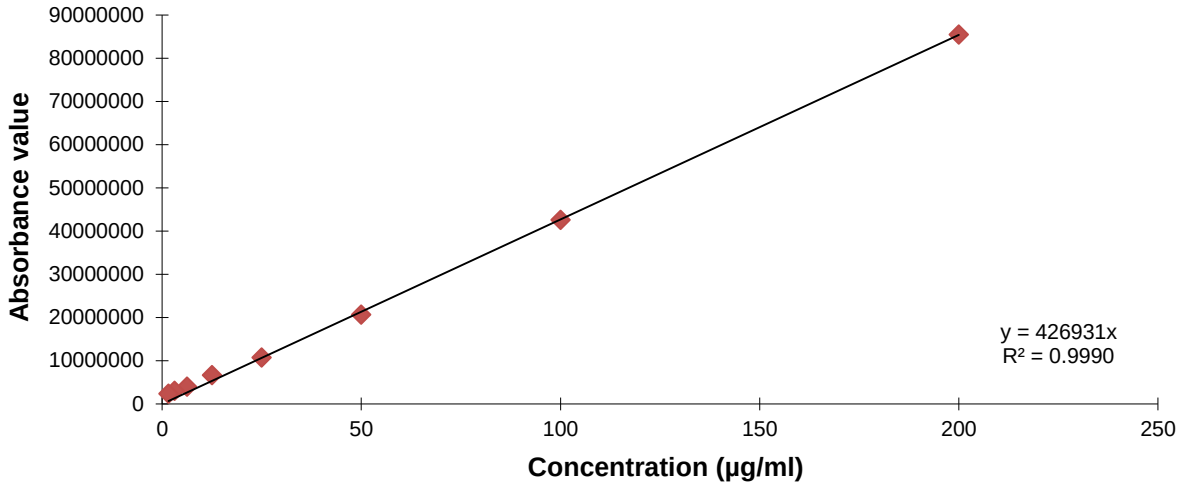

Figure 3.15: The linear regression graph for Lucifer yellow, where the mean absorbance is plotted as a function of concentration

From the data portrayed in the graph (Figure 3.15), it is clear that an R2 value of 0.9990 was obtained. It can therefore be concluded that the method for Lucifer yellow quantification met the criteria for linearity.

3.5.7.2 Accuracy

Table 3.24 displays the percentage (%) recovery, standard deviation (SD) and the % relative standard deviation (%RSD) obtained for Lucifer yellow from the solutions with different concentrations. The results confirmed that the analytical method yielded an acceptable mean recovery of 98.220%.

Table 3.24: The accuracy results for Lucifer yellow samples

Concentration spiked (µg/ml)	Mean Fluorescence detection values (n = 3)			Averages	Recovery (µg/ml)	Recovery (%)
	Replicate 1	Replicate 2	Replicate 3			
25	10693041	10714077	10927119	10778079	25.24	99.68
25	10523399	10491295	10755895	10590196	24.80	97.98
25	10466494	10341750	10656560	10488268	24.56	96.88
100	41978864	41732568	42242508	41984647	98.33	98.33
100	41063132	41255820	41647048	41322000	96.78	96.78
100	40974144	40671872	41195408	40947141	95.90	95.90
200	87158856	85099968	83108240	85122355	199.36	100.97
200	85666640	83763640	81582224	83670835	195.96	99.21
200	84991264	82558032	80648296	82732531	193.76	98.26
					Mean	**98.22**
					SD	**1.581**
					%RSD	**1.610**

3.5.7.3 Precision

3.5.7.3.1 Intra-day Precision

The results illustrated in Table 3.25, clearly show that the %RSD values for repeated readings of three concentrations of Lucifer yellow are in accordance with the specified guideline of ≤ 2%.

Table 3.25: Intra-day precision results for Lucifer yellow over three different concentrations

Theoretical concentration (µg/ml)	Mean Fluorescence detection values (n = 3)			Averages	Standard deviation	%RSD
	08:00	12:00	16:00			
200	79442771	77993939	78087216	78507975	810899.02	**1.033**
100	38835647	39694828	38623353	39051276	567350.42	**1.453**
3.125	2689654	2722712	2693780	2702049	18013.42	**0.667**

3.5.7.3.2 Inter-day Precision

An acceptable inter-day precision was obtained for Lucifer yellow at the various concentrations. The specified value of ≤ 5% RSD was met, as can be seen in Table 3.26.

Table 3.26: Inter-day precision results for Lucifer yellow on three consecutive days

Theoretical concentration (µg/ml)	Mean Fluorescence detection values (n = 3)			Averages	Standard deviation	%RSD
	Day 1	Day 2	Day3			
200	76501232	73564691	73144917	74403613	1828675.88	**2.458**
100	38838208	38933215	37771447	38514290	645072.46	**1.675**
3.125	2710923	2775503	2626173	2704200	74891.86	**2.769**

3.5.7.4 Ruggedness and robustness

The Lucifer yellow stability was only tested over a 5 hour period, as the transport samples were measured immediately after the experiment was completed. The results summarised in Table 3.27 confirmed that Lucifer yellow is stable for the duration of the experiment, which lasted not more than 3 hours.

Table 3.27: The stability of Lucifer yellow in solution over a time period of 5 hours

Time (h)	Mean Absorbance of three readings (n = 3)	%Remaining	% Degraded
0	39283437	100.00	0.00
1	38599623	98.26	1.74
2	38186411	97.21	2.79
3	38120679	97.04	2.96
4	38062449	96.89	3.11
5	37921725	96.53	3.47

3.5.7.5 Limit of detection and quantification

The slope of the linear regression curve and the standard deviation of the blanks for DMEM are shown in Table 3.28 which was used to determine the limit of detection and quantification. The

LOD and LOQ for Lucifer yellow were calculated to be 0.4455 µg/ml and 1.3499 µg/ml, respectively.

Table 3.28: The mean fluorescence detection and standard deviation values of the blanks as well as the slope of the standard curve of Lucifer yellow

Replicates	Fluorescence detection value of the blanks
1	2523834
2	2454568
3	2381007
4	2499075
5	2433254
6	2349858
7	2473084
8	2403364
9	2364117
Means	**2431351.22**
SD	**57641.854**
Slope	**426979.43**

3.6 Conclusion

The HPLC methods for each of the individual analytes, as well as the fluorometric method for Lucifer yellow, were found to be functional and complied with the criteria for the validation parameters. Therefore, the developed methods are sufficient for the analysis of Caco-2 transport samples.

CHAPTER 4: ARTICLE FOR PUBLICATION IN CURRENT DRUG DELIVERY

This chapter is presented as a research article submitted for publication in "*Current Drug Delivery*". It is formatted according to the journal's instructions to authors, which are included in Appendix C. In addition, the detailed apparent permeability coefficients and efflux ratio values of this study are presented in Appendix B. All the *in vitro* data that were gathered from the experiments are presented in Appendix A.

Absorptive and Secretory Transport of Selected Artemisinin Derivatives across Caco-2 Cell Monolayers

Jaco Heyns[a], Clarissa Willers[a], Richard K. Haynes[a], Ho N. Wong[a], Josias Hamman[a] and Chrisna Gouws*[a]

[a]*Pharmacen™, Centre of Excellence for Pharmaceutical Sciences, North-West University, Private Bag X6001, Potchefstroom 2520, South Africa*

Abstract: Malaria continues to be a major health concern and affects more than 200 million people a year. Drugs currently used for treatment of malaria are increasingly rendered ineffectual by the ongoing emergence of parasite resistance. For any new drugs, however, knowledge of their membrane permeability is an essential pre-requisite for eventual use. Treatment failure and emergence of resistance can occur as a result of reduced availability of the drug at the desired site of action. Cell-based permeability assays such as Caco-2 cell monolayers serve as a model for predicting drug absorption and efflux, and provide an estimate of drug bioavailability.

Here we have studied the bi-directional transport of new anti-malarial compounds, artemisone and artemiside, as well as reference compounds, namely the known anti-malarial drug artemether, and caffeine and atenolol.

The Caco-2 cell monolayer model was used to assess the membrane permeation properties of these compounds, and to identify if they are subject to P-gp associated efflux, in the presence and absence of verapamil. The effect of piperine on the transport of the compounds that were identified to be P-gp substrates was also assessed. Samples withdrawn from the acceptor chambers at pre-determined time intervals were analysed by means of high-performance liquid chromatography (HPLC).

Transport results in terms of the absorptive direction revealed that artemisone and artemether had low absorption rates relative to the reference compounds. It was further demonstrated that artemisone is slightly effluxed, and although both artemether and artemiside were susceptible to P-gp mediated efflux, it appears that other efflux proteins may also be involved.

The low permeability of anti-malarial drugs must be borne in mind during development of effective dosage regimens of new drugs.

Keywords: Anti-malarial drug, Caco-2, drug permeability, efflux, herb-drug interactions, P-glycoprotein.

1. INTRODUCTION

Malaria, a tropical disease caused by protozoan *Plasmodium* parasites, remains a major health concern globally. According to the 2016 World Malaria Report, published by the World Health Organization (WHO), approximately 212 million cases of infections and 429 000 deaths have been reported in 2015 of which 92% occurred in Africa, 6% in South-East Asia and 2% in the Eastern Mediterranean regions [1]. The *Plasmodium falciparum* parasite was responsible for 99% of these deaths, and 70% of the total number of deaths occurred in children under the age of 5 years. Thus, there is need to maintain the substantial effort to prevent or control malaria outbreaks worldwide. Since the 1940s, the development of anti-malarial drugs formed an important contributing factor in controlling malaria infections [2]. Well-known drugs such as chloroquine, quinine, mefloquine, pyrimethamine, proguanil, sulfadoxine and more recently, the derivatives dihydroartemisinin, artemether and artesunate of the Chinese anti-malarial drug artemisinin (Figure **1A**), have contributed immensely to the fight against malaria [3-5]. However, the emergence of resistance of the parasites towards some of these drugs, including most recently, against the artemisinins, renders the development of improved anti-malarial drugs an urgent task [1, 6]. Drug-resistant malaria and the mechanisms involved have previously been reviewed extensively [3].

*Address correspondence to Chrisna Gouws at Pharmacen™, Centre of Excellence for Pharmaceutical Sciences, North-West University, Private Bag X6001, Potchefstroom 2520, South Africa; Tel: +27-18-285-2505; Fax: +27-87-231-5432; E-mail: chrisna.gouws@nwu.ac.za

Artemisone and artemiside (Figure **1B**) are newer derivatives of the Chinese anti-malarial drug artemisinin. They are readily prepared from dihydroartemisinin, and are potently active both *in vitro* and *in vivo* against *P. falciparum* [7], and also against cerebral malaria in a murine model [8-9]. With these activities, the potential for developing these as anti-malarial drugs needs to be assessed. At the same time, it is important to assess their membrane permeability. Drug absorption is the result from passive diffusion, uptake and efflux transporters, as well as gastrointestinal metabolism [10].

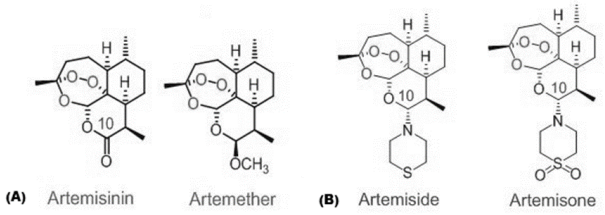

Figure **1**: (**A**) Structures of artemisinin and the clinical derivative, artemether. (**B**) The amino-artemisinins, artemiside and artemisone.

The *in vitro* membrane permeability of these drugs across intestinal epithelial cell monolayers can provide an indication of their uptake and potential bioavailability after oral administration. It is also important to determine if any of these drugs are substrates for P-glycoprotein (P-gp) efflux transporters expressed by the Caco-2 cell line. If this is the case, the possibility exists that the malaria parasite may acquire resistance against these drugs via an efflux mechanism. Good characterisation of the efflux potential of anti-malarial drugs is also important as it could be related to interactions when considering combination therapy.

Efflux of drugs and the transporter proteins involved has been reviewed comprehensively. The mammalian adenosine triphosphate (ATP)-binding cassette (ABC) transporters that play an essential role in the transport of clinically relevant anti-malarial drugs, are primarily located in the plasma membrane where they can efflux structurally diverse drugs, through an ATP-dependent mechanism that can take place against concentration gradients [11].

Plasmodium falciparum has numerous proteins on the membrane of the digestive vacuole that are used to transport different compounds across the membrane [3, 6]. Genetic mutations can occur, which result in changes in the expression level of these transporters [12]. The efflux capabilities of the parasite can thereby be enhanced, leading to the reduced sensitivity of the parasite to anti-malarial drugs [13-14]. A homolog of the well-known P-gp transporter, responsible for several efflux-related drug resistance instances in humans [15], was identified in the*P. falciparum* parasite. The amplification of this *P. falciparum* multidrug resistance transporter 1 (PfMDR1) have been associated with the reduced sensitivity to artemisinin or its derivatives artemether, artesunate and dihydroartemisinin, lumefantrine, quinine and mefloquine [16-17].

Given that the majority of malaria-endemic countries suffer from high poverty rates, rural communities cannot afford to travel to healthcare facilities or cover the expenses of standard anti-malarial drugs. As such, individuals in these communities rather visit their traditional medical practitioners for easily accessible and affordable plant medicines to treat malaria and other ailments [18-20]. It is a common tendency, especially in developing countries, to use herbal remedies alternatively or concomitantly with prescribed Western drugs [21-22]. The belief that herbal medicines are strictly beneficial for human health, seeing as it is of natural and organic origin should be treated with caution [22]. When plant medicines are simultaneously used with conventional drugs, the treatment efficacy may be altered by means of herb-drug interactions [23]. Oga *et al.* [22] comprehensively reviewed the underlying mechanisms responsible for herb-drug interactions, of which the inhibition or induction of efflux drug transporters is applicable to this study. The phytoconstituent, piperine, present in black pepper (*Piper nigrum*) has been shown to inhibit the function of the human P-gp transporter [24-25] and was used in this study to potentially enhance bioavailability of the selected compounds by reducing P-gp mediated efflux.

The aim of this study was to measure the bi-directional permeability of artemether, the clinically used artemisinin derivative (Figure **1A**), and compare this with the newer derivatives artemisone and artemiside. The Caco-2 cell monolayer model would be used to assess the membrane permeation properties of these compounds, and to identify if they are subject to P-gp associated efflux. The effect of piperine on the transport of the compounds that are identified to be P-gp substrates would also be assessed.

2. MATERIALS AND METHOD

2.1. Study design

The bi-directional transport (i.e. absorption and efflux) of artemether, artemisone and artemiside was measured across Caco-2 cell monolayers in Transwell® 6-well plates in the absence and presence of the P-gp inhibitor, verapamil. Caffeine (highly membrane permeable) and atenolol (poorly membrane permeable) were included as reference compounds to rank the extent of membrane permeation of the selected artemisinin derivatives. Lucifer yellow was used as an integrity marker to confirm the cell monolayer integrity, while the known P-gp substrate, vinblastine, was used to confirm the appropriateness of the cell-based model for the study of efflux-based transport. The transport of caffeine, atenolol and Lucifer yellow was only tested in the apical to basolateral direction, whereas vinblastine studies were conducted in both directions. Bi-directional transport of the artemisinin derivatives that showed P-gp transporter related efflux was

investigated in the presence of piperine, which is known to inhibit P-gp function [24-25]. All the transport assays were conducted in triplicate.

2.2. Materials and reagents

Artemisone and artemiside were prepared and purified as previously described [7] and purity assessed by means of HPLC. Vinblastine, piperine and Lucifer yellow were purchased from Sigma-Aldrich (Johannesburg, South Africa), whereas verapamil hydrochloride and artemether (Batch no. 060510) were purchased from DB Fine Chemicals (Johannesburg, South Africa). The Caco-2 cell line was purchased from the European Collection of Cell Cultures (ECACC) (Public Health England, Salisbury, UK). Dulbecco's Modified Eagle Medium (DMEM) (HyClone, high-glucose, cat. no. SH30243.01) and phosphate buffered saline (PBS) (HyClone, 1X, 0.0067 M, cat. no. SH30256.01) was obtained from Separations (Johannesburg, South Africa). From The Scientific Group (Johannesburg, South Africa), amphotericin B (Biochrom, 250 µg/ml, cat. no. A2612) and HEPES-Buffer (Biochrom, 1 M, cat. no. L1613) were purchased. Non-essential amino acids (NEAA) (Lonza, 100X, cat. no. BE13-114E), L-glutamine (Lonza, 200 mM, cat. no. BE17-605E), Penicillin/Streptomycin (Pen-Strep) (Lonza, 10000U Penicillin/ml/ 10000U Streptomycin/ml, cat. no. DE17-602E) and trypsin EDTA (Lonza, cat. no. BE17-161F) was obtained from Whitehead Scientific (Cape Town, South Africa). Trypan Blue was purchased at Sigma-Aldrich (Johannesburg, South Africa). Foetal bovine serum (FBS) (Gibco Life Technologies, cat. no. 10270) was obtained from Thermo Fisher Scientific Inc. (Massachusetts, USA).

2.3. Caco-2 cell culturing, sub-culturing and seeding

The Caco-2 cells were cultured in high-glucose DMEM, supplemented with 10% FBS, 1% NEAA, 1% Pen-Strep, 2 mM L-glutamine and 1% amphotericin B. Their incubation took place at 37°C in a 95% humidified atmosphere with 5% carbon dioxide (CO_2) in an ESCO CelCulture CO_2 incubator (Esco Technologies, Inc., CCL-170B, PA, USA). The growth medium was replaced every second day and regular visual inspections under a light microscope (Nikon Eclipse, TS100, Nikon Instruments Inc., New York, USA) were carried out to estimate the confluence and to ensure that no bacteria were present.

The cells were sub-cultured by trypsination at approximately 50% confluency [26]. Briefly, the growth medium in the culturing flask was removed and the cells rinsed twice with 10 ml PBS. A volume of 3 ml trypsin was added and evenly distributed over the cell layer. The flask was incubated for 5 min at 37°C. After complete detachment of the cells, 6 ml preheated growth medium was added to deactivate the enzyme. The cell suspension was gently pipetted to ensure all cells were rinsed from the bottom of the flask, transferred to a 15 ml centrifuge tube and centrifuged for 5 min at 140 x *g*. The cell pellet was re-suspended in 5 ml growth medium and divided to a ratio between 1:4 and 1:15 into new flasks and filled with preheated growth medium to a final volume of 15 ml. The cells were returned to the incubator to grow under normal culturing conditions. For experimental purposes, Caco-2 cells between passages 50 and 60 were used.

The Caco-2 cells were seeded onto Transwell® 6-well plates (Corning Costar® Corporation, Tewksbury, Massachusetts, USA) with a pore diameter of 0.4 µm and a surface area of 4.67 cm^2. Prior to seeding, the viable cells in a cell suspension obtained by trypsinisation (as described above) were counted in the presence of Trypan blue by means of a haemocytometer (Marienfeld-Superior, 0.0025 mm^2, Germany). The cell suspension was diluted to a concentration of 20 000 cells per ml with growth media and 2.5 ml of the final cell suspension was pipetted into each apical chamber of the plate wells, whereas 2.5 ml growth medium was dispensed into each basolateral chamber. To ensure the formation of intact epithelial cell monolayers on these membrane filters, the cells were cultured for 21 to 24 days with growth medium replaced every second day.

2.4. Preparation of test solutions

The compounds were dissolved initially in small volumes of methanol, prior to further dilution. A final concentration of 5% methanol was not exceeded for all solutions applied to the cells. Stock solutions of artemiside, artemisone, artemether and vinblastine were prepared at a concentration of 200 µM and diluted to a final concentration of 100 µM with either DMEM (for transport in the apical-to-basolateral direction) or DMEM buffered with HEPES (for transport in the basolateral-to-apical direction). A stock solution of verapamil at a concentration of 100 µM was prepared in either DMEM or DMEM buffered with HEPES. Combined test solutions (100 µM drug and 50 µM verapamil or piperine, [27]) were prepared by adding equal volumes of each stock solution to make up the required test solution in either DMEM or HEPES-buffered DMEM. Stock solutions of caffeine, atenolol and Lucifer yellow were prepared at a concentration of 1 mg/ml and diluted with DMEM to working solutions of 40 µg/ml (caffeine and atenolol) [28] and 50 µg/ml (Lucifer yellow) [29]. After preparation, test solutions and replacement media were heated in a circulating water bath at 37°C for 30 min prior to each transport study.

2.5. In vitro bi-directional transport studies

Prior to the transport studies, the transepithelial electrical resistance (TEER) of each cell monolayer was measured with a Millicell ERS II meter (Millipore, Billerica, MA, USA) to indicate the integrity of the monolayers. A resistance of at least 150 Ω (equivalent to 700 Ω.cm^2) was required before initiation of the transport studies [30].

2.5.1. Transport in the apical-to-basolateral direction

For the transport in the apical-to-basolateral (AP-BL) direction (uptake), the growth medium was removed from the basolateral compartments of the Transwell® plates. A volume of 2.5 ml preheated DMEM buffered with HEPES was added to the basolateral compartments and the plates incubated for 30 min at 37°C. After incubation, the TEER was measured. The growth medium was removed from the apical compartment and replaced with 2.5 ml of each test solution in DMEM. The TEER was immediately measured again, after the addition of the test solutions. Samples (200 µl) were withdrawn from the basolateral compartment at time intervals of 20, 40, 60, 80, 100 and 120 min, and replaced with an equal volume of preheated DMEM buffered with HEPES. The TEER was measured at the end of the transport study to confirm that the cell monolayer was still intact after exposure to the test solutions.

2.5.2. Transport in the basolateral-to-apical direction

For the transport in the basolateral-to-apical (BL-AP) direction (efflux), the growth medium was removed from the apical compartment of the Transwell® plates. A volume of 2.5 ml preheated DMEM was added to the apical compartments and the plates incubated for 30 min at 37°C. After incubation, the TEER was measured. The growth medium was removed from the basolateral compartment and replaced with 2.5 ml of each test solution in DMEM with HEPES. The TEER was measured immediately after the addition of test solutions. Samples (200 µl) were withdrawn from the apical compartment at time intervals of 20, 40, 60, 80, 100 and 120 min, and replaced with 200 µl of preheated DMEM. The TEER of each cell monolayer was measured at the end of the experiment to confirm if the integrity of the cell monolayer was still intact.

2.6. Sample analyses

All transport samples withdrawn at the time intervals described above, except for the Lucifer yellow samples, were analysed with validated high-performance liquid chromatography (HPLC) analyses to determine the concentration of the selected compounds in the acceptor compartments. The Lucifer yellow marker was quantified with fluorescence spectroscopy on a microplate reader.

2.6.1. Fluorescence quantification

The quantification of the membrane integrity marker, Lucifer yellow, was performed with a SpectraMax® Paradigm® Multi-Mode Detection Platform Microplate Reader (Molecular Devices, LLC, California, USA), equipped with SoftMax® Pro-Microplate Data acquisition and analysis software.

For Lucifer yellow quantification, each sample withdrawn at 20 min intervals was loaded into a black, flat bottom 96-well plate (Product #3916, Corning®, New York, USA). A standard curve was prepared for Lucifer yellow at various concentrations ranging from 50 µg/ml to 1.563 µg/ml, using DMEM as solvent. This serial dilution range was loaded in triplicate onto the solid black plate. Blanks of DMEM and DMEM buffered with HEPES were loaded in six replicates. Care was taken to ensure the correct spatial arrangement of the samples on the 96-well plate. The fluorescence was measured at an excitation wavelength of 485 nm and emission wavelength of 535 nm [31]. The limit of detection (LOD) and the limit of quantification (LOQ) for Lucifer yellow were calculated to be 0.446 µg/ml and 1.350 µg/ml, respectively.

Linear regression was performed on the standard curve (fluorescence plotted as a function of concentration (µg/ml)). The slope and Y-intercept of the linearity graph was determined and used to calculate the concentration of Lucifer yellow present in the samples. This was done after each sample was corrected for background noise and dilution. From these results, the cumulative transport (percentage over time) and apparent permeability coefficients (P_{app}) were calculated.

2.6.2. HPLC conditions

The chromatographic separation was carried out on Agilent 1100 and 1200 series HPLC systems (Agilent® Technologies, Palo Alto, California, U.S.A) equipped with pumps, autosamplers, UV detectors and Chemstation Rev.A.08.03 Agilent® Technologies, data acquisition and analysis software (Hewlet-Packard, Palo Alto, California, U.S.A). Analysis were run on a Venusil XBP C18(2) column, 150 x 4.6 mm, 5 µm, 100 Å (Agela Technologies, Newark, DE). All the HPLC methods were validated with respect to linearity, accuracy, precision, limit of detection and limit of quantification (data not shown), prior to analyses of the transport samples.

An isocratic elution mode was used with a flow rate of 1.0 ml/min and sample injections of 50 µl were made automatically by the autosampler.

2.6.2.1. Vinblastine

The analysis of vinblastine was performed on the Agilent 1200 HPLC series under the following conditions: the mobile phase consisted of a mixture of acetonitrile and water with 0.005 M di-potassium hydrogen phosphate (Na_2HPO_4) in a ratio of (75:25) and adjusted to a pH of 6 by using 2 M hydrochloric acid. The UV detector was set at 220 nm. The LOD for vinblastine was 0.020 µg/ml, and the LOQ was 0.060 µg/ml.

2.6.2.2. Artemiside

Analysis of artemiside was performed on the Agilent 1100 HPLC series under the following conditions: the mobile phase was a mixture of acetonitrile and water (75:25), buffered with

0.1% orthophosphoric acid. The UV detector was set at 205 nm. The LOD for artemiside was 0.009 µg/ml, and the LOQ was 0.027 µg/ml.

2.6.2.3. Artemisone

Analysis of artemisone was performed on the Agilent 1100 HPLC series under the following conditions: the mobile phase was a mixture of acetonitrile and water (70:30), buffered with 0.1% orthophosphoric acid. The UV detector was set at 200 nm. The LOD for artemisone was 0.012 µg/ml, and the LOQ 0.037 µg/ml.

2.6.2.4. Artemether

Analysis of artemether was performed on the Agilent 1100 HPLC series under the following conditions: the mobile phase was a mixture of acetonitrile and water (70:30). The UV detector was set at 216 nm. The LOD for artemether was 0.025 µg/ml, and the LOQ 0.075 µg/ml.

2.7. Data processing and statistical analysis

The drug concentrations obtained from the transport samples were corrected for dilution and expressed as cumulative drug transport (percentage of total dose) at specific time points. The apparent permeability coefficient (P_{app}) values were calculated according to the following equation [32]:

$$P_{app} = dQ/dt(1/(A.C_0.60))$$

where dQ/dt represents the increased amount of drug present in the acceptor compartment over time (cm/s), A is the surface area of the cell monolayer exposed to the test solution (cm^2) and C_0 is the initial drug concentration present (µg/ml). "60" is used in the equation to correct the transport values measured as a function of time in minutes, to be expressed in seconds for P_{app} (i.e. the P_{app} values are expressed in cm/s).

The efflux ratio values, for the drugs applied in both directions, were calculated according to the following equation [32]:

$$ER = P_{app}(BL\text{-}AP)/P_{app}(AP\text{-}BL)$$

where P_{app} (AP-BL) is the permeability coefficient value in the apical-to-basolateral direction, and P_{app} (BL-AP) indicates the permeability coefficient value in the basolateral-to-apical direction.

Statistical analyses of the transport data were performed using Statistica 12.0 (Statsoft, Inc., Tulsa, Oklahoma, USA) to determine if statistically significant differences exist between the P_{app} values of the experimental groups and the control groups in each direction. Furthermore, the efflux ratio was also analysed between each experimental group and its control (drug alone). The T-test was done to assess statistically significant differences between the various treatments and their controls, and statistical significance was defined as $p < 0.05$. This was followed by a nonparametric Mann-Whitney U test, where statistical significance was defined as $p < 0.1$.

Kinetic analysis on the apical to basolateral transport was done with the software program DDSolver, which is an add-in program in Microsoft Excel. This software program is used for non-linear fitting of data to conduct kinetic analysis. Both the zero order and first order models were fitted and the following kinetic parameters are reported: k0 = zero order rate constant, k1 = first order rate constant. To evaluate the goodness of fit, the correlation coefficient (R_obs–pre) and coefficient of determination (COD) are also shown.

3. RESULTS AND DISCUSSIONS:

3.1. Integrity and efflux of the Caco-2 cell culture model

The integrity of the Caco-2 cell monolayer was validated with Lucifer yellow (LY), which was used as an exclusion marker due to the inability of this hydrophilic molecule to permeate across intact biological membranes. A comparative study was done between LY and LY with 5% methanol, and the permeation rate of both was determined as 0.156×10^{-6} cm/s and 0.210×10^{-6} cm/s, respectively, as shown in Table **1**. These P_{app} values are similar to values reported by Bhushani *et al.* [29] and Wahlang *et al.* [31], where the intactness of membranes was tested. This also demonstrated that the 5% methanol used to dissolve the anti-malarial drugs would not interrupt the integrity of the Caco-2 monolayer.

Table **1**: The apparent permeability coefficient (P_{app}) values for Lucifer yellow and the reference compounds for absorptive transport.

Compounds	P_{app} (AP-BL) ($\times 10^{-6}$ cm/s)*
Lucifer yellow	0.156 ± 0.080
Lucifer yellow (5% methanol)	0.210 ± 0.096
Caffeine	17.059 ± 0.636
Atenolol	4.836 ± 1.574

*Mean ± standard deviation of mean (n = 3). Key to abbreviations: AP-BL – apical-to-basolateral direction.

Vinblastine is a known P-gp substrate and was used to validate the ability of the Caco-2 cell model to efflux compounds under the culturing conditions used in this study [33]. The P_{app} values in both directions for vinblastine alone and in combination with verapamil are presented in Figure **2.**

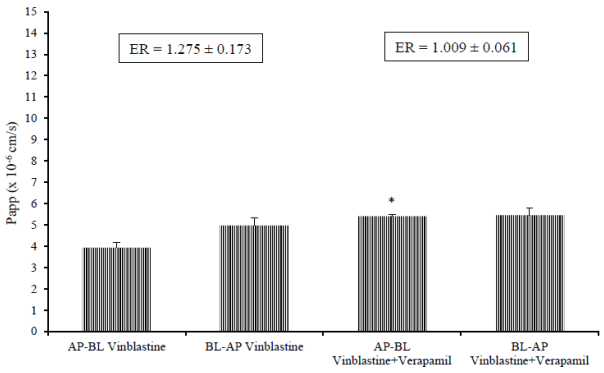

Figure 2: Bi-directional P_{app} values for vinblastine in the presence and absence of verapamil (n = 3, error bars indicate the standard deviation, * statistically significantly different from the control group).

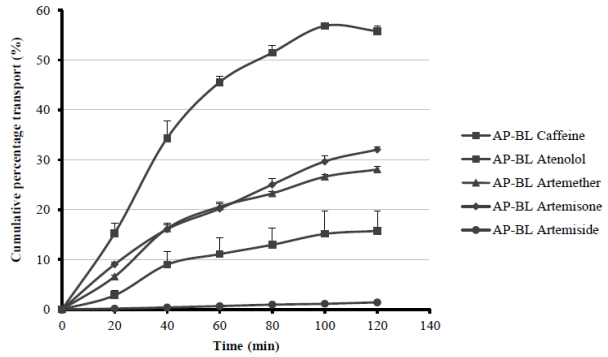

Figure 3: Cumulative percentage transport of the artemisinin derivatives and two reference compounds, caffeine and atenolol (n = 3; error bars indicate standard deviation).

Table 2: Kinetic analysis of the transport data of the artemisinin derivatives and two reference compounds in the apical to basolateral direction

Compound	**Zero order model**		
	k0	**R_obs–pre**	**COD**
Caffeine	0.575	0.943	0.837
Atenolol	0.152	0.966	0.913
Artemether	0.272	0.963	0.892
Artemisone	0.298	0.984	0.940
Artemiside	0.011	0.998	0.993
	First order model		
	k1	**R_obs–pre**	**COD**
Caffeine	0.009	0.980	0.954
Atenolol	0.002	0.972	0.932
Artemether	0.003	0.972	0.932
Artemisone	0.004	0.992	0.974
Artemiside	0.000	0.998	0.992

Key to abbreviations: k0 = zero order rate constant, k1 = first order rate constant, R_obs–pre = correlation coefficient and COD = coefficient of determination

It can be seen that verapamil, a known inhibitor of P-gp and standard inhibitor used in Caco-2 based transport studies, induced a statistically significant increase (T-test, $p < 0.05$; Mann-Whitney U test, $p < 0.1$) to the absorptive transport of vinblastine (AP-BL). The efflux ratio (ER) value of vinblastine also decreased in combination with verapamil (ER = 1.009), and although it was not statistically significantly different from the ER value for vinblastine alone (ER = 1.275) with the T-test ($p = 0.065$), it was significant with the Mann-Whitney U test ($p = 0.081$). This decrease indicated the suitability of the Caco-2 cell culture for investigation of the efflux of compounds via the P-gp efflux transporter protein. To confirm this, additional validation was performed (results not shown) with the fluorescent model marker, Rhodamine 123 (Rh123). Transport of Rh123 across the Caco-2 monolayer was measured in the absence and presence of 100 µM verapamil. Verapamil decreased the ER of Rh123 from 5.523 to 1.342, confirming the suitability of the Caco-2 model for efflux studies.

3.2. Absorptive and secretory transport of artemisone in the presence and absence of verapamil and piperine

Bi-directional transport of artemisone was measured in the presence and absence of verapamil. Figure **3** depicts the percentage cumulative transport of artemisone in the AP-BL direction as well as the transport of the reference compounds, caffeine (reference compound for high membrane permeation) and atenolol (reference compound for low membrane permeation), while Table 2 depicts the kinetic analysis of the transport data. As illustrated, artemisone exhibited an intermediate level of absorptive transport (32.03%) across the Caco-2 cell monolayers when compared to the two reference compounds (56.85% and 15.75%, respectively). This indicates that although artemisone will probably not be completely absorbed from the gastrointestinal tract, it cannot be classified as a poorly absorbable compound. These results differ slightly from a previous study which found artemisone to be absorbed completely (AP-BL P_{app} of 37-60 x 10^{-6} cm/s), but the concentrations applied were only 10 and 20 µM [10]. They also found the P_{app} values to decrease as the concentrations artemisone increased, and it may be possible to extrapolate that a further increase in concentration would result in a further decrease in transport.

The P_{app} values for artemisone are presented in Figure **4**. The P_{app} value for artemisone transport in the AP-BL direction (9.326 x 10^{-6} cm/s) was lower than that of artemisone in the BL-AP direction (11.496 x 10^{-6} cm/s). This indicates that efflux of the compound takes place. An increase in the uptake

of artemisone in the AP-BL direction occurred in the presence of the P-gp inhibitor, verapamil, but it was not statistically significant when compared to artemisone alone (Figure **4**). The decrease in the efflux of artemisone in the BL-AP direction was significantly ($p < 0.05$) different from artemisone in the absence of verapamil.

Although the extent of efflux was decreased by verapamil, it was not completely inhibited, suggesting that artemisone may not be a specific substrate of P-gp efflux transporters. This correlates well with previous findings [10], where it was also concluded that artemisone is not a substrate for efflux by P-gp transporters. Given that Caco-2 cells not only express P-gp transporters, but the majority of intestinal transporters responsible for drug disposition [34-36], the possibility exists that artemisone may be a substrate for other transporter proteins.

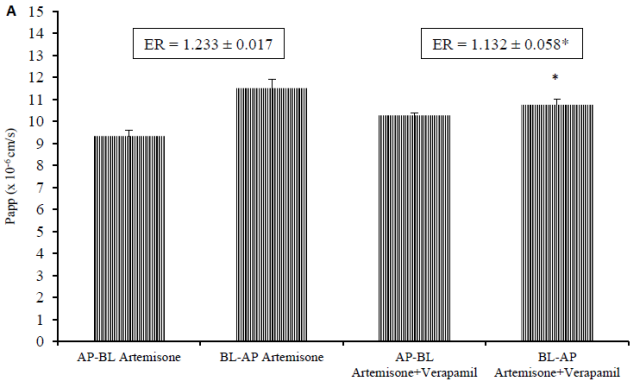

Figure 4: Bi-directional P_{app} values for artemisone in the absence and presence of verapamil ($n = 3$, error bars indicate the standard deviation, * statistically significantly different from the control group).

As indicated in Figure **4**, the efflux ratio value of artemisone was decreased from 1.233 to 1.132 in the presence of verapamil; supporting the finding that artemisone is actively effluxed. This constituted a statistically significant effect (T-test; $p < 0.05$).

The bi-directional transport of artemisone was investigated in the presence of piperine (Figure **5**), to evaluate its potential to enhance the absorption of artemisone. Although the piperine had a relatively small effect on the uptake (AP-BL) of artemisone, the efflux (BL-AP) was significantly reduced.

In addition, the presence of piperine which has been shown to inhibit P-gp [24-25], resulted in a statistically significant (T-test; $p < 0.05$) reduction in the efflux ratio to a value of 1.134. Artemisone is therefore probably a weak substrate for P-gp.

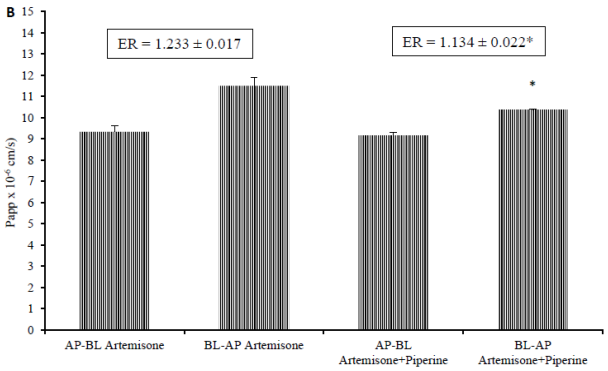

Figure 5: Bi-directional P_{app} values for artemisone in the absence and presence of piperine ($n = 3$, error bars indicate the standard deviation, * statistically significantly different from the control group).

3.3. Absorptive and secretory transport of artemether in the presence and absence of verapamil

As seen from the relative cumulative percentage transport in Figure **3**, artemether also had an intermediate level of absorptive transport (28.06%) compared to the two reference compounds (56.85% and 15.75%, respectively) with slightly lower absorptive transport than that of artemisone. Based on this Caco-2 model, artemether will probably not be completely absorbed from the gastrointestinal tract, similar to artemisone, although it cannot be classified as a poorly absorbed compound.

The P_{app} values for artemether were calculated, and presented in Figure **6**. As indicated, a statistically significant increase ($p < 0.05$) in the P_{app} value for artemether transport in the AP-BL direction (8.367×10^{-6} cm/s) occurred in the presence of verapamil, but artemether in the BL-AP direction (8.852×10^{-6} cm/s) was slightly lowered in the presence of verapamil with no statistical significance. This once again indicates the presence of active efflux, but not necessarily by means of P-gp transporter only.

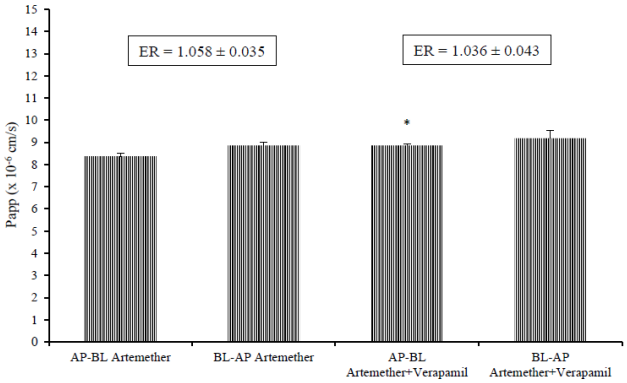

Figure 6: Bi-directional P_{app} values for artemether in the presence and absence of verapamil (n = 3, error bars indicate the standard deviation, * statistically significantly different from the control group).

From the data portrayed in Figure **6**, it can be deduced that the presence of verapamil did not inhibit the extent of efflux of artemether, since the ratio of the P_{app} values in the AP-BL to BL-AP directions remained very consistent with and without inhibition of P-gp by verapamil. These results suggest that, although artemether is actively effluxed, it may not be a substrate of the P-gp transporter specifically. This could indicate that another of the efflux proteins may be involved [34-36]. It would also mean that a combination between artemether and piperine (a P-gp inhibitor) would not be useful to increase the bioavailability of artemether. From Figure **6**, the efflux ratio of artemether was reduced from 1.058 to 1.036 in the presence of verapamil, which is neglible and according to the T-test and Mann-Whitney U test it was also not statistically significant. This supports the conclusion that artemether efflux is not a result of P-gp transporters.

A previous study also indicated that artemether was not an inhibitor of P-gp, and since inhibitors of P-gp are frequently also substrates of P-gp, this finding supports the results of the present study [37].

3.4. Absorptive and secretory transport of artemiside in the presence and absence of verapamil and piperine

From the data of Figure **3**, it is clear that artemiside had a relatively low level of absorptive transport (1.40%), since it was significantly lower than that of the poorly absorbed reference compound, atenolol (15.75%). This indicates that artemiside will probably have a poor bioavailability from a membrane permeation perspective. To clarify if efflux was a contributing factor to the low absorptive transport, the different P_{app} values for artemiside were calculated, and presented in Figure **7**. As indicated, the P_{app} value of artemiside transport in the AP-BL direction (0.424 x 10^{-6} cm/s) was much lower than that of artemiside in the BL-AP direction (0.912 x 10^{-6} cm/s). This suggested that this compound is susceptible to efflux.

The presence of verapamil increased the uptake of artemiside in the AP-BL direction, and there was statistical significance between the two groups in the AP-BL direction. However, verapamil did not reduce the efflux of artemiside in the BL-AP direction. Although the extent of absorptive transport was slightly increased by the P-gp inhibitor, verapamil, the lack of efflux reduction suggest that other efflux transporters may be involved and artemiside may not be a selective substrate for P-gp. As seen in Figure **7**, the efflux ratio of artemiside was decreased from 2.100 to 1.468 in the presence of verapamil, but the difference between the two groups is not statistically significant, thus supporting the fact that artemiside is only effluxed to some extent by P-gp.

Figure 7: Bi-directional P_{app} values for artemiside in the presence and absence of verapamil (n = 3, error bars indicate the standard deviation, # statistically significantly different from the control group).

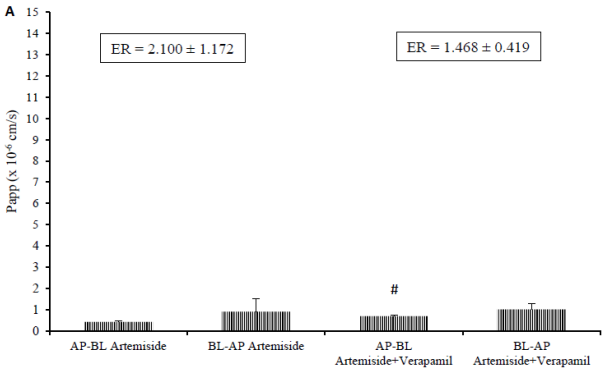

The bi-directional transport of artemiside was also investigated in the presence of piperine, to evaluate its potential to enhance the absorption of artemiside. Piperine had a statistically significant reduction in the apparent permeation coefficient of artemiside in the AP-BL direction from 0.755 x 10^{-6} cm/s to 0.432 x 10^{-6} cm/s (Figure **8**). However, the P_{app} value of artemiside in the BL-AP direction (0.906 x 10^{-6} cm/s) was also significantly increased in the presence of piperine (1.790 x 10^{-6} cm/s).

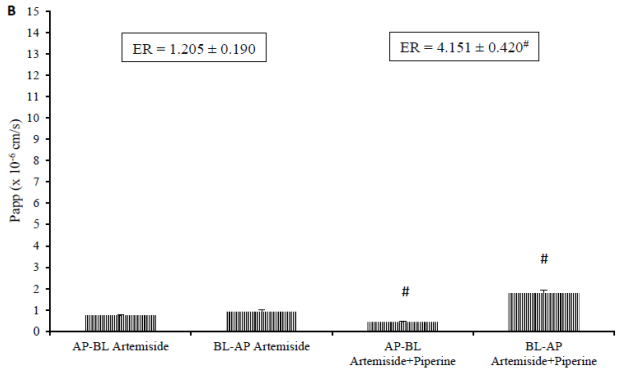

Figure 8: Bi-directional P_{app} values for artemiside in the presence and absence of piperine (n = 3, error bars indicate the standard deviation, # statistically significantly different from the control group).

In addition, piperine which is known to inhibit P-gp displayed a statistically significant increase to the efflux ratio (4.151) when compared to the control group to a value of 1.205 (Figure **8**). This increase in the efflux ratio was unexpected, but it could indicate that the efflux of artemiside may be caused by efflux proteins other than P-gp, and the piperine has an inducing effect on these transporters.

CONCLUSION

The anti-malarial compounds artemisone, artemether and artemiside appear to have intermediate to low membrane permeation properties. These artemisinin derivatives have been shown to be effluxed to various degrees, and artemisone revealed greater efflux affected by P-gp in comparison to artemiside and artemether. It is clear that all of these compounds are substrates of efflux transporters to varying extents, which cannot be related to P-gp alone. Addition of piperine to increase absorptive transport of these compounds had limited success, possibly as a result of the limited P-gp related efflux. The results also suggested that some of the transporters involved in the efflux of these compounds may potentially be induced by piperine.

It is important to keep in mind that a reduction in drug bioavailability due to mutations in transporter genes in the parasite may lead to insufficient amounts of drug reaching the site of action, leading to treatment failure and resistance to anti-malarial drugs [38]. Therefore, further investigation is needed to establish if efflux proteins other than P-gp may be involved in the secretory transport of these anti-malarial compounds, and if these proteins can be inhibited in an effort to increase bioavailability of these drugs.

CONFLICT OF INTEREST

The authors declare no conflict of interest, financial or otherwise. This research was funded under the Flagship Project Scheme of the South African Medical Research Council (MRC) with funds from the National Treasury under its Economic Competiveness and Support Package. The financial assistance of the NRF is hereby also acknowledged.

The views, opinions and findings expressed in this material are those of the authors only, and are not necessarily linked to the MRC or to the NRF.

ACKNOWLEDGEMENTS

Contributions of the authors: H.N.W. obtained and purified artemisone and artemiside; S.H., C.G. designed the experiments; C.W.; J.H. sub-cultured and seeded the Caco-2 mammalian cells on Transwell® plates; J.H. performed the *in vitro* transport studies; J.H., C.W., S.H., C.G. processed and analyzed the data; J.H., C.W., C.G. wrote the first draft of the paper; C.W., C.G., S.H., R.K.H. revised the paper for publishing.

REFERENCES

[1] WHO. *World Malaria Report 2016.* WHO: France, **2016**.

[2] Mehlotra, R.K.; Henry-Halldin, C.N.; Zimmerman, P.A. Application of pharmacogenomics to malaria: a holistic approach for successful chemotherapy. *Pharmacogenomics,* **2009,** *10* (3), 435-449.

[3] Petersen, I.; Eastman, R.; Lanzer, M. Drug-resistant malaria: molecular mechanisms and implications for public health. *FEBS Lett.,* **2011,** *585* (11), 1551-1562.

[4] Muller, I.B.; Hyde, J.E. Antimalarial drugs: modes of action and mechanisms of parasite resistance. *Future Microbiol.,* **2010,** *5* (12), 1857-1873.

[5] Meshnick, S.R.; Dobson, M.J. The history of antimalarial drugs. In: *Antimalarial Chemotherapy: Mechanisms of Action, Resistance, and New Directions in Drug Discovery;* Rosenthal, P.J., Ed.; Humana Press Inc.: Totowa, N.J., **2001**; pp 15-25.

[6] Cui, L.; Mharakurwa, S.; Ndiaye, D.; Rathod, P.K.; Rosenthal, P.J. Antimalarial Drug Resistance: Literature Review and Activities and Findings of the ICEMR Network. *Am. J. Trop. Med. Hyg.,* **2015,** *93* (3 Suppl), 57-68.

[7] Haynes, R.K.; Fugmann, B.; Stetter, J.; Rieckmann, K.; Heilmann, H.D.; Chan, H.W.; Cheung, M.K.; Lam, W.L.; Wong, H.N.; Croft, S.L.; Vivas, L.; Rattray, L.; Stewart, L.; Peters, W.; Robinson, B.L.; Edstein, M.D.; Kotecka, B.; Kyle, D.E.; Beckermann, B.; Gerisch, M.; Radtke, M.; Schmuck, G.; Steinke, W.; Wollborn, U.; Schmeer, K.; Romer, A. Artemisone-a highly active antimalarial drug of the artemisinin class. *Angew. Chem. Int. Ed. Engl.,* **2006,** *45* (13), 2082-2088.

[8] Waknine-Grinberg, J.H.; Hunt, N.; Bentura-Marciano, A.; McQuillan, J.A.; Chan, H.W.; Chan, W.C.; Barenholz, Y.; Haynes, R.K.; Golenser, J. Artemisone effective against murine cerebral malaria. *Malaria J.*, **2010,** *9*, 227.

[9] Guo, J.; Guiguemde, A.W.; Bentura-Marciano, A.; Clark, J.; Haynes, R.K.; Chan, W.C.; Wong, H.N.; Hunt, N.H.; Guy, R.K.; Golenser, J. Synthesis of artemiside and its effects in combination with conventional drugs against severe murine malaria. *Antimicrob. Agents Chemother.*, **2012,** *56* (1), 163-173.

[10] Senarathna, S.M.D.K.G.; Page-Sharp, M.; Crowe, A. The interactions of P-glycoprotein with antimalarial drugs, including substrate affinity, inhibition and regulation. *PLoS ONE*, **2016,** *11* (4), e0152677.

[11] Schinkel, A.H.; Jonker, J.W. Mammalian drug efflux transporters of the ATP binding cassette (ABC) family: an overview. *Adv. Drug Deliv. Rev.*, **2012,** *64*, 138-153.

[12] Fidock, D.A.; Nomura, T.; Talley, A.K.; Cooper, R.A.; Dzekunov, S.M.; Ferdig, M.T.; Ursos, L.M.B.; Sidhu, A.b.S.; Naude, B.; Deitsch, K.W.; Su, X.-Z.; Wootton, J.C.; Roepe, P.D.; Wellems, T.E. Mutations in the *P.falciparum* digestive vacuole transmembrane protein PfCRT and evidence for their role in chloroquine resistance. *Mol. Cell.*, **2000,** *6* (4), 861-871.

[13] Lehane, A.M.; van Schalkwyk, D.A.; Valderramos, S.G.; Fidock, D.A.; Kirk, K. Differential drug efflux or accumulation does not explain variation in the chloroquine response of *Plasmodium falciparum* strains expressing the same isoform of mutant PfCRT. *Antimicrob. Agents Chemother.*, **2011,** *55* (5), 2310-2318.

[14] Lehane, A.M.; Kirk, K. Efflux of a range of antimalarial drugs and 'chloroquine resistance reversers' from the digestive vacuole in malaria parasites with mutant PfCRT. *Mol. Microbiol.*, **2010,** *77* (4), 1039-1051.

[15] Lin, J.H.; Yamazaki, M. Role of P-glycoprotein in pharmacokinetics: clinical implications. *Clin. Pharmacokinet.*, **2003,** *42* (1), 59-98.

[16] Sidhu, A.B.; Uhlemann, A.C.; Valderramos, S.G.; Valderramos, J.C.; Krishna, S.; Fidock, D.A. Decreasing *pfmdr1* copy number in *Plasmodium falciparum* malaria heightens susceptibility to mefloquine, lumefantrine, halofantrine, quinine, and artemisinin. *J. Infect. Dis.*, **2006,** *194*, 528-535.

[17] Lanteri, C.A.; Chaorattanakawee, S.; Lon, C.; Saunders, D.L.; Rutvisuttinunt, W.; Yingyuen, K.; Bathurst, I.; Ding, X.C.; Tyner, S.D. *Ex vivo* activity of endoperoxide antimalarials, including artemisone and arterolane, against multidrug-resistant *Plasmodium falciparum* isolates from Cambodia. *Antimicrob. Agents Chemother.*, **2014,** *58* (10), 5831-5840.

[18] Muthaura, C.N.; Keriko, J.M.; Derese, S.; Yenesew, A.; Rukunga, G.M. Investigation of some medicinal plants traditionally used for treatment of malaria in Kenya as potential sources of antimalarial drugs. *Exp. Parasitol.*, **2011,** *127* (3), 609-626.

[19] WHO. *WHO Traditional Medicine Strategy 2002-2005*. WHO: Geneva, Switzerland, **2002**.

[20] WHO. *WHO Traditional Medicine Strategy*. WHO: Geneva, Switzerland, **2013**.

[21] Mukherjee, P.K.; Wahile, A. Integrated approaches towards drug development from Ayurveda and other Indian system of medicines. *J. Ethnopharmacol.*, **2006,** *103*, 25-35.

[22] Oga, E.F.; Sekine, S.; Shitara, Y.; Horie, T. Pharmacokinetic Herb-Drug Interactions: Insight into Mechanisms and Consequences. *Eur. J. Drug Metab. Pharmacokinet.*, **2016,** *41* (2), 93-108.

[23] Barnes, J.; Anderson, L.A.; Phillipson, J.D. *Herbal Medicines*. 3rd ed.; Pharmaceutical Press: London, UK, **2007**.

[24] Han, Y.; Chin Tan, T.M.; Lim, L.Y. *In vitro* and *in vivo* evaluation of the effects of piperine on P-gp function and expression. *Toxicol. Appl. Pharmacol.*, **2008,** *230* (3), 283-289.

[25] Bhardwaj, R.K.; Glaeser, H.; Becquemont, L.; Klotz, U.; Gupta, S.K.; Fromm, M.F. Piperine, a major constituent of black pepper, inhibits human P-glycoprotein and CYP3A4. *J. Pharmacol. Exp. Ther.*, **2002,** *302* (2), 645-650.

[26] Natoli, M.; Leoni, B.D.; D'Agnano, I.; Zucco, F.; Felsani, A. Good Caco-2 cell culture practices. *Toxicol. In Vitro*, **2012,** *26* (8), 1243-1246.

[27] Chen, Y.; Wang, Y.; Zhou, J.; Gao, X.; Qu, D.; Liu, C. Study on the mechanism of intestinal absorption of epimedins a, B and C in the Caco-2 cell model. *Molecules*, **2014,** *19* (1), 686-698.

[28] Shikanga, E.A.; Hamman, J.H.; Chen, W.; Combrinck, S.; Gericke, N.; Viljoen, A.M. *In vitro* permeation of mesembrine alkaloids from *Sceletium tortuosum* across porcine buccal, sublingual, and intestinal mucosa. *Planta Med.*, **2012,** *78* (3), 260-268.

[29] Bhushani, J.A.; Karthik, P.; Anandharamakrishnan, C. Nanoemulsion based delivery system for improved bioaccessibility and Caco-2 cell monolayer permeability of green tea catechins. *Food Hydrocoll.*, **2016,** *56*, 372-382.

[30] Alqahtani, S.; Mohamed, L.A.; Kaddoumi, A. Experimental models for predicting drug absorption and metabolism. *Expert Opin. Drug Metab. Toxicol.*, **2013,** *9* (10), 1-14.

[31] Wahlang, B.; Pawar, Y.B.; Bansal, A.K. Identification of permeability-related hurdles in oral delivery of curcumin using the Caco-2 cell model. *Eur. J. Pharm. Biopharm.*, **2011,** *77* (2), 275-282.

[32] Tarirai, C.; Viljoen, A.M.; Hamman, J.H. Effects of dietary fruits, vegetables and a herbal tea on the *in vitro* transport of cimetidine: comparing the Caco-2 model with porcine jejunum tissue. *Pharm. Biol.*, **2012,** *50* (2), 254-263.

[33] Ogihara, T.; Kamiya, M.; Ozawa, M.; Fujita, T.; Yamamoto, A.; Yamashita, S.; Ohnishi, S.; Isomura, Y. What kinds of substrates show P-glycoprotein-dependent intestinal absorption? Comparison of verapamil with vinblastine. *Drug Metab. Pharmacokinet.*, **2006,** *21* (3), 238-244.

[34] Brück, S.; Strohmeier, J.; Busch, D.; Drozdzik, M.; Oswald, S. Caco-2 cells - expression, regulation and function of drug transporters compared with human jejunal tissue. *Biopharm. Drug Dispos.,* **2017,** *38* (2), 115-126.

[35] Olander, M.; Wisniewski, J.R.; Matsson, P.; Lundquist, P.; Artursson, P. The Proteome of Filter-Grown Caco-2 Cells With a Focus on Proteins Involved in Drug Disposition. *J. Pharm. Sci.,* **2016,** *105* (2), 817-827.

[36] Hayeshi, R.; Hilgendorf, C.; Artursson, P.; Augustijns, P.; Brodin, B.; Dehertogh, P.; Fisher, K.; Fossati, L.; Hovenkamp, E.; Korjamo, T.; Masungi, C.; Maubon, N.; Mols, R.; Mullertz, A.; Monkkonen, J.; O'Driscoll, C.; Oppers-Tiemissen, H.M.; Ragnarsson, E.G.; Rooseboom, M.; Ungell, A.L. Comparison of drug transporter gene expression and functionality in Caco-2 cells from 10 different laboratories. *Eur. J. Pharm. Sci.,* **2008,** *35* (5), 383-396.

[37] Oga, E.F.; Sekine, S.; Shitara, Y.; Horie, T. Potential P-glycoprotein-mediated drug-drug interactions of antimalarial agents in Caco-2 cells. *Am. J. Trop. Med. Hyg.,* **2012,** *87* (1), 64-69.

[38] Paloque, L.; Ramadani, A.P.; Mercereau-Puijalon, O.; Augereau, J.M.; Benoit-Vical, F. *Plasmodium falciparum*: multifaceted resistance to artemisinins. Malaria J., 2016, 15, 1-12.

Received: March 20, 2014. Revised: April 16, 2014. Accepted: April 20, 2014

CHAPTER 5: FINAL CONCLUSIONS AND FUTURE RECOMMENDATIONS

5.1 Final conclusions

The biopharmaceutical and pharmacokinetic properties of drugs that are orally administrated need to be investigated since these aspects ultimately determine the efficacy of drugs. Drug absorption after oral administration takes place across the intestinal epithelium from the gastro-intestinal lumen into the blood circulation, while secretory transport (i.e. efflux from the epithelial cells back into the lumen) reduces the bioavailability of drugs. One of these transporters, P-glycoprotein (P-gp), lowers the uptake of drug molecules by actively pumping them from the epithelial cells back into the gastro-intestinal lumen (Chan *et al.*, 2004:26).

Malaria is one of the world's biggest health concerns since more than 200 million people are affected each year and increasing resistance to anti-malarial drugs causing treatment failure and recrudescence of malaria implores the need to discover new drugs. New promising artemisinin derivatives are currently being developed, but limited information on the membrane permeability properties of these drugs are available. It was important to investigate the absorptive and secretory transport of these drugs across intestinal epithelia as an indication of their bioavailability, and to identify if they are efflux transporter substrates, which may contribute to poor bioavailability and/or occurrence of drug resistance.

Bi-directional studies of these compounds were executed on the well-known Caco-2 *in vitro* cell monolayer model, after validation of both the model and the analytical methods. The validation results presented in Chapter 3 clearly indicated that the integrity of the Caco-2 cell monolayer was intact using the culturing method described, and this integrity was not compromised by the presence of methanol in the experimental solutions. The efflux of vinblastine also confirmed the expression of P-gp transporters by the Caco-2 cells. It was further demonstrated that the various analytical methods used to quantify the compounds met each validation criteria, and therefore were adequate for sample analysis during transport studies.

The results from this study have revealed that the permeability of artemether and artemisone was relatively moderate in relation to the reference compounds, caffeine and atenolol, but artemiside demonstrated very limited permeability. This could indicate potential bioavailability problems, and could be a result of excessive first-pass metabolism or marked efflux. Bi-directional transport in the absence and presence of verapamil, a known P-gp inhibitor, revealed artemisone and

artemiside to be susceptible to P-gp related efflux to some extent. However, P-gp related efflux of artemiside appeared to be very limited. The data also showed that artemiside and artemether had a statistically significant increase ($p < 0.05$) in absorption in the presence of verapamil, but only a minor increase in efflux. This suggests that efflux proteins other than P-gp may be involved in the active secretory transport of these artemisinin derivatives.

Piperine, an active constituent used in traditional medicine, is known to inhibit the P-gp transporter proteins. It is therefore a valuable compound to be combined with drugs that are susceptible to efflux in an effort to increase their bioavailability. In this study, since artemether did not appear to be a P-gp substrate, only the effect of piperine on the bi-directional transport of artemiside and artemisone was investigated. The efflux of artemisone was decreased more by piperine than by verapamil, which was statistically significant according to the Dunnett post-hoc test. On the contrary, the efflux of artemiside was significantly increased by piperine, which was statistically significant (according to the T-test). This unexpected increase in the efflux could possibly indicate that other efflux proteins are involved with artemiside and that piperine has a stimulating effect on these transporters.

Since resistance of the *Plasmodium* parasite has been ascribed to mainly two mechanism, namely drug transporter alterations resulting in reduced availability of the drugs at the site of action and, secondly, drug target modification (Paloque *et al.*, 2016); it is important to know which transporters are involved in the active secretion of anti-malarial compounds.

5.2 Future recommendation

The results that were obtained from this study suggested that the artemisinin derivatives are effluxed to different extents. The efflux of artemiside and artemether needs further investigation to identify which efflux transporters are responsible for their active transport in the secretory direction. Furthermore, the extent of efflux by the parasite should be investigated to identify potential resistance via this mechanism.

Even though the Caco-2 cell culture model is morphological and physiological similar to that of the human gastrointestinal epithelium, it could be helpful if the results were compared to other *in vitro* and *in vivo* methods. Comparison to other methods may clarify some of the results of this preliminary study, as every method has its own advantages and disadvantages. The Ussing chamber is recommended to examine the anti-malarial drug transport across excised jejunal tissue of pigs, while *in vivo* studies can be conducted in laboratory animals such as mice or rats.

Since the artemisinin derivatives did not have high permeation across the Caco-2 cell monolayers, a further recommendation would be to evaluate the contribution of first-pass metabolism during movement across the intestinal epithelium. This could provide another target (e.g. enzyme inhibition) to potentially increase the bioavailability of the drugs.

BIBLIOGRAPHY

Ahuja, S. 2007. HPLC Method Development for Pharmaceuticals, Volume 8, edited by S. Ahuja & S. Rasmussen
https://books.google.co.za/books?hl=en&lr=&id=yRAjTMwbaGYC&oi=fnd&pg=PP1&dq=HPLC+Method+Development+for+Pharmaceuticals&ots=GvOzr7rGt-&sig=aJcsr5tnD8Zd8sCnUNiWbvcygqg#v=onepage&q=HPLC%20Method%20Development%20for%20Pharmaceuticals&f=false
Date of access: 23 October 2017.

Ajazuddin, Alexander, A., Qureshi, A., Kumari, L., Vaishnav, P., Sharma, M., Saraf, S. & Saraf, S. 2014. Role of herbal bioactives as a potential bioavailability enhancer for Active Pharmaceutical Ingredients. *Fitoterapia*, 97:1-14.

Alam, M.A., Al-Jenoobi, F.I. & Al-Mohizea, A.M. 2012. Everted gut sac model as a tool in pharmaceutical research: limitations and applications. *The Journal of Pharmacy and Pharmacology*, 64(3):326-336.

Ali, S., Najmi, M.H., Tarning, J. & Lindegardh, N. 2010. Pharmacokinetics of artemether and dihydroartemisinin in healthy Pakistani male volunteers treated with artemether-lumefantrine. *Malaria Journal,* 9:275.

Alqahtani, S., Mohamed, L.A. & Kaddoumi, A. 2013. Experimental models for predicting drug absorption and metabolism. *Expert Opinion on Drug Metabolism & Toxicology*, 9(10):1-14.

Amaratunga, C., Lim, P., Suon, S., Sreng, S., Mao, S., Sopha, C., Sam, B., Dek, D., Try, V., Amato, R., Blessborn, D., Song, L., Tullo, G.S., Fay, M.P., Anderson, J.M., Tarning, J. & Fairhurst, R.M. 2016. Dihydroartemisinin–piperaquine resistance in *Plasmodium falciparum* malaria in Cambodia: a multisite prospective cohort study. *The Lancet. Infectious Diseases*, 16(3):357-365.

Amato, R., Lim, P., Miotto, O., Amaratunga, C., Dek, D., Pearson, R.D., Almagro-Garcia, J., Neal, A.T., Sreng, S., Suon, S., Drury, E., Jyothi, D., Stalker, J., Kwiatkowski, D.P. & Fairhurst, R.M. 2017. Genetic markers associated with dihydroartemisinin–piperaquine failure in *Plasmodium falciparum* malaria in Cambodia: a genotype-phenotype association study. *The Lancet. Infectious Diseases*, 17(2):164-173.

Anderson, J.M. & Van Itallie, C.M. 2009. Physiology and Function of the Tight Junction. *Cold Spring Harbor Perspectives in Biology*, 1(2):1-16.

Ashley, E.A., Dhorda, M., Fairhurst, R.M., Amaratunga, C., Lim, P., Suon, S., Sreng, S., Anderson, J.M., Mao, S., Sam, B., Sopha, C., Chuor, C.M., Nguon, C., Sovannaroth, S., Pukrittayakamee, S., Jittamala, P., Chotivanich, K., Chutasmit, K., Suchatsoonthorn, C., Runcharoen, R., Hien, T.T., Thuy-Nhien, N.T., Thanh, N.V., Phu, N.H., Htut, Y., Han, K-T., Aye, K.H., Mokuolu, O.A., Olaosebikan, R.R., Folaranmi, O.O., Mayxay, M., Khanthavong, M., Hongvanthong, B., Newton, P.N., Onyamboko, M.A., Fanello, C.I., Tshefu, A.K., Mishra, N., Valecha, N., Phyo, A.P., Nosten, F., Yi, P., Tripura, R., Borrmann, S., Bashraheil, M., Peshu, J., Faiz, M.A. Ghose, A., Hossain, M.A., Samad, R., Rahman, M.R., Hasan, M.M., Islam, A., Miotto, O., Amato, R., MacInnis, B., Stalker, J., Kwiatkowski, D.P., Bozdech, Z., Jeeyapant, A., Cheah, P.Y., Sakulthaew, T., Chalk, J., Intharabut, B. Silamut, K., Lee, S.J., Vihokhern, B., Kunasol, C., Imwong, M., Tarning, J., Taylor, W.J., Yeung, S., Woodrow, C.J., Flegg, J.A., Das, D., Smith, J., Venkatesan, M., Plowe, C.V. Stepniewska, K., Guerin, P.J., Dondorp, A.M. Day, N.P., & White, N.J. 2014. Spread of Artemisinin Resistance in *Plasmodium falciparum* Malaria. *The New England Journal of Medicine*, 371:411-423.

Balimane, P.V., Chong, S. & Morrison, R.A. 2000. Current methodologies used for evaluation of intestinal permeability and absorption. *Journal of Pharmacological and Toxicological Methods*, 44(1):301-312.

Barthe, L., Woodley, J.F., Kenworthy, S., & Houin, G. 1998. An improved everted gut sac as a simple and accurate technique to measure paracellular transport across the small intestines. *European Journal of Drug Metabolism and Pharmacokinetics*, 23(2):313-323.

Bell, D. & Winstanley, P. 2005. Current issues in the treatment of uncomplicated malaria in Africa. *British Medical Bulletin*, 71(1):29-43.

Belorgey, D., Lanfranchi, D.A. & Davioud-Charvet, E. 2013. 1,4-Naphthoquinones and Others NADPH-Dependent Glutathione Reductase-Catalyzed Redox Cyclers as Antimalarial Agents. *Current Pharmaceutical Design*, 19(14):1-44.

Bhardwaj, R.K., Glaeser, H., Becquemont, L., Klotz, U., Gupta, S.K. & Fromm, M.F. 2002. Piperine, a Major Constituent of Black Pepper, Inhibits Human P-glycoprotein and CYP3A4. *Journal of Pharmacology and Experimental Therapeutics*, 302(2):645-650.

Blumberg, L.H. 2015. Recommendations for the treatment and prevention of malaria: Update for the 2015 season in South Africa. *South African Medical Journal,* 105(3):175-178

Borrmann, S., Adegnika, A.A., Missinou, M.A., Binder, R.K., Issifou, S., Schindler, A., Matsiegui, P.B., Kun, J.F., Krishna, S., Lell, B. & Kremsner, P.G. 2003. Short-Course Artesunate Treatment of Uncomplicated *Plasmodium falciparum* Malaria in Gabon. *Antimicrobial Agents and Chemotherapy*, 47(3):901-904.

Bourdy, G., Willcox, M.L., Ginsburg, H., Rasoanaivo, P., Graz, B. & Deharo, E. 2008. Ethnopharmacology and malaria: New hypothetical leads or old efficient antimalarials? *International Journal for Parasitology*, 38(1):33-41.

Bressolle, F., Bromet-Petit, M. & Audran, M. 1996. Validation of liquid chromatographic and gas chromatographic methods Applications to pharmacokinetics. *Journal of Chromatography. B, Biomedical Applications*, 686(1):3-10.

Brijlal, N., Khoza, N., Mbonane, N., Meyiwa, S., Moodley, S., Parbhoo, T., Pillay, E., Lubbe, M. & Bodenstein, J. 2011. The attitudes and knowledge of pharmacists towards the use of herbal medicine. *South African Pharmaceutical Journal*, 78(7):35-37.

Carter, R. & Mendis, K.N. 2002. Evolutionary and Historical Aspects of the Burden of Malaria. *Clinical Microbiology Reviews*, 15(4):564-594.

CDC. Centers of Disease Control and Prevention. Date of access: 28 Jun. 2016. https://www.cdc.gov/malaria/about/biology/

Chan, L.M.S., Lowes, S. & Hirst, B.H. 2004. The ABCs of drug transport in intestine and liver: efflux proteins limiting drug absorption and bioavailability. *European Journal of Pharmaceutical Sciences*, 21(1):25-51.

Colombo, D., Lunardon, L. & Bellia, G. 2014. Cyclosporine and Herbal Supplement Interactions. *Journal of Toxicology*:1-6.

Cordier, W. & Steenkamp, V. 2011. Drug interactions in African herbal remedies. *Drug Metabolism and Drug Interactions*, 26(2):53-63.

Cox, F.E. 2010. History of the discovery of the malaria parasites and their vectors. *Parasites & Vectors*, 3(1):1-9.

Cui, L., Mharakurwa, S., Ndiaye, D., Rathod, P.K. & Rosenthal, P.J. 2015. Antimalarial Drug Resistance: Literature Review and Activities and Findings of the ICEMR Network. *The American Journal of Tropical Medicine and Hygiene*, 93(3):57-68.

Daugherty, A.L. & Mrsny, R.J. 1999. Transcellular uptake mechanisms of the intestinal epithelial barrier Part one. *Pharmaceutical Science & Technology Today*, 2(4):144-151.

De Ridder, S., Van der Kooy, F. & Verpoorte, R. 2008. Artemisia annua as a self-reliant treatment for malaria in developing countries. *Journal of Ethnopharmacology*, 120(3):302-314.

Dixit, P., Jain, D.K. & Dumbwani, J. 2012. Standardization of an *ex vivo* method for determination of intestinal permeability of drugs using everted rat intestine apparatus. *Journal of Pharmacological and Toxicological Methods*, 65(1):13-17.

Dong, M.W. 2006. Modern HPLC for Practicing Scientists. New Jersey: John Wiley & Sons, Inc. 286 p.

El-Kattan, A & Varma, M. 2012. Oral Absorption, Intestinal Metabolism and Human Oral Bioavailability. *In*: PAXTON, J, ed. *Topics on Drug Metabolism*, Croactia: InTech. 1-34 p.

Estudante, M., De Mello-Sampayo, C., Sahin, S., Morais, J. & Benet, L.Z. 2015. The utility of *in vitro* trials that use Caco-2 cell systems as a replacement for animal intestinal permeability and human bioequivalence measurements in drug development. *Biomedical and Biopharmaceutical Research*, 12(1):117-126.

Estudante, M., Morais, J.G., Soveral, G. & Benet, L.Z. 2013. Intestinal drug transporters: An overview. *Advanced Drug Delivery Reviews*, 65(10):1340-1356.

Fasinu, P.S., Bouic, P.J. & Rosenkranz, B. 2012. An Overview of the Evidence and Mechanisms of Herb–Drug Interactions. *Frontiers in Pharmacology*, 3:1-19.

Fenwick, N., Griffen, G. & GAuthier, C. 2009. The welfare of animals used in science: How the “Three Rs” ethic guides improvements. *The Canadian Veterinary Journal*, 50(5):523-530.

Gavhane, Y.N. & Yadav, A.V. 2012. Loss of orally administered drugs in GI tract. *Saudi Pharmaceutical Journal*, 20(4):331-344.

Greenwood, B.M. & Targett, G.A. 2011. Malaria vaccines and the new malaria agenda. *Clinical Microbiology and Infection*, 17(11):1600-1607.

Guo, J., Guiguemde, A.W., Bentura-Marciano, A., Clark, J., Haynes, R.K., Chan, W.C., Wong, H.N., Hunt, N.H., Guy, R.K. & Golenser, J. 2012. Synthesis of artemiside and its effects in combination with controventional drugs against severe murine malaria. *Antimicrobial Agents and Chemotherapy*, 56(1):163-173.

Gurley, B.J. 2012. Pharmacokinetic Herb-Drug Interactions (Part 1): Origins, Mechanisms, and the Impact of Botanical Dietary Supplements. *Planta Medica*, 78(13):1478-1489.

Gurley, B.J., Fifer, E.K. & Gardner, Z. 2012. Pharmacokinetic Herb-Drug Interactions (Part 2): Drug Interactions Involving Popular Botanical Dietary Supplements and Their Clinical Relevance. *Planta Medica*, 78(13):1490-1514.

Haynes, R.K., Chan, W.C., Wong, H.N., Li, K.Y., Wu, W.K., Fan, K.M., Sung, H.H., Williams, I.D., Prosperi, D., Melato, S., Coghi, P. & Monti, D. 2010. Facile oxidation of leucomethylene blue and dihydroflavins by artemisinins: relationship with flavoenzyme function and antimalarial mechanism of action. *ChemMedChem*, 5(8):1282-1299.

Ho, W.E., Peh, H.Y. & Chan, T.K., Wong, W.S.F. 2014. Artemisinins: Pharmacological actions beyond anti-malarial. *Pharmacology & Therapeutics*, 142(1):126-139.

Holmstock, N., Annaert, P. & Augustijns, P. 2012. Boosting of HIV Protease Inhibitors by Ritonavir in the Intestine: The Relative Role of Cytochrome P450 and P-Glycoprotein Inhibition Based on Caco-2 Monolayers versus *In Situ* Intestinal Perfusion in Mice. *Drug Metabolism and Disposition*, 40(8):1473-1477.

Hunter, J. & Hirst, B.H. 1997. Intestinal secretion of drugs. The role of P-glycoprotein and related drug efflux systems in limiting oral drug absorption. *Advanced Drug Delivery Reviews*, 25(2-3):129-157.

Hyde, J.E. 2005. Drug-resistant malaria. *Trends in Parasitology*, 21(11):494-498.

Izzo, A.A. 2005. Herb–drug interactions: an overview of the clinical evidence. *Fundamental & Clinical Pharmacology*, 19(1):1-16.

Karamati, S.A., Hassanzadazar, H., Bahmani, M. & Rafieian-Kopaei, M. 2014. Herbal and chemical drugs effective on malaria. *Asian Pacific Journal of Tropical Disease*, 4(Suppl 2):599-600.

Kerns, E.H. & Di, L. 2008. Permeability. *In*: *Drug-like Properties: Concepts, Structure Design and Methods: from ADME to Toxicity Optimization*, San Diego: Academic Press. 86-99 p.

Küblbeck, J., Hakkarainen, J.J., Petsalo, A., Vellonen, K., Tolonen, A., Reponen, P., Forsberg, M.M. & Honkakoski, P. 2016. Genetically Modified Caco-2 Cells With Improved Cytochrome P450 Metabolic Capacity. *Journal of Pharmaceutical Sciences*, 105(2):941-949.

Kumar, A., Kishore, L., Kaur, N. & Nair, A. 2012. Method development and validation: Skills and tricks. *Chronicles of Young Scientists*, 3(1):3-11.

Le Ferrec, E., Chesne, C., Artusson, P., Brayden, D., Fabre, G., Gires, P., Guillou, F., Rousset, M., Rubas, W. & Scarino, M.L. 2001. *In vitro* models of the intestinal barrier. *Alternatives to Laboratory Animals*, 29(6):649-668.

Lehane, A.M. & Kirk, K. 2008. Chloroquine Resistance-Conferring Mutations in *pfcrt* Give Rise to a Chloroquine-Associated H^+ Leak from the Malaria Parasite's Digestive Vacuole. *Antimicrobial Agents and Chemotherapy*, 52(12):4374-4380.

Li, C., Wang, Q., Ren, T., Zhang, Y., Lam, C.W.K., Chow, M.S.S. & Zuo, Z. 2016. Non-linear pharmacokinetics of piperine and its herb-druginteractions with docetaxel in Sprague-Dawley rats. *Journal of Pharmaceutical and Biomedical Analysis*, 128:286-293.

Lin, J.H. & Yamazaki, M. 2003. Role of P-Glycoprotein in Pharmacokinetics: Clinical Implications. *Clinical Pharmacokinetics*, 42(1):59-98.

Liu, C.X., Yi, X.L., Si, D.Y., Xiao, X.F., He, X. & Li, Y.Z. 2011. Herb-drug Interactions Involving Drug Metabolizing Enzymes and Transporters. *Current Drug Metabolism*, 12(9):835-849.

Liu, M.Z., Zhang, Y.L., Zeng, M.Z., He, F.Z., Luo, Z.Y., Luo, J.Q., Wen, J.G., Chen, X.P., Zhou, H.H. & Zhang, W. 2015. Pharmacogenomics and Herb-Drug Interactions: Merge of Future and Tradition. *Evidence-based Complementary and Alternative Medicine*:1-8.

Luo, Z., Liu, Y., Zhao, B., Tang, M., Dong, H., Zhang, L., Lv, B. & Wei, L. 2013. *Ex vivo* and *in situ* approaches used to study intestinal absorption. *Journal of Pharmacological and Toxicological Methods*, 68(2):208-216.

Makanga, M. 2014. A review of the effects of artemether-lumefantrine on gametocyte carriage and disease transmission. *Malaria Journal*, 13:291-315.

Malviya, R., Bansal, V., Pal, O.P. & Sharma, P.K. 2010. High performance liquid chromatography: A short review. *Journal of Global Pharma Technology*, 2(5):22-26.

Marchetti, S., Mazzanti, R., Beijnen, J.H. & Schellens, J.H. 2007. Concise Review: Clinical Relevance of Drug–Drug and Herb–Drug Interactions Mediated by the ABC Transporter ABCB1 (MDR1, P-glycoprotein). *The Oncologist*, 12(8):927-941.

Medana, I.M. & Turner, G.D. 2006. Human cerebral malaria and the blood–brain barrier. *International Journal for Parasitology*, 36(5):555-568.

Mita, T., Tanabe, K. & Kita, K. 2009. Spread and evolution of *Plasmodium falciparum* drug resistance. *Parasitology International*, 58(3):201-209.

Miyake, M., Koga, T., Kondo, S., Yoda, N., Emoto, C., Mukai, T. & Toguchi, H. 2017. Prediction of drug intestinal absorption in human using the Ussing chamber system: A comparison of intestinal tissues from animals and humans. *European Journal of Pharmaceutical Sciences*, 96:373-380.

Moreno, A. & Joyner, C. 2015. Malaria vaccine clinical trials: what's on the horizon. *Current Opinion in Immunology*, 35:98-106.

Müller, I.B. & Hyde, J.E. 2010. Antimalarial drugs: modes of action and mechanisms of parasite resistance. *Future Microbiology*, 5(12):1857-1873.

Nožinić, D., Milić, A., Mikac, L., Ralić, J., Padovan, J. & Antolović, R. 2010. Assessment of Macrolide Transport Using PAMPA, Caco-2 and MDCKII-hMDR1 Assays. *Croatica Chemica Acta*, 83(3):323-331.

Oga, E.F., Sekine, S., Shitara, Y. & Horie, T. 2012. P-glycoprotein mediated efflux in Caco-2 cell monolayers: the influence of herbals on digoxin transport. *Journal of Ethnopharmacology*, 144(3):612-617.

Olliaro, P. 2001. Mode of action and mechanisms of resistance for antimalarial drugs. *Pharmacology & Therapeutics*, 89(2):207-219.

Pal, D. & Mitra, A.K. 2006. MDR- and CYP3A4-mediated drug–herbal interactions. *Life Sciences*, 78(18):2131-2145.

Paloque, L., Ramadani, A.P., Mercereau-Puijalon, O., Augereau, J.M. & Benoit-Vical, F. 2016. *Plasmodium falciparum*: multifaceted resistance to artemisinins. *Malaria Journal*, 15:1-12.

Panchagnula, R. & Thomas, R.S. 2000. Biopharmaceutics and pharmacokinectics in drug research. *International Journal of Pharmaceutics*, 201(2):131-150.

Percário, S., Moreira, D.R., Gomes, B.A.Q., Ferreira, M.E.S., Gonçalves, A.C.M., Laurindo, P.S.O.C., Vilhena, T.C., Dolabela, M.F. & Green, M.D. 2012. Oxidative Stress in Malaria. *International Journal of Molecular Sciences*, 13(12):16346-16372.

Petersen, I., Eastman, R. & Lanzer, M. 2011. Drug-resistant malaria: Molecular mechanisms and implications for public health. *FEBS Letters*, 585(11):1551-1562.

Posadzki, P., Watson, L. & Ernst, E. 2013. Herb–drug interactions: an overview of systematic reviews. *British Journal of Clinical Pharmacology*, 75(3):603-618.

Rahman, T., Hosen, I., Islam, M.M.T, & Shekhar, H.U. 2012. Oxidative stress and human health. *Advances in Bioscience and Biotechnology*, 3(7A):997-1019.

Rosenberg, M.F., Callaghan, R., Ford, R.C. & Higgins, C.F. 1997. Structure of the Multidrug Resistance P-glycoprotein to 2.5 nm Resolution Determined by Electron Microscopy and Image Analysis. *The Journal of Biological Chemistry*, 272(16):10685-10694.

Sanchez, C.P., Dave, A., Stein, W.D. & Lanzer, M. 2010. Transporters as mediators of drug resistance in *Plasmodium falciparum*. *International Journal for Parasitology*, 40(10):1109-1118.

Sanchez, C.P., Stein, W.D. & Lanzer, M. 2007. Is PfCRT a channel or a carrier? Two competing models explaining chloroquine resistance in *Plasmodium falciparum*. *Trends in Parasitology*, 23(7):332-339.

Schellack, G. 2011. Drug dosage forms and the routes of drug administration. *Nursing Pharmacology and Medicine Management*, 15(6):10-15.

Shabir, G.A. 2003. Validation of high-performance liquid chromatography methods for pharmaceutical analysis. Understanding the differences and similarities between validation requirements of the US Food and Drug Administration, the US Pharmacopeia and the International Conf. *Journal of Chromatography A*, 987(1-2):57-66.

Shabir, G.A. 2004. A Practical Approach to Validation of HPLC Methods Under Current Good Manufacturing Practices. *Journal of Validation Technology*:29-37.

Shah, P., Jogani, V., Bagchi, T. & Misra, A. 2006. Role of Caco-2 Cell Monolayers in Prediction of Intestinal Drug Absorption. *Biotechnology Progress*, 22(1):186-198.

Sharom, F.J. 2008. ABC multidrug transporters: structure, function and role in chemoresistance. *Pharmacogenomics*, 9(1):105-127.

Sharom, F.J. 2014. Complex interplay between the P-glycoprotein multidrug efflux pump and the membrane: its role in modulating protein function. *Frontiers in Oncology*:1-19.

Shoba, G., Joy, D., Joseph, T., Majeed, M., Rajendran, R. & Srinivas, P.S. 1998. Influence of Piperine on the Pharmacokinetics of Curcumin in Animals and Human Volunteers. *Planta medica*, 64(4):353-356.

Sidhu, A.B., Uhlemann, A.C., Valderramos, S.G., Valderramos, J.C., Krishna, S. & Fidock, D.A. 2006. Decreasing *pfmdr1* copy number in *Plasmodium falciparum* malaria heightens susceptibility to mefloquine, lumefantrine, halofantrine, quinine, and artemisinin. *The Journal of Infectious Diseases*, 194(4):528-535.

Sidhu, A.B.S., Verdier-Pinard, D. & Fidock, D.A. 2002. Chloroquine Resistance in *Plasmodium falciparum* Malaria Parasites Conferred by *pfcrt* Mutations. *Science*, 298(5591):210-213.

Singh, R. 2013. HPLC method development and validation – An overview. *Journal of Pharmaceutical Education and Research*, 4(1):26-33.

Sjöberg, Å., Lutz, M., Tannergren, C., Wingolf, C., Borde, A. & Ungell, A.L. 2013. Comprehensive study on regional human intestinal permeability and prediction of fraction absorbed of drugs using the Ussing chamber technique. *European Journal of Pharmaceutical Sciences*, 48(1-2):166-180.

Sun, H., Chow, E.C.Y., Liu, S., Du, Y. & Pang, K.S. 2008. The Caco-2 cell monolayer: usefulness and limitations. *Expert Opinion on Drug Metabolism and Toxicology*, 4(4):395-411.

Takala-Harrison, S. & Laufer, M.K. 2015. Antimalarial drug resistance in Africa: key lessons for the future. *Annals of the New York Academy of Sciences*, 1342:62-67.

Thammana, M. 2016. A Review on High Performance Liquid Chromatography (HPLC). *Journal of Global Pharma Technology*, 2(5):22-26.

Trampuz, A., Jereb, M., Muzlovic, I. & Prabhu, R.M. 2003. Clinical review: Severe malaria. *Clinical Care*, 7(4):315-323.

Valderramos, S.G. & Fidock, D.A. 2006. Transporters involved in resistance to antimalarial drugs. *Trends in Pharmacological Sciences*, 27(11):594-601.

Van Breemen, R.B. & Li, Y. 2005. Caco-2 cell permeability assays to measure drug absorption. *Expert Opinion on Drug Metabolism & Toxicology*, 1(2):175-185.

Vander Heyden, Y., Nijhuis, A., Smeyers-Verbeke, J., Vandeginste, B.G. & Massart, D.L. 2001. Guidance for robustness/ruggedness tests in method validation. *Journal of Pharmaceutical and Biomedical Analysis*, 24(5-6):723-753.

Wahlang, B., Pawar, Y.B. & Bansal, A.K. 2011. Identification of permeability-related hurdles in oral delivery of curcumin using the Caco-2 cell model. *European Journal of Pharmaceutics and Biopharmaceutics*, 77(2):275-282.

Waknine-Grinberg, J.H., Hunt, N., Bentura-Marciano, A., McQuillan, J.A., Chan, H., Chan, W., Berenholz, Y., Haynes, R.K. & Golenser, J. 2010. Artemisone effective against murine cerebral malaria. *Malaria Journal*, 9:1-15.

Wessler, J.D., Grip, L.T., Mendell, J. & Giugliano, R.P. 2013. The P-Glycoprotein Transport System and Cardiovascular Drugs. *Journal of the American College of Cardiology*, 61(25):2495-2502.

White, N.J. 2011. Determinants of relapse periodicity in *Plasmodium vivax* malaria. *Malaria Journal,* 10:297

White, N.J. 1997. Assessme+nt of the Pharmacodynamic Properties of Antimalarial Drugs *In vivo*. *Antimicrobial Agents and Chemotherapy*, 41(7):1413-1422.

WHO. 2015. *World Malaria Report*. WHO: Geneva, Switzerland.

WHO. 2015. *Guidelines for the treatment of Malaria,* Third edition. WHO: Geneva, Switzerland

WHO. 2016. Artemisinin and artemisinin-based combination therapy resistance. Status report. WHO: Geneva, Switzerland.

WHO. 2016. *World Malaria Report*. WHO: Geneva, Switzerland.

Widmaier, E.P., Raff, H. & Strang, K.T. 2011. Movement of Molecules Across Cell Membranes. *In*: *Vander's Human Physiology: The Mechanism of Body Function*, 12th ed. McGraw-Hill. 102 p.

Willers, C., Wentzel, J.F., Du Plessis, L.H., Gouws, C. & Hamman, J.H. 2017. Efflux as a mechanism of antimicrobial drug resistance in clinical relevant microorganisms: the role of efflux inhibitors. *Expert Opinion on Therapeutic Targets*, 21(1):23-36.

Wilson, K. & Walker, J. 2000. Chromatographic techniques. *In*: *Practical biochemistry: Principles and techniques*, 5th ed. Cambridge: Cambridges University Press. 619-686 p.

Zhang, D., Luo, G., Ding, X. & Lu, C. 2012. Preclinical experimental models of drug metabolism and disposition in drug discovery and development. *Acta Pharmaceutica Sinica B*, 2(6):549-561.

APPENDIX A

IN VITRO TRANSPORT DATA ACROSS CACO-2 CELL MONOLAYERS AND THE RESPECTIVE TEER VALUES

EXPERIMENTAL DATA

1. Transepithelial electrical resistance (TEER) values

All the values of TEER is measured in ohm (Ω)

Table A-1.1: TEER value of caffeine AP-BL

	Begin (0 min)	After incubation with DMEM+HEPES	After test compounds	End (120 min)
Well 1	137	228	134	168
Well 2	259	203	141	160
Well 3	284	207	149	184
Mean	**227**	**213**	**141**	**171**
SD	**78.653**	**13.429**	**7.506**	**12.220**
%RSD	**34.700**	**6.314**	**5.311**	**7.160**

Table A-1.2: TEER value of atenolol AP-BL

	Begin (0 min)	After incubation with DMEM+HEPES	After test compounds	End (120 min)
Well 4	207	181	138	178
Well 5	204	185	152	179
Well 6	205	196	163	186
Mean	**205**	**187**	**151**	**181**
SD	**1.528**	**7.767**	**12.530**	**4.359**
%RSD	**0.744**	**4.146**	**8.298**	**2.408**

Table A-1.3: TEER value of Lucifer yellow AP-BL

	Begin (0 min)	After incubation with DMEM+HEPES	After test compounds	End (120 min)
Well 1	344	374	238	269
Well 2	365	382	253	282
Well 3	298	325	226	258
Mean	**336**	**360**	**239**	**270**
SD	**34.269**	**30.860**	**13.528**	**12.014**
%RSD	**0.102**	**0.086**	**0.057**	**0.045**

Table A-1.4: TEER value of Lucifer yellow (5% methanol) AP-BL

	Begin (0 min)	After incubation with DMEM+HEPES	After test compounds	End (120 min)
Well 4	321	338	216	219
Well 5	323	337	205	212
Well 6	309	328	227	233
Mean	**318**	**334**	**216**	**221**
SD	**7.572**	**5.508**	**11.000**	**10.693**
%RSD	**2.384**	**1.647**	**5.093**	**4.831**

Table A-1.5: TEER value of artemiside AP-BL

	Begin (0 min)	After incubation with DMEM+HEPES	After test compounds	End (120 min)
Well 1	228	194	169	159
Well 2	251	242	200	189
Well 3	241	234	198	178
Mean	**240**	**223**	**189**	**175**
SD	**11.533**	**25.716**	**17.349**	**15.177**
%RSD	**4.805**	**11.515**	**9.180**	**8.656**

Table A-1.6: TEER value of artemiside BL-AP

	Begin (0 min)	After incubation with DMEM+HEPES	After test compounds	End (120 min)
Well 4	201	165	168	164
Well 5	169	136	113	147
Well 6	178	162	164	150
Mean	**183**	**154**	**148**	**154**
SD	**16.503**	**15.948**	**30.665**	**9.074**
%RSD	**9.034**	**10.333**	**20.673**	**5.905**

Table A-1.7: TEER value of artemiside & verapamil AP-BL

	Begin (0 min)	After incubation with DMEM+HEPES	After test compounds	End (120 min)
Well 1	262	246	223	221
Well 2	286	262	227	221
Well 3	275	255	228	219
Mean	**274**	**254**	**226**	**220**
SD	**12.014**	**8.021**	**2.646**	**1.155**
%RSD	**4.379**	**3.154**	**1.171**	**0.524**

Table A-1.8: TEER value of artemiside & verapamil BL-AP

	Begin (0 min)	After incubation with DMEM+HEPES	After test compounds	End (120 min)
Well 4	239	205	198	207
Well 5	232	196	191	192
Well 6	236	216	198	204
Mean	**236**	**206**	**196**	**201**
SD	**3.512**	**10.017**	**4.041**	**7.937**
%RSD	**1.490**	**4.870**	**2.065**	**3.949**

Table A-1.9: TEER value of artemiside AP-BL

	Begin (0 min)	After incubation with DMEM+HEPES	After test compounds	End (120 min)
Well 1	338	351	259	307
Well 2	338	344	259	299
Well 3	328	360	268	294
Mean	**335**	**352**	**262**	**300**
SD	**5.774**	**8.021**	**5.196**	**6.557**
%RSD	**1.725**	**2.281**	**1.983**	**2.186**

Table A-1.10: TEER value of artemiside BL-AP

	Begin (0 min)	After incubation with DMEM+HEPES	After test compounds	End (120 min)
Well 4	343	261	277	308
Well 5	314	257	277	275
Well 6	325	272	299	283
Mean	**327**	**263**	**284**	**289**
SD	**14.640**	**7.767**	**12.702**	**17.214**
%RSD	**4.473**	**2.950**	**4.467**	**5.963**

Table A-1.11: TEER value of artemiside & piperine AP-BL

	Begin (0 min)	After incubation with DMEM+HEPES	After test compounds	End (120 min)
Well 1	371	374	216	301
Well 2	384	362	208	285
Well 3	328	335	234	265
Mean	**361**	**357**	**219**	**284**
SD	**29.309**	**19.975**	**13.317**	**18.037**
%RSD	**8.119**	**5.595**	**6.071**	**6.359**

Table A-1.12: TEER value of artemiside & piperine BL-AP

	Begin (0 min)	After incubation with DMEM+HEPES	After test compounds	End (120 min)
Well 4	362	285	306	303
Well 5	319	250	272	260
Well 6	357	248	280	284
Mean	**346**	**261**	**286**	**282**
SD	**23.516**	**141.619**	**110.057**	**114.981**
%RSD	**6.797**	**54.260**	**38.482**	**40.725**

Table A-1.13: TEER value of artemisone AP-BL

	Begin (0 min)	After incubation with DMEM+HEPES	After test compounds	End (120 min)
Well 1	558	560	261	324
Well 2	550	564	234	394
Well 3	529	546	265	366
Mean	**546**	**557**	**253**	**361**
SD	**14.978**	**9.452**	**16.862**	**35.233**
%RSD	**2.745**	**1.698**	**6.656**	**9.751**

Table A-1.14: TEER value of artemisone BL-AP

	Begin (0 min)	After incubation with DMEM+HEPES	After test compounds	End (120 min)
Well 4	555	341	387	419
Well 5	533	338	383	351
Well 6	532	321	362	376
Mean	**540**	**333**	**377**	**382**
SD	**13.000**	**10.786**	**13.429**	**34.395**
%RSD	**2.407**	**3.236**	**3.559**	**9.004**

Table A-1.15: TEER value of artemisone & verapamil AP-BL

	Begin (0 min)	After incubation with DMEM+HEPES	After test compounds	End (120 min)
Well 1	545	547	255	330
Well 2	557	568	302	322
Well 3	537	556	266	318
Mean	**546**	**557**	**274**	**323**
SD	**10.066**	**10.536**	**24.583**	**6.110**
%RSD	**1.843**	**1.891**	**8.961**	**1.890**

Table A-1.16: TEER value of artemisone & verapamil BL-AP

	Begin (0 min)	After incubation with DMEM+HEPES	After test compounds	End (120 min)
Well 4	565	340	378	434
Well 5	545	277	321	425
Well 6	561	275	329	406
Mean	**557**	**297**	**343**	**422**
SD	**10.583**	**36.964**	**30.860**	**14.295**
%RSD	**1.900**	**12.432**	**9.006**	**3.390**

Table A-1.17: TEER value of artemisone & piperine AP-BL

	Begin (0 min)	After incubation with DMEM+HEPES	After test compounds	End (120 min)
Well 1	394	404	232	255
Well 2	411	416	237	239
Well 3	400	405	285	278
Mean	**402**	**408**	**251**	**257**
SD	**8.622**	**6.658**	**29.263**	**19.604**
%RSD	**2.146**	**1.631**	**11.643**	**7.618**

Table A-1.18: TEER value of artemisone & piperine BL-AP

	Begin (0 min)	After incubation with DMEM+HEPES	After test compounds	End (120 min)
Well 4	440	312	312	277
Well 5	446	315	317	296
Well 6	425	331	342	313
Mean	**437**	**319**	**324**	**295**
SD	**10.817**	**10.214**	**16.073**	**18.009**
%RSD	**2.475**	**3.199**	**4.966**	**6.098**

Table A-1.19: TEER value of artemether AP-BL

	Begin (0 min)	After incubation with DMEM+HEPES	After test compounds	End (120 min)
Well 1	525	488	244	336
Well 2	511	482	257	332
Well 3	530	526	307	369
Mean	**522**	**499**	**269**	**346**
SD	**9.849**	**23.861**	**33.262**	**20.306**
%RSD	**1.887**	**4.785**	**12.350**	**5.874**

Table A-1.20: TEER value of artemether BL-AP

	Begin (0 min)	After incubation with DMEM+HEPES	After test compounds	End (120 min)
Well 4	519	327	364	393
Well 5	517	418	456	427
Well 6	507	535	389	373
Mean	**514**	**427**	**403**	**398**
SD	**6.429**	**104.270**	**47.571**	**27.301**
%RSD	**1.250**	**24.438**	**11.804**	**6.865**

Table A-1.21: TEER value of artemether & verapamil AP-BL

	Begin (0 min)	After incubation with DMEM+HEPES	After test compounds	End (120 min)
Well 1	245	242	202	199
Well 2	258	254	232	216
Well 3	245	232	221	203
Mean	**249**	**243**	**218**	**206**
SD	**7.506**	**11.015**	**15.177**	**8.888**
%RSD	**3.010**	**4.539**	**6.951**	**4.315**

Table A-1.22: TEER value of artemether & verapamil BL-AP

	Begin (0 min)	After incubation with DMEM+HEPES	After test compounds	End (120 min)
Well 4	244	224	208	199
Well 5	238	225	220	208
Well 6	241	240	225	223
Mean	**241**	**230**	**218**	**210**
SD	**3.000**	**8.963**	**8.737**	**12.124**
%RSD	**1.245**	**3.903**	**4.014**	**5.774**

Table A-1.23: TEER value of vinblastine AP-BL

	Begin (0 min)	After incubation with DMEM+HEPES	After test compounds	End (120 min)
Well 1	340	352	233	202
Well 2	324	307	226	235
Well 3	360	372	276	230
Mean	**341**	**344**	**245**	**222**
SD	**18.037**	**33.292**	**27.074**	**17.786**
%RSD	**5.284**	**9.687**	**11.051**	**8.000**

Table A-1.24: TEER value of vinblastine BL-AP

	Begin (0 min)	After incubation with DMEM+HEPES	After test compounds	End (120 min)
Well 4	321	201	233	194
Well 5	328	235	231	196
Well 6	355	217	226	188
Mean	**335**	**218**	**230**	**193**
SD	**17.954**	**17.010**	**3.606**	**4.163**
%RSD	**5.365**	**7.815**	**1.568**	**2.161**

Table A-1.25: TEER value of vinblastine & verapamil AP-BL

	Begin (0 min)	After incubation with DMEM+HEPES	After test compounds	End (120 min)
Well 1	335	344	244	208
Well 2	325	334	248	208
Well 3	352	371	272	206
Mean	**337**	**350**	**255**	**207**
SD	**13.650**	**19.140**	**15.144**	**1.155**
%RSD	**4.047**	**5.474**	**5.947**	**0.557**

Table A-1.26: TEER value of vinblastine & verapamil BL-AP

	Begin (0 min)	After incubation with DMEM+HEPES	After test compounds	End (120 min)
Well 4	330	247	240	205
Well 5	324	245	238	203
Well 6	337	225	226	212
Mean	**330**	**239**	**235**	**207**
SD	**6.506**	**12.166**	**7.572**	**4.726**
%RSD	**1.970**	**5.090**	**3.227**	**2.287**

2. Transport data across the Caco-2 cell monolayer

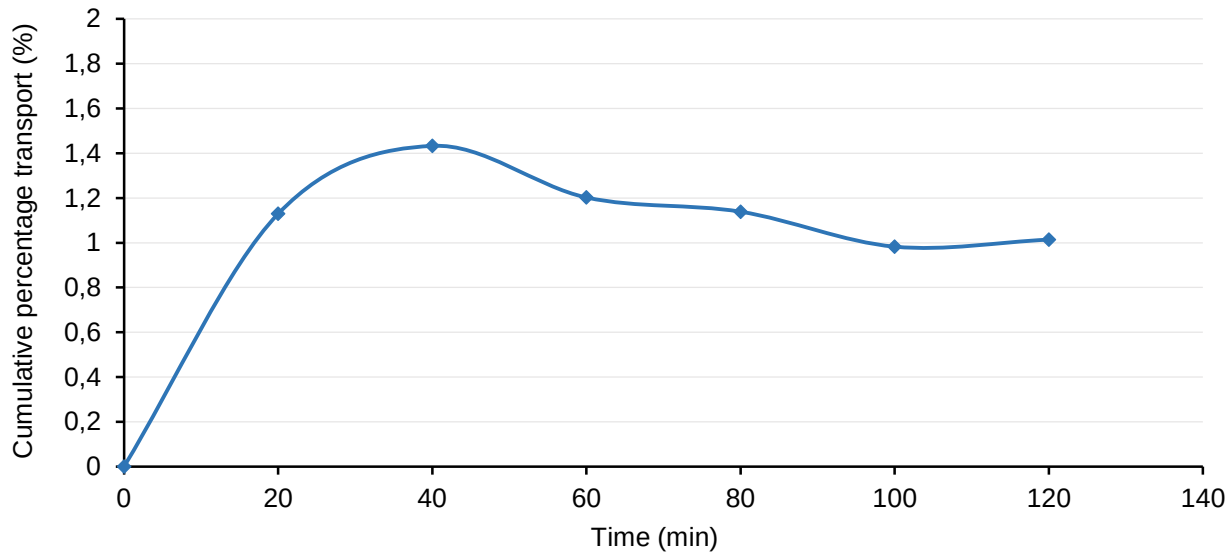

Figure A-2.1: Cumulative percentage transport of Lucifer yellow on three Caco-2 cell monolayers in the AP-BL direction

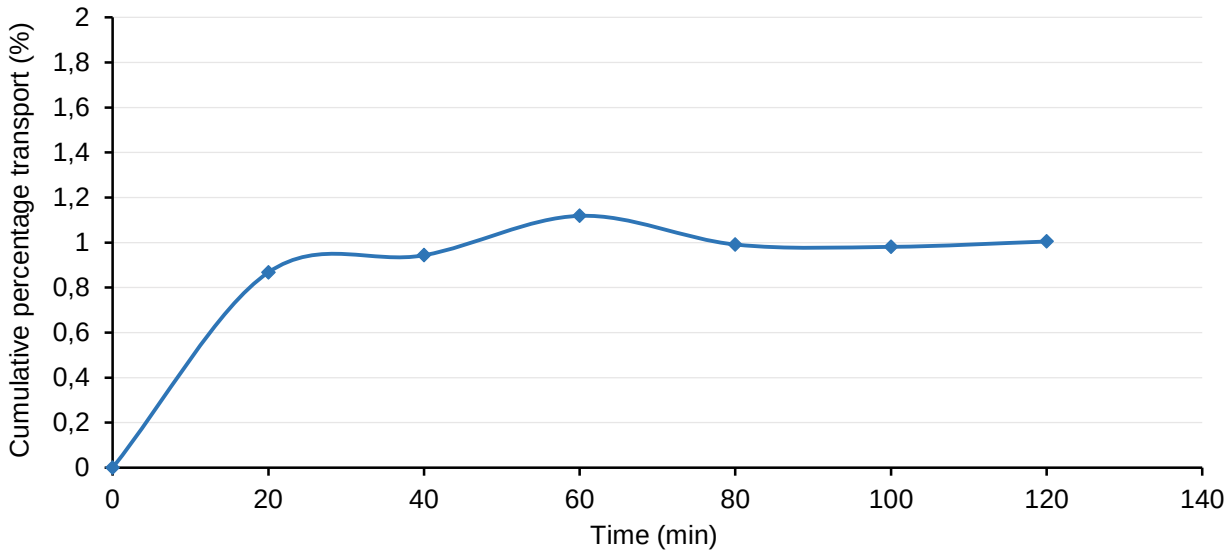

Figure A-2.2: Cumulative percentage transport of Lucifer yellow with a volume of 5% methanol on three Caco-2 cell monolayers in the AP-BL direction

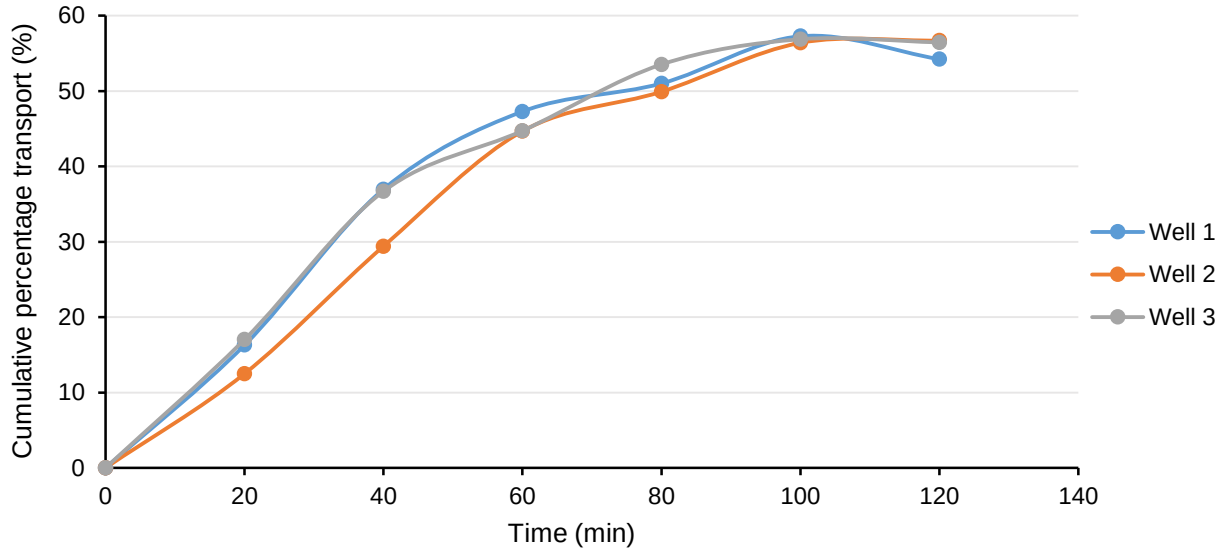

Figure A-2.3: Cumulative percentage transport of caffeine on three Caco-2 cell monolayers in the AP-BL direction

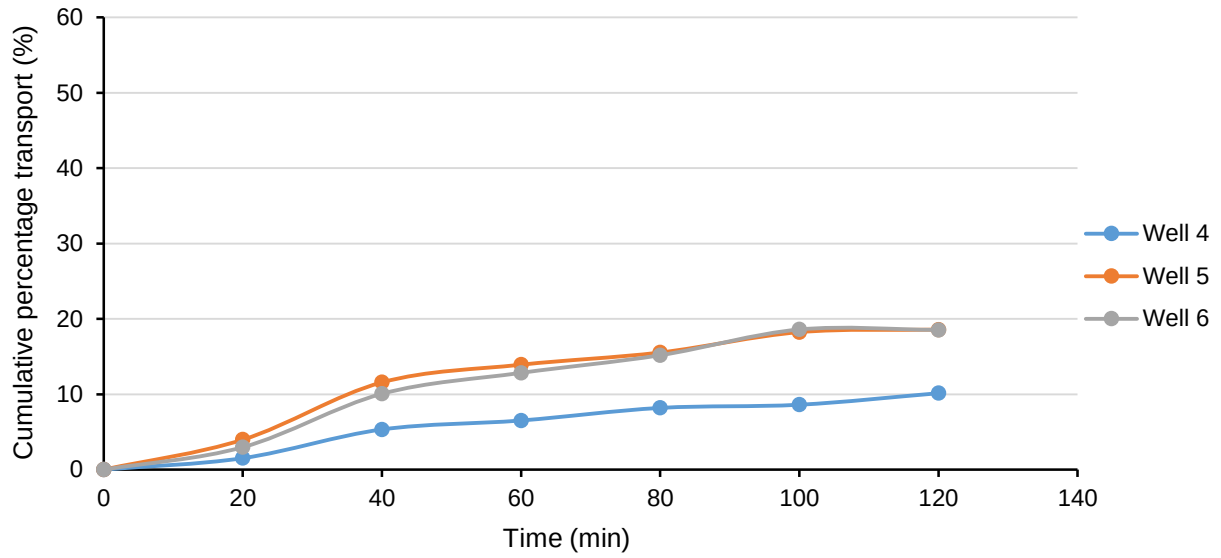

Figure A-2.4: Cumulative percentage transport of atenolol on three Caco-2 cell monolayers in the AP-BL direction

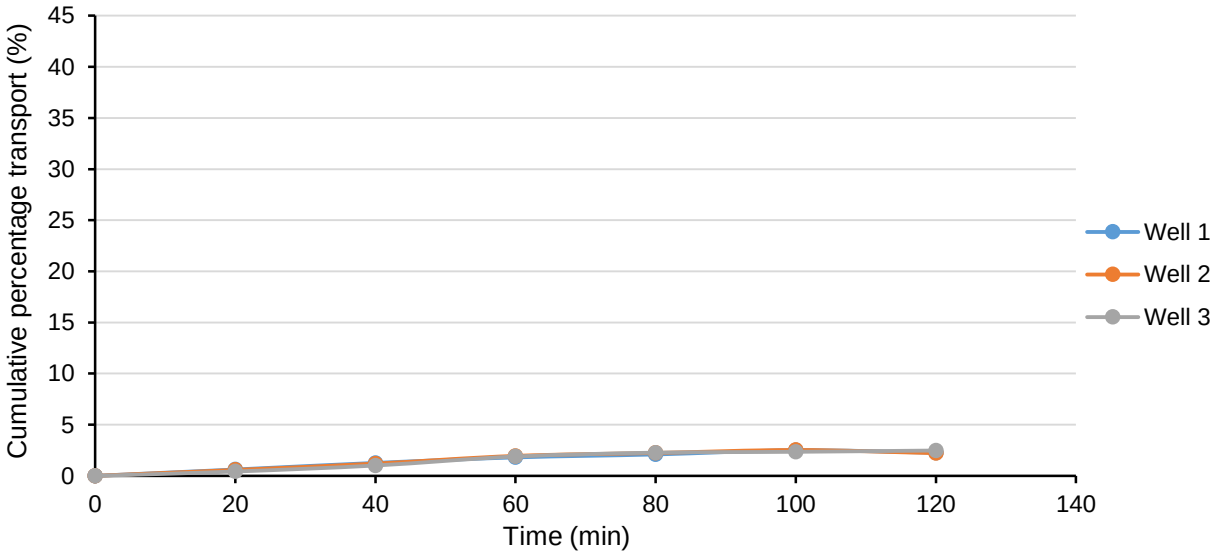

Figure A-2.5: Cumulative percentage transport of artemiside on three Caco-2 cell monolayers in the AP-BL direction

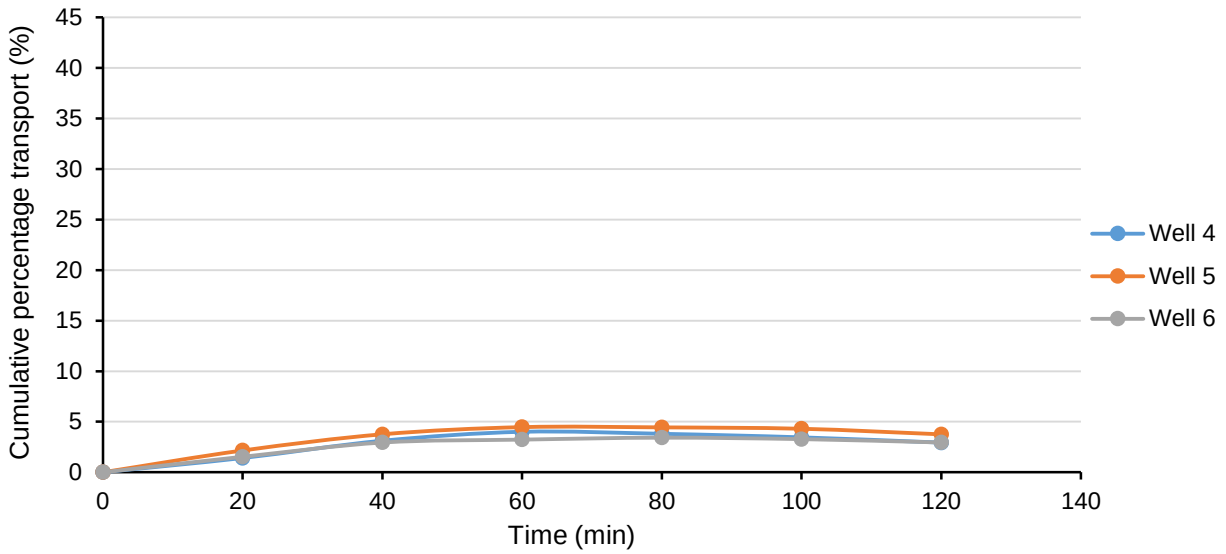

Figure A-2.6: Cumulative percentage transport of artemiside on three Caco-2 cell monolayers in the BL-AP direction

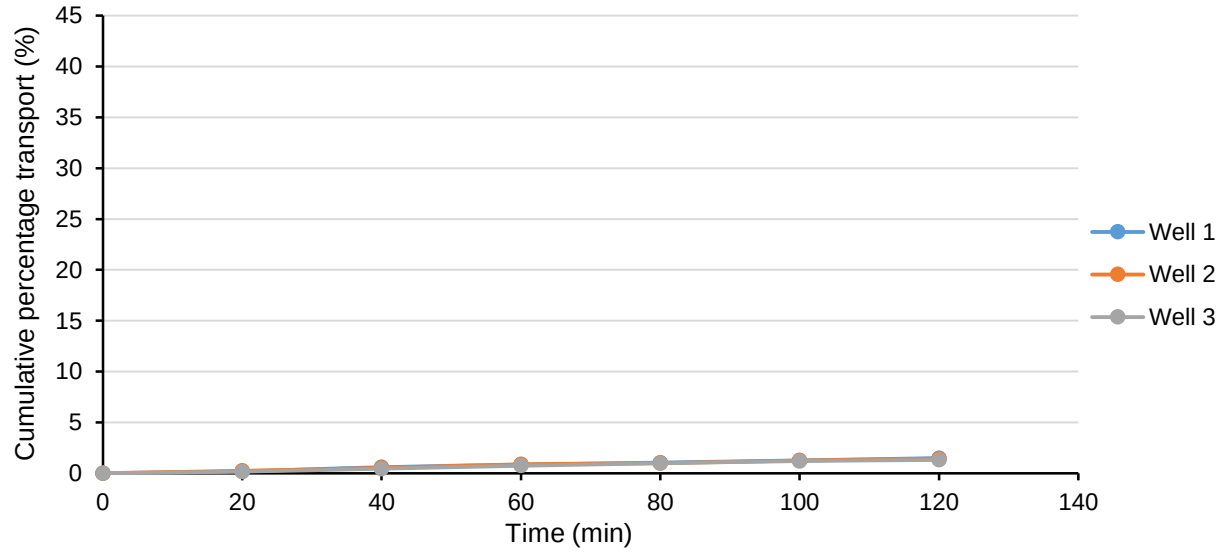

Figure A-2.7: Cumulative percentage transport of artemiside on three Caco-2 cell monolayers in the presence of piperine in the AP-BL direction

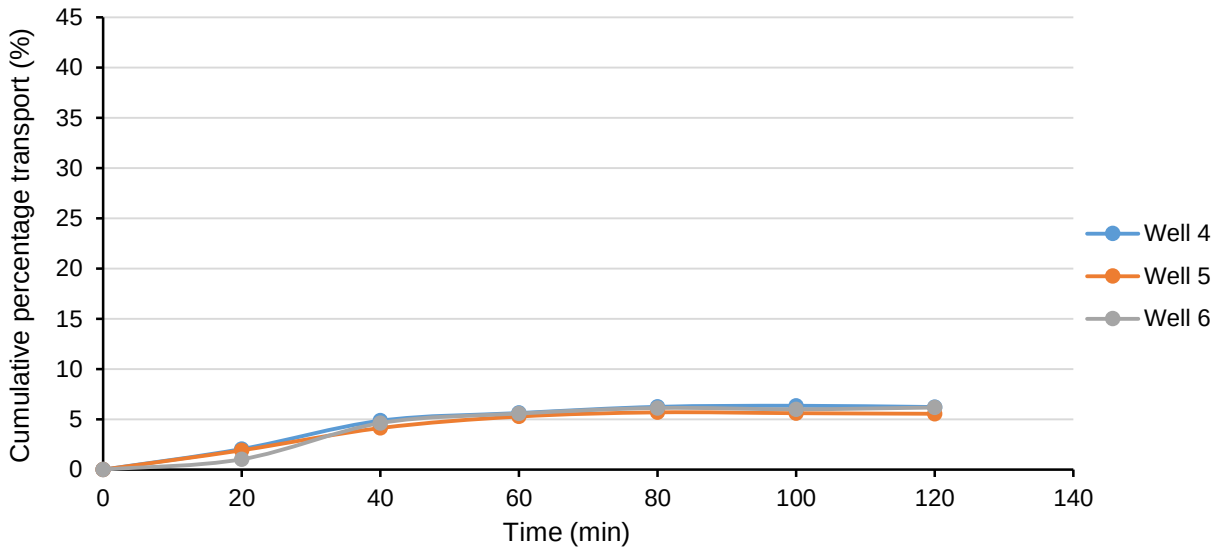

Figure A-2.8: Cumulative percentage transport of artemiside on three Caco-2 cell monolayers in the presence of piperine in the BL-AP direction

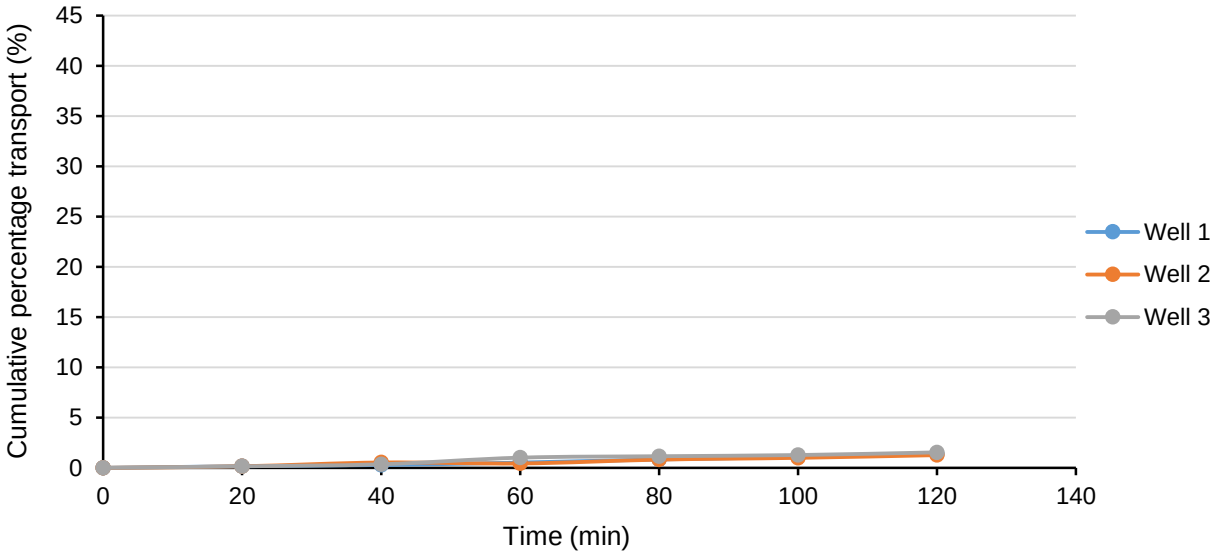

Figure A-2.9: Cumulative percentage transport of artemiside on three Caco-2 cell monolayers in the AP-BL direction

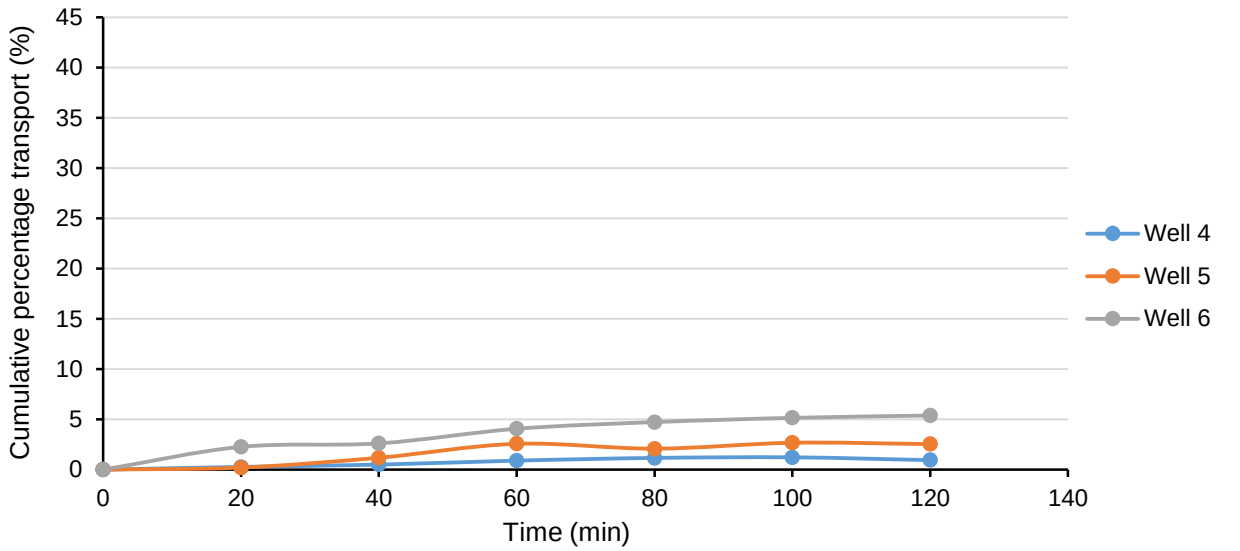

Figure A-2.10: Cumulative percentage transport of artemiside on three Caco-2 cell monolayers in the presence of piperine in the BL-AP direction

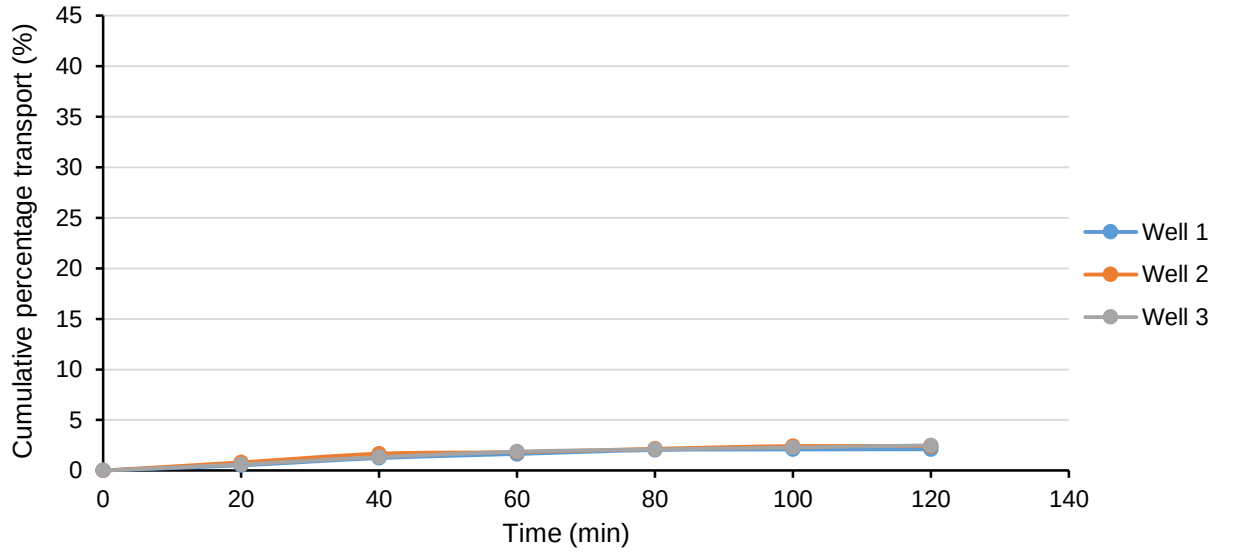

Figure A-2.11: Cumulative percentage transport of artemiside on three Caco-2 cell monolayers in the presence of verapamil in the AP-BL direction

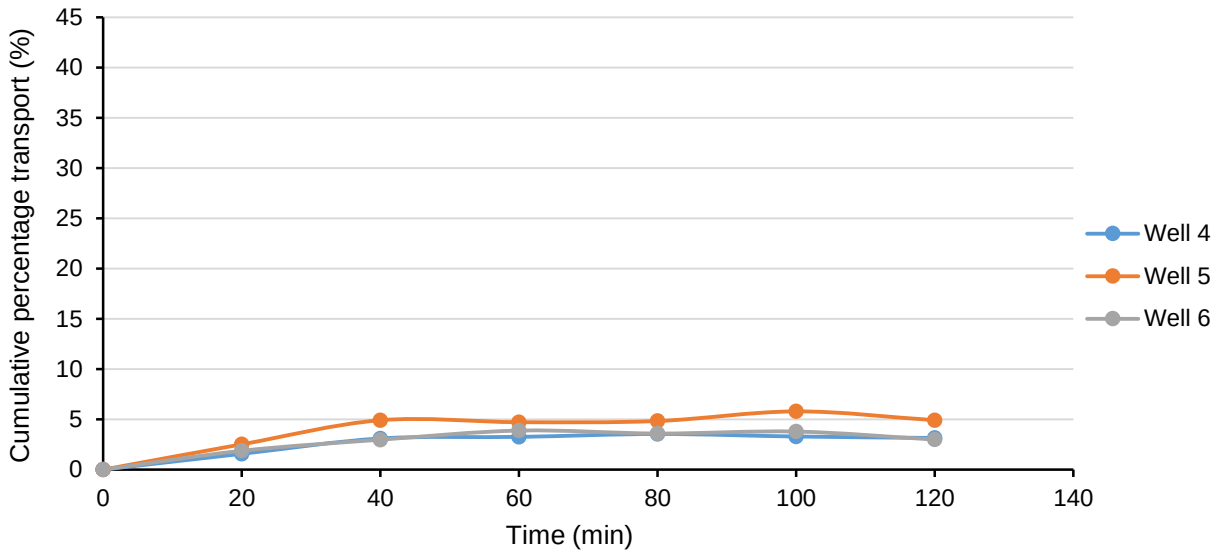

Figure A-2.12: Cumulative percentage transport of artemiside on three Caco-2 cell monolayers in the presence of verapamil in the BL-AP direction

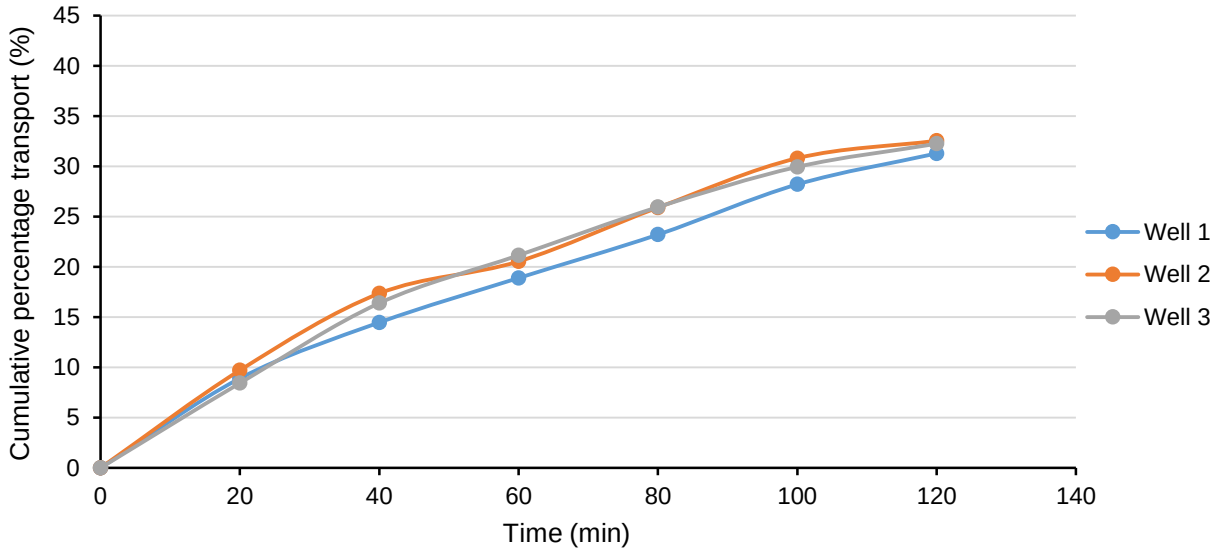

Figure A-2.13: Cumulative percentage transport of artemisone on three Caco-2 cell monolayers in the AP-BL direction

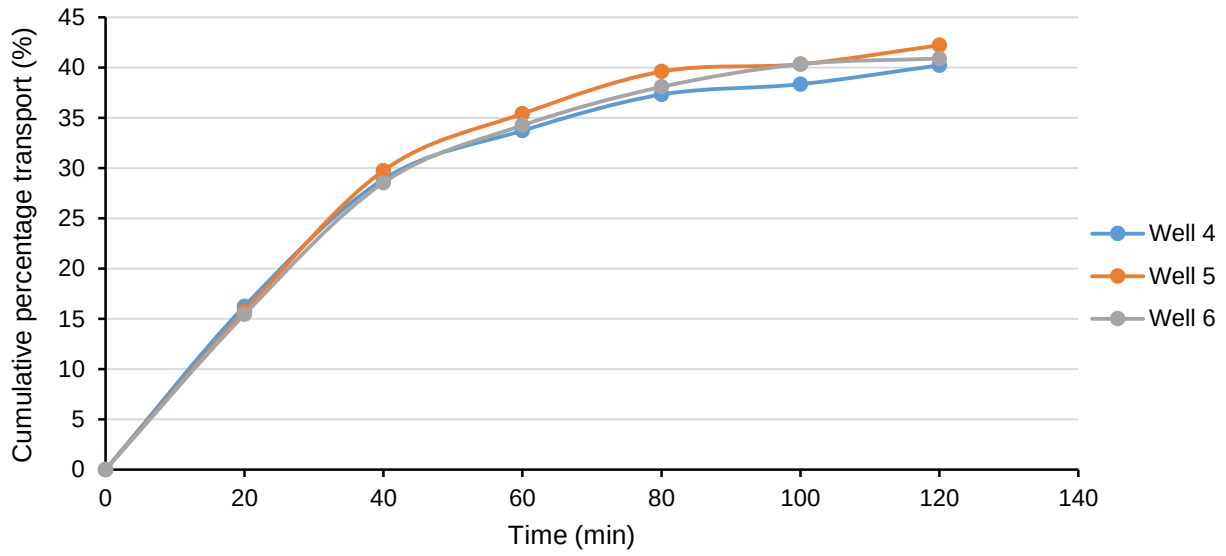

Figure A-2.14: Cumulative percentage transport of artemisone on three Caco-2 cell monolayers in the BL-AP direction

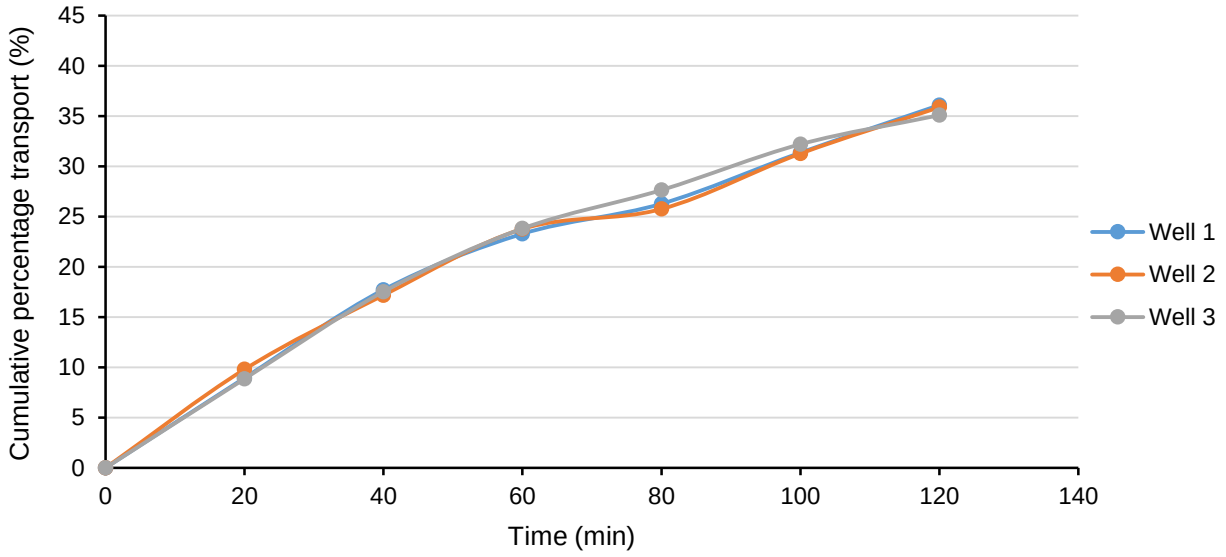

Figure A-2.15: Cumulative percentage transport of artemisone on three Caco-2 cell monolayers in the presence of verapamil in the AP-BL direction

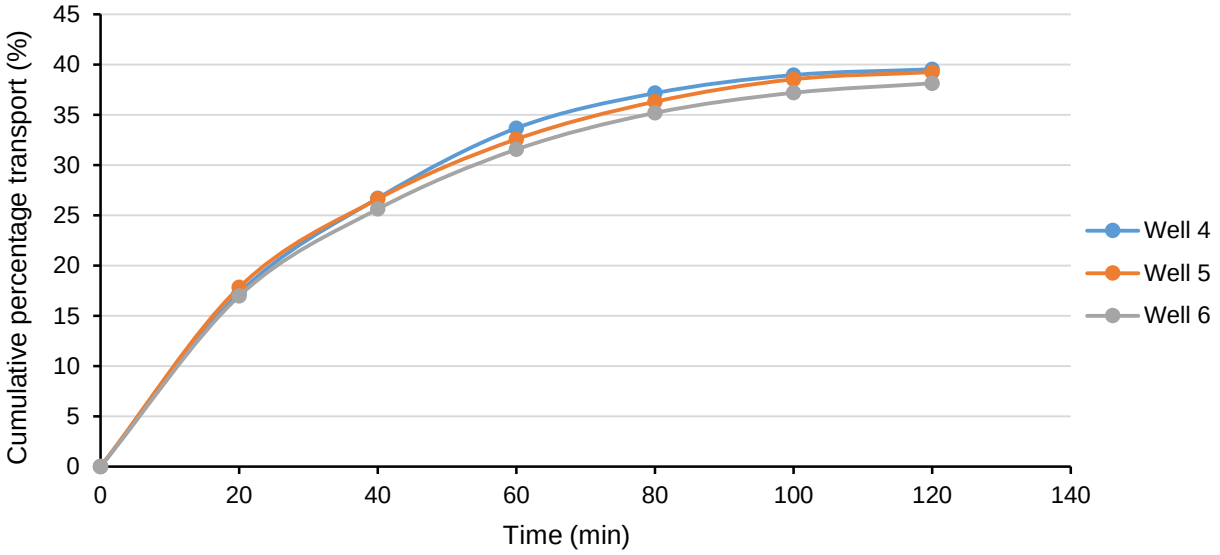

Figure A-2.16: Cumulative percentage transport of artemisone on three Caco-2 cell monolayers in the presence of verapamil in the BL-AP direction

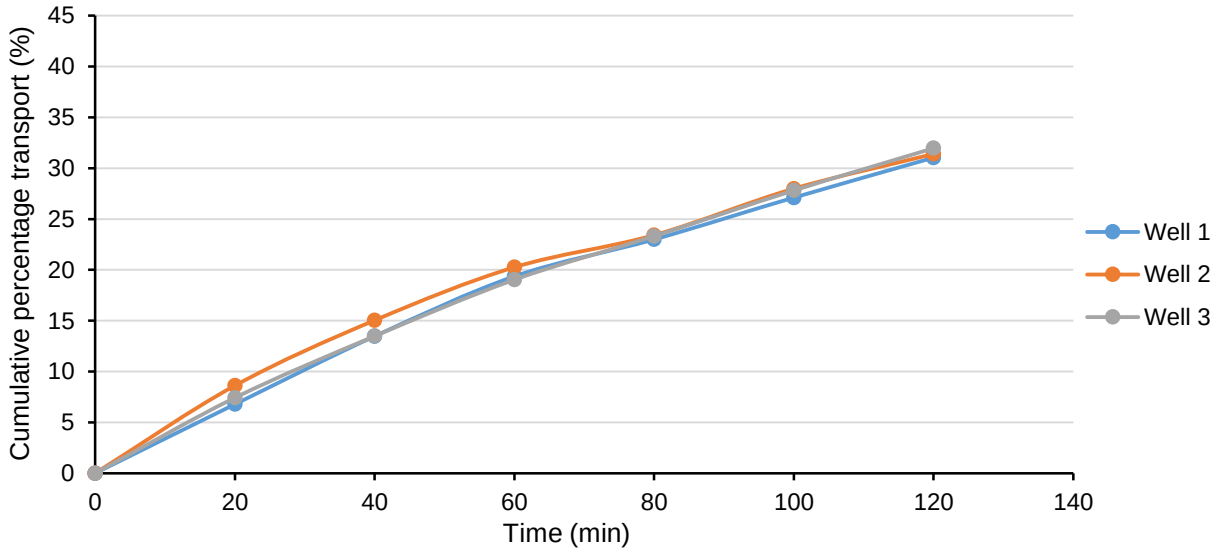

Figure A-2.17: Cumulative percentage transport of artemisone on three Caco-2 cell monolayers in the presence of piperine in the AP-BL direction

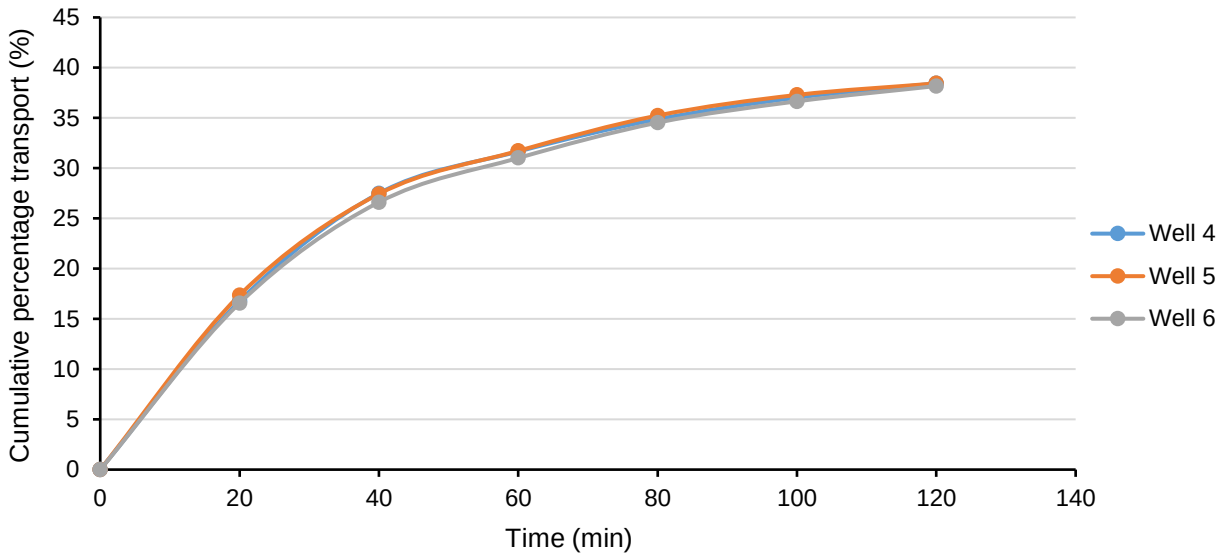

Figure A-2.18: Cumulative percentage transport of artemisone on three Caco-2 cell monolayers in the presence of piperine in the BL-AP direction

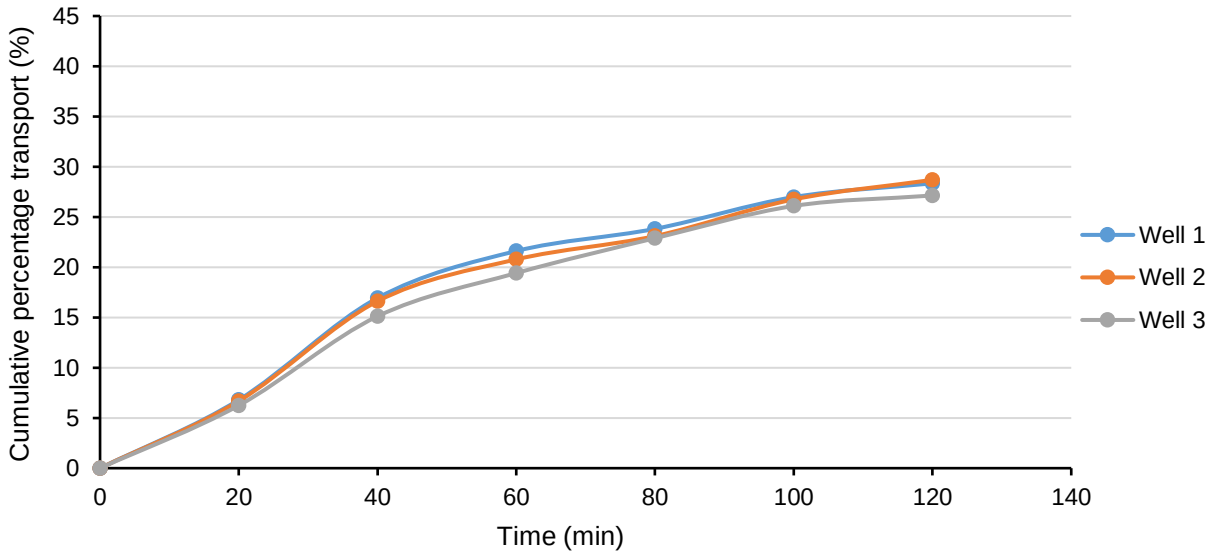

Figure A-2.19: Cumulative percentage transport of artemether on three Caco-2 cell monolayers in the AP-BL direction

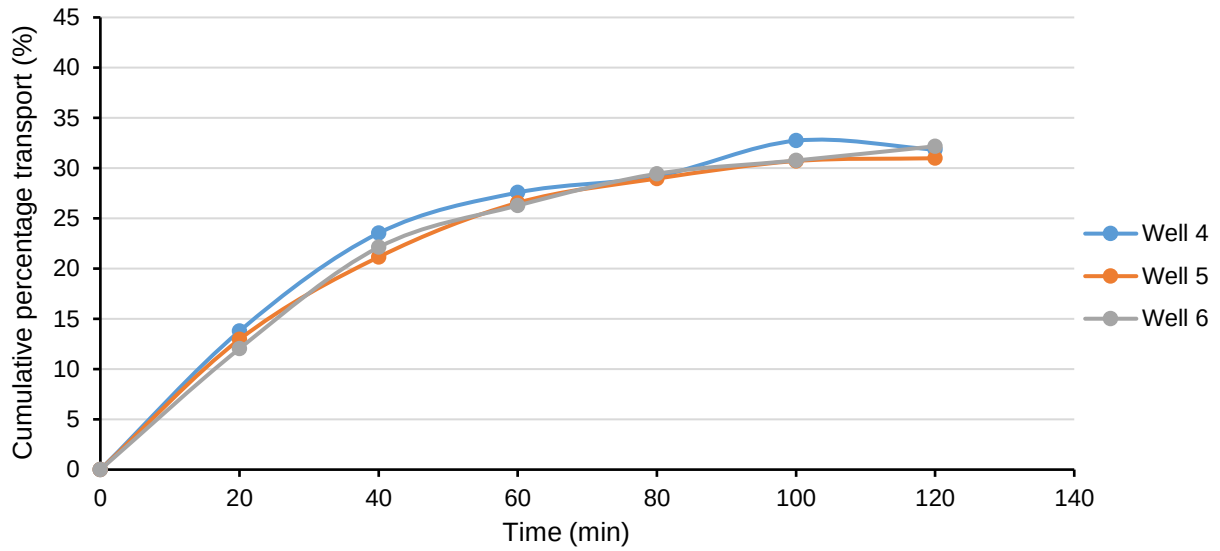

Figure A-2.20: Cumulative percentage transport of artemether on three Caco-2 cell monolayers in the BL-AP direction

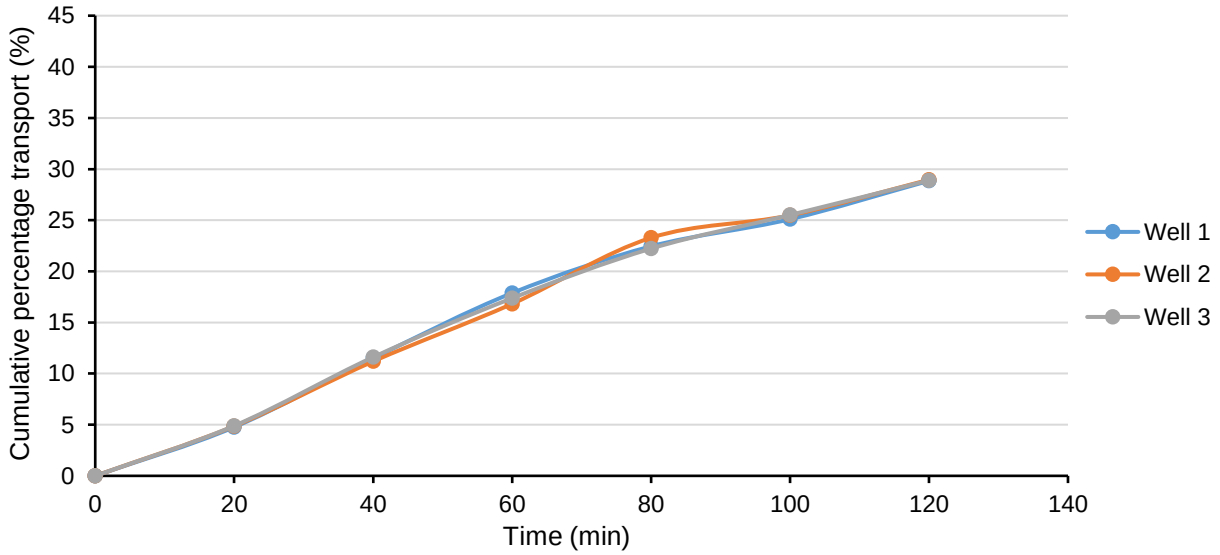

Figure A-2.21: Cumulative percentage transport of artemether on three Caco-2 cell monolayers in the presence of verapamil in the AP-BL direction

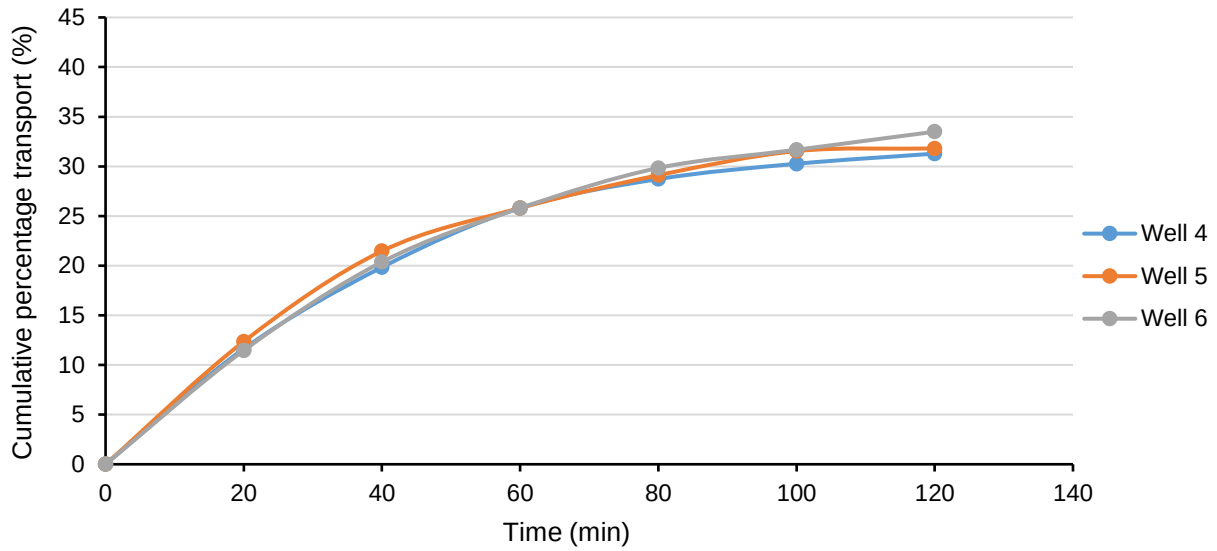

Figure A-2.22: Cumulative percentage transport of artemether on three Caco-2 cell monolayers in the presence of verapamil in the BL-AP direction

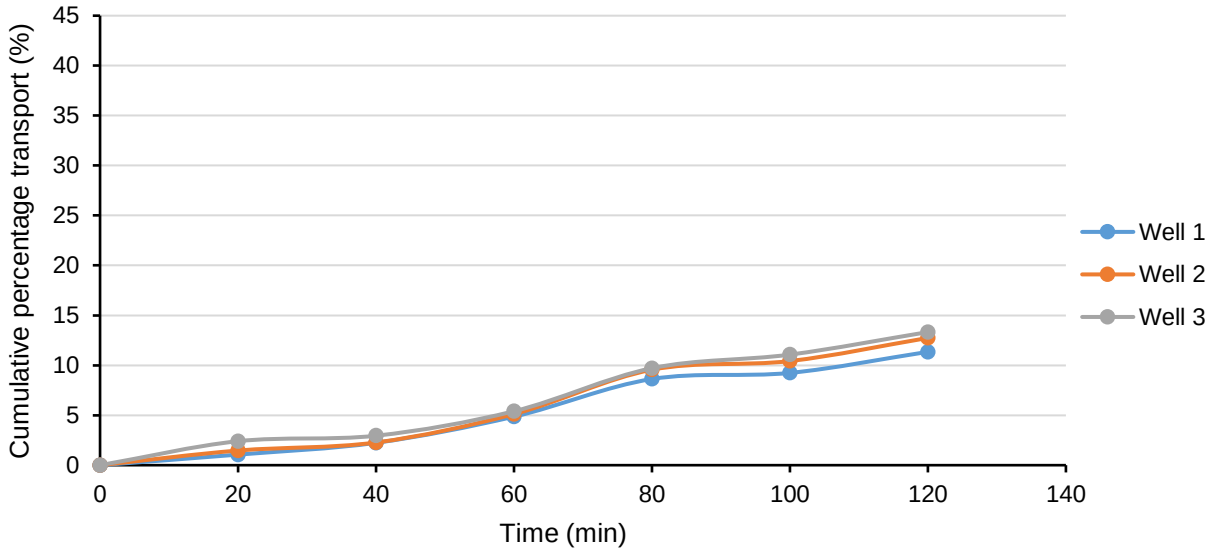

Figure A-2.23: Cumulative percentage transport of vinblastine on three Caco-2 cell monolayers in the AP-BL direction

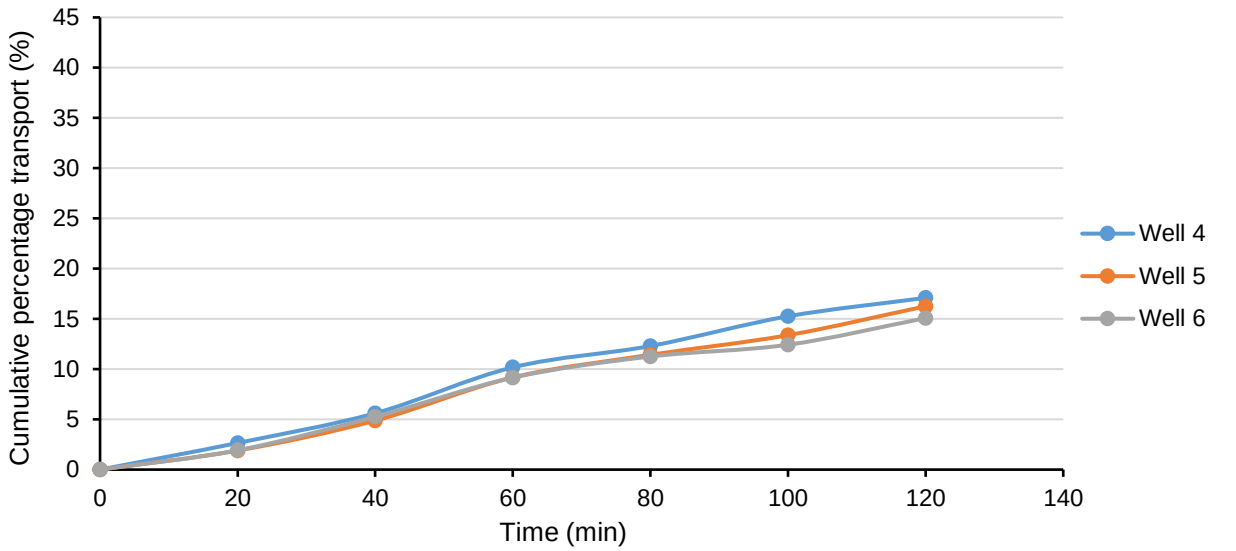

Figure A-2.24: Cumulative percentage transport of vinblastine on three Caco-2 cell monolayers in the BL-AP direction

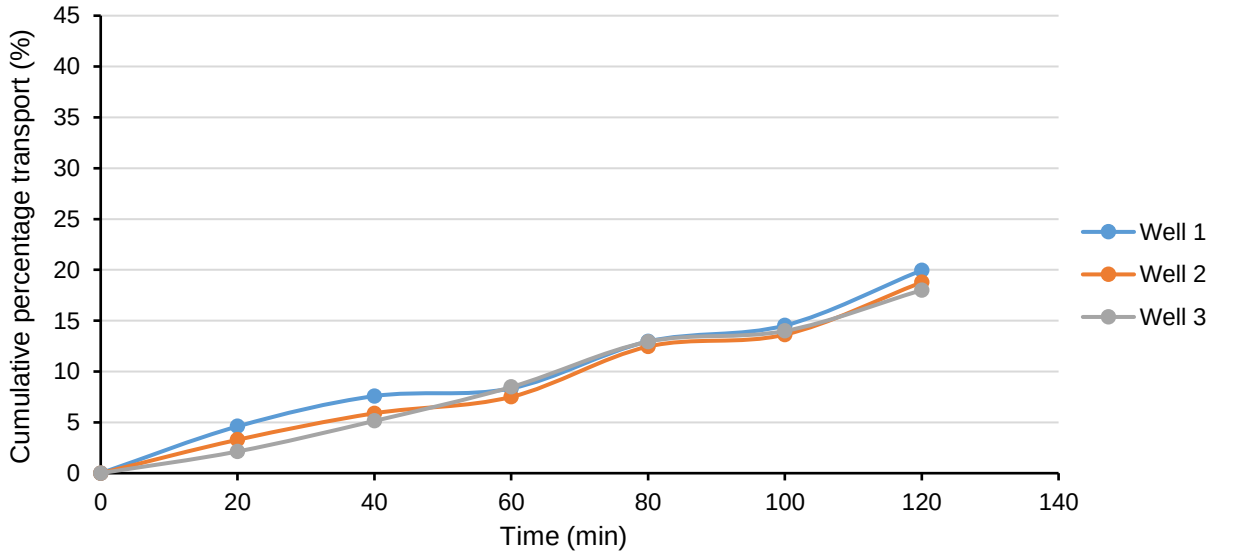

Figure A-2.25: Cumulative percentage transport of vinblastine on three Caco-2 cell monolayers in the presence of verapamil in the AP-BL direction

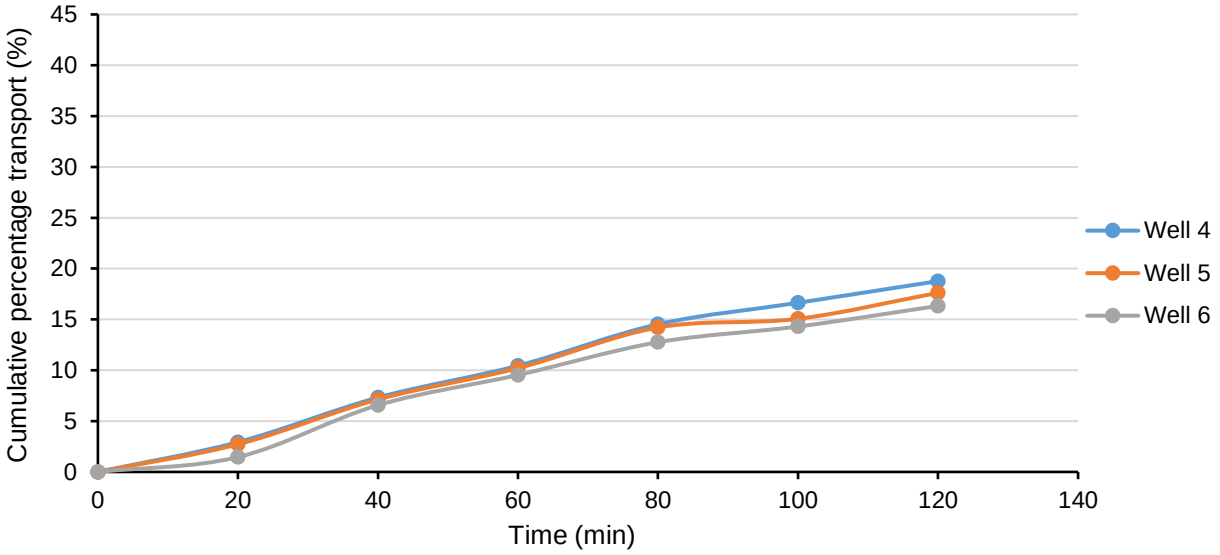

Figure A-2.26: Cumulative percentage transport of vinblastine on three Caco-2 cell monolayers in the presence of verapamil in the BL-AP direction

APPENDIX B

APPARENT PERMEABILITY COEFFICIENT VALUES (P_{APP}) AND EFFLUX RATIOS OF ALL THE EXPERIMENTAL DATA

Table B-1: The apparent permeability coefficients (P_{app}) values and efflux ratios for the selected artemisinin derivatives in the presence and absence of verapamil and piperine (# artemiside with piperine is statistically significantly different from artemiside alone according to the student t-test, * statistically significantly different from the control group based on Dunnett's post-hoc analysis; ND – not determined). (CaptionTop_Tbl_Fig)

Experimental group	P_{app} (A-B) (x 10^{-6})	P_{app} (B-A) (x 10^{-6})	Efflux ratio
Vinblastine	3,915 ± 0,257	4,964 ± 0,3502	1,275 ± 0,173
Vinblastine + verapamil	5,400 ± 0,065*	5,447 ± 0,324	1,009 ± 0,061
Artemisone	9,326 ± 0,283	11,496 ± 0,407	1,233 ± 0,017
Artemisone + verapamil	10,259 ± 0,101	10,746 ± 0,256*	1,132 ± 0,058*
Artemisone + piperine	9,158 ± 0,167	10,382 ± 0,0182*	1,134 ± 0,022*
Artemether	8,367 ± 0,133	8,852 ± 0,161	1,058 ± 0,035
Artemether + verapamil	8,857 ± 0,06903*	9,173 ± 0,358	1,036 ± 0,043
Artemiside	0,424 ± 0,0607	0,912 ± 0,596	2,100 ± 1,172
Artemiside + verapamil	0,695 ± 0,0427#	1,019 ± 0,289	1,468 ± 0,419
Artemiside	0,755 ± 0,0392	0,906 ± 0,115	1,205 ± 0,190
Artemiside + piperine	0,432 ± 0,0165#	1,790 ± 0,143#	4,151 ± 0,420#
Lucifer yellow	0,156 ± 0,0796	ND	ND
Lucifer yellow (5% methanol)	0,2096 ± 0,0958	ND	ND
Caffeine	17,059 ± 0,636	ND	ND
Atenolol	4,836 ± 1,574	ND	ND

APPENDIX C

FORMATTING GUIDELINES STIPULATED BY THE JOURNAL CURRENT DRUG DELIVERY FOR ARTICLE SUBMISSION

Title: (The Title of the Article should be Precise and Brief and Must Not be More Than 120 Characters. Authors should avoid the Use of Non-Standard Abbreviations. The Title Must be Written in Title Case Except for articles, conjunctions and prepositions.)

Principal Author[a], Corresponding author[*b], Co-author[1], Co-author[2a] and Co-author[3a]

(The author will be required to provide their full names, the institutional affiliations and the location, with an asterisk in front of the name of the principal/corresponding author).

[a]*Department Name, Faculty Name, University Name, City, Country;* [b]*Department Name, Faculty Name, University Name, City, Country*

Abstract: The abstract should not exceed 250 words for review papers summarizing the essential features of the article.

Keywords: 6 to 8 keywords must be provided.

1. INTRODUCTION

The Introduction section should include the background and aims of the research in a comprehensive manner, for the researchers.

1.1. Section headings

Section headings should be numbered sequentially, left aligned and have the first letter capitalized, starting with the introduction. Sub-section headings however should be in lower-case and italicized with their initials capitalized. They should be numbered as 1.1, 1.2, etc. A page break may be inserted to keep a heading along with its text.

1.2. General guidelines for the preparation of your text

Please provide soft copies of all the materials (main text in MS Word or Tex/LaTeX), figures/illustrations in TIFF, PDF or JPEG, and chemical structures drawn in ChemDraw (CDX)/ISISDraw (TGF) as separate files, while a PDF version of the entire manuscript must also be included, embedded with all the figures/illustrations/tables/chemical structures etc. It is advisable that the document files related to a manuscript submission should always have the name of the corresponding author as part of the file name, i.e., “Cilli MS text.doc”, “Cilli MS Figure 1” etc.

It is imperative that before submission, authors should carefully proofread the files for special characters, mathematical symbols, Greek letters, equations, tables, references and images, to ensure that they appear in proper format.

*Address correspondence to this author at the Department of xxxy, Faculty of xxx, xxx University, P.O. Box: 0000-000, City, Country; Tel/Fax: ++0-000-000-0000, +0-000-000-0000; E-mails: author@institute.xxx

References, figures, tables, chemical structures etc. should be referred to in the text at the appropriate place where they have been first discussed. Figure legends/ captions should also be provided.

1.3. Figures/Illustrations:

All authors must strictly follow the guidelines below for preparing illustrations for publication. If the figures are found to be sub-standard, then the manuscripts will be rejected/ and the authors offered the option of figure improvement professionally by Eureka Science. The costs for such improvement will be charged to the authors.

Illustrations should be provided as separate files, embedded in the text file, and must be numbered consecutively in the order of their appearance. Each figure should include only a single illustration which should be cropped to minimize the amount of space occupied by the illustration.

If a figure is in separate parts, all parts of the figure must be provided in a single composite illustration file.

Photographs should be provided with a scale bar if appropriate, as well as high-resolution component files.

1.3.1. Scaling/Resolution:

Line Art image type is normally an image based on lines and text. It does not contain tonal or shaded areas. The preferred file format should be TIFF or EPS, with the color mode being Monochrome 1-bit or RGB, in a resolution of 900-1200 dpi.

Halftone image type is a continuous tone photograph containing no text. It should have the preferred file format TIFF, with color mode being RGB or Grayscale, in a resolution of 300 dpi.

Combination image type is an image containing halftone , text or line art elements. It should have the preferred file format TIFF, with color mode being RGB or Grayscale, in a resolution of 500-900 dpi.

1.3.2. Formats:

Illustrations may be submitted in the following file formats:

- Illustrator
- EPS (preferred format for diagrams)
- PDF (also especially suitable for diagrams)
- PNG (preferred format for photos or images)
- Microsoft Word (version 5 and above; figures must be a single page)
- PowerPoint (figures must be a single page)
- TIFF
- JPEG (conversion should be done using the original file)
- BMP
- CDX (ChemDraw)
- TGF (ISISDraw)

Bentham Science does not process figures submitted in GIF format.

For TIFF or EPS figures with considerably large file size restricting the file size in online submissions is advisable. Authors may therefore convert to JPEG format before submission as this result in significantly reduced file size and upload time, while retaining acceptable quality. JPEG is a ‘lossy’ format, however. In order to maintain acceptable image quality, it is recommended that JPEG files are saved at High or Maximum quality.

Zipit or Stuffit tools should not be used to compress files prior to submission as the resulting compression through these tools is always negligible.

Please refrain from supplying:

a) Graphics embedded in word processor (spreadsheet, presentation) document.

b) Optimized files optimized for screen use (like GIF, BMP, PICT, WPG) because of the low resolution.

c) Files with too low a resolution.

d) Graphics that are disproportionately large for the content.

1.3.3. Image Conversion Tools:

There are a number of software packages available, many of them freeware or shareware, capable of converting to and from different graphics formats, including PNG.

General tools for image conversion include Graphic Converter on the Macintosh, Paint Shop Pro, for Windows, and ImageMagick, available on Macintosh, Windows and UNIX platforms.

Bitmap images (e.g. screenshots) should not be converted to EPS as they result in a much larger file size than the equivalent JPEG, TIFF, PNG or BMP, and poor quality. EPS should only be used for images produced by vector-drawing applications such as Adobe Illustrator or CorelDraw. Most vector-drawing applications can be saved in, or exported as, EPS format. If the images were originally prepared in an Office application, such as Word or PowerPoint, original Office files should be directly uploaded to the site, instead of being converted to JPEG or another format of low quality.

1.3.4. Color Figures/Illustrations:

Color figures publication in the journal: The cost for each individual page of color figures is US$ 950.

Color figures should be supplied in CMYK not RGB colors.

1.3.5. Chemical Structures:

Chemical structures MUST be prepared in ChemDraw/ CDX and provided as a separate file.

1.4 Tables:

Tables should be embedded in the text exactly according to their appropriate placement in the submitted manuscript. Table number in bold font i.e. Table 1, should follow a title. The title should be in small case with the first letter in caps.

Data Tables should be submitted in Microsoft Word table format.

1.5. Construction of references

All references should be numbered sequentially [in square brackets] in the text and listed in the same numerical order in the reference section. The reference numbers must be finalized and the bibliography must be fully formatted before submission.

Sample references are provided at the end of this template in the reference section. Correct reference format and list must be provided in the article.

2. MATERIALS AND METHOD (FOR RESEARCH ARTICLES ONLY)

This section provides details of the methodology used along with information on any previous efforts with corresponding references. Any details for further modifications and research should be included.

3. EXPERIMENTAL: (FOR RESEARCH ARTICLES ONLY)-

Repeated information should not be reported in the text of an article. A calculation section must include experimental data, facts and practical development from a theoretical perspective.

4. RESULTS AND DISCUSSIONS: (FOR RESEARCH ARTICLES ONLY)-

The Results and discussions may be presented individually or combined in a single section with short and informative headings.

5. STANDARD PROTOCOL ON APPROVALS, REGISTRATIONS, PATIENT CONSENTS & ANIMAL PROTECTION:

All clinical investigations must be conducted according to the declaration of helsinki principles. Authors must comply with the guidelines of the international committee of medical journal editors (www.icmje.org) with regard to the patient's consent for research or participation in a study.

CONCLUSION

The concluding lines of the article may be presented in a short section of conclusion.

LIST OF ABBREVIATIONS

If abbreviations are used in the text either they should be defined in the text where first used, or a list of abbreviations can be provided.

CONFLICT OF INTEREST

Financial contributions and any potential conflict of interest must be clearly acknowledged under the heading ‘Conflict of Interest’. Authors must list the source(s) of funding for the study. This should be done for each author.

ACKNOWLEDGEMENTS

All individuals listed as authors must have contributed substantially to the design, performance, analysis, or reporting of the work and are required to indicate their specific contribution. Anyone (individual/company/institution) who has substantially contributed to the study for important intellectual content, or who was involved in the article’s drafting the manuscript or revising must also be acknowledged.

Guest or honorary authorship based solely on position (e.g. research supervisor, departmental head) is discouraged.

SUPPLEMENTARY MATERIAL

Supportive/Supplementary material intended for publication must be numbered and referred to in the manuscript but should not be a part of the submitted paper. List all Supportive/Supplementary Material and include a brief caption line for each file describing its contents.

REFERENCES

Journal Reference:

[1] Bard, M.; Woods, R.A.; Bartón, D.H.; Corrie, J.E.; Widdowson, D.A. Sterol mutants of Saccharomyces cerevisiae: chromatographic analyses. *Lipids*, **1977**, *12*(8), 645-654.

[2] Zhang, W.; Brombosz, S.M.; Mendoza, J.L.; Moore, J.S. A high-yield, one-step synthesis of o-phenylene ethynylene cyclic trimer via precipitation-driven alkyne metathesis. *J. Org. Chem.*, **2005**, *70*, 10198-10201.

Book Reference:

[3] Crabtree, R.H. *The Organometallic Chemistry of the Transition Metals*, 3rd ed.; Wiley & Sons: New York, **2001**.

Book Chapter Reference:

[4] Wheeler, D.M.S.; Wheeler, M.M. In: *Studies in Natural Products Chemistry*; Atta-ur-Rahman, Ed.; Elsevier Science B. V: Amsterdam, **1994**; Vol. 14, pp. 3-46.

Conference Proceedings:

[5] Jakeman, D.L.; Withers, S.G.E. In: *Carbohydrate Bioengineering: Interdisciplinary Approaches* In: Proceedings of the 4th Carbohydrate Bioengineering Meeting, Stockholm, Sweden, June 10-13, 2001; Teeri, T.T.; Svensson, B.; Gilbert, H.J.; Feizi, T., Eds.; Royal Society of Chemistry: Cambridge, UK, **2002**; pp. 3-8.

URL (WebPage):

[6] National Library of Medicine. Specialized Information Services: Toxicology and Environmental Health. sis.nlm.nih.gov/Tox/ToxMain.html (Accessed May 23, **2004**).

Patent:

[7] Hoch, J.A.; Huang, S. Screening methods for the identification of novel antibiotics. U.S. Patent 6,043,045, March 28, 2000.

Thesis:

[8] Mackel, H. *Capturing the Spectra of Silicon Solar Cells*. PhD Thesis, The Australian National University: Canberra, December **2004**.

E-citations:

[9] Citations for articles/material published exclusively online or in open access (free-to-view), must contain the accurate Web addresses (URLs) at the end of the reference(s), except those posted on an author's Web site (unless editorially essential), e.g. 'Reference: Available from: URL'.

Some important points to remember:

- All references must be complete and accurate.
- All authors must be cited and there should be no use of the phrase *et al.*
- Date of access should be provided for online citations.
- Journal names should be abbreviated according to the Index Medicus/MEDLINE.
- Punctuation should be properly applied as mentioned in the examples given above.
- Superscript in the in-text citations and reference section should be avoided.
- Abstracts, unpublished data and personal communications (which can only be included if prior permission has been obtained) should not be given in the references section. The details may however appear in the footnotes.
- The authors are encouraged to use a recent version of EndNote (version 5 and above) or Reference Manager (version 10) when formatting their reference list, as this allows references to be automatically extracted.

Received: March 20, 2014 Revised: April 16, 2014 Accepted: April 20, 2014